9-29-2022 1:00 PM

Absence of Enhancer of Zeste Homolog 2 Promotes the Progression of KRAS-Driven Pancreatic Ductal Adenocarcinoma

Xiaoyi Wang, *The University of Western Ontario*

Supervisor: Dr. Christopher Pin, *The University of Western Ontario*

A thesis submitted in partial fulfillment of the requirements for the Master of Science degree in Physiology and Pharmacology

Abstract

Pancreatic ductal adenocarcinoma (PDAC) is predicted to be the second deadliest cancer by 2030. Previous studies showed constitutive activation of *KRAS* ($KRAS^{G12D}$) is a key genetic driver of PDAC, accelerated by deletion of the epigenetic regulator Enhancer of Zeste Homologue 2 (EZH2). However, contradictory findings suggest multiple roles for EZH2. The goal of this study was to define EZH2's contribution to early $KRAS^{G12D}$-driven PDAC. *I hypothesized that EZH2 restricts $KRAS^{G12D}$ initiation of PDAC in response to injury.* To address this hypothesis, genetically modified mice with targeted deletion of the SET domain of *Ezh2* +/- $KRAS^{G12D}$ were exposed to cerulein-induced pancreatic injury and examined for pancreatic lesions. Histological analysis for markers of tissue damage and inflammation showed loss of EZH2 caused no difference in the pre-neoplastic lesion formation but did affect progression, and reduced immune cell infiltration, suggesting a role for EZH2 in limiting early progression of $KRAS^{G12D}$-mediated PDAC.

Keywords: PDAC, EZH2, KRAS, pancreatitis.

Summary for Lay Audience

In this study, I examined the role of an enzyme Enhancer of Zeste Homologue 2 (EZH2) in the most common type of pancreatic cancer called pancreatic ductal carcinoma (PDAC) in the presence of *KRAS* mutation in mice. The majority of PDAC patients bear *KRAS* mutations in their genome. Our previous work showed that there are no differences in the severity of pancreatic tissue injury whether you delete *EZH2* or not. However, other studies indicate that *EZH2* deletion make the effects of *KRAS* mutation much stronger on the development of PDAC. Therefore, I wanted to know if the loss of *EZH2* is beneficial or harmful for pancreatic tissue recovery from injury in the context of *KRAS* mutation. My work showed that the loss of *EZH2* results in more progressive pancreatic lesions, which increase the possibility of developing into cancer. In addition, I observed more immune cells appeared around the pancreatic lesions of mice lacking *Ezh2* expression. My results suggest that *EZH2* plays an important role in the development of pancreatic cancer and may be a potential target for anti-cancer therapy.

Co-Authorship Statement

Xiaoyi (Jessie) Wang completed all the experiments and data analysis included in this project except for **Figure 3.8 B-C**, which were done by Fatemeh Mousavi. Scoring of tissue damage was done by Liena Zhao.

Acknowledgments

First of all, I would like to thank my supervisor Dr. Christopher Pin for your guidance, patience, and encouragement throughout this project. I'm extremely grateful for this amazing opportunity and for your constant support. It's impossible for me to complete this project during the past two years without your knowledge and valuable feedbacks. There is no doubt that you are the best mentor in my life. Many thanks to you!

Next, I would like to thank my parents, Jun Wang and Jun Ma, for all the care, love, mental and financial supports. I will never have a chance to study abroad in Canada and achieve my goal without my parents' support. Thank you for always being there for me during the tough times, and I'm so proud to be your daughter. I would also like to thank Vic for your companion over these years, I love you so much!

To my committee members, Dr. Sean Gill and Dr. Len Luyt. Thank you for providing critical feedbacks and comments that helped me improve my project. I feel really lucky and honored to have you in my committee.

Finally, I would like to thank all the past and current Pin lab members for helping me with learning essential technical skills and for improving my knowledge. Thank you, Kurt, for supporting me with your knowledge at the beginning. To Phyo and Mellisa, who helped me a lot with lab techniques and mouse work. A special thanks to Fatemeh, who supported my project with all the bioinformatics, and Emilie, who is a truly knowledgeable and kind person that is always there to address my questions.

Table of Contents

List of Tables

List of Figures

List of Abbreviation

AB	Alcian Blue
ADM	Acinar-to-Buct cell Metaplasia
AKT	Protein kinase B
AP	Acute Pancreatitis
AP-1	Activator Protein 1
apCAF	Antigen-presenting Cancer-Associated Fibroblast
AR	Androgen Receptor
bHLH	Basic Helix-Loop-Helix
C3	Complement 3
CAF	Cancer-Associated Fibroblast
CCL2	Chemokine (c-c motif) Ligand 2
CD	Cluster of Differentiation
CDE	Choline Deficient Ethionine
CDKN2A	Cyclin Dependent Kinase Inhibitor 2a
CIP	Cerulein Induced Pancreatitis
CK19	Cytokeratin 19
CP	Chronic Pancreatitis
CPA1	Carboxypeptidase A1
CRPC	Castration-Resistant Prostate Cancer
CVB	Group B Coxsackieviruses
CXC	Cysteine-rich
CXCL1	Chemokine (c-x-c motif) Ligand 1
CXCL12	Chemokine (c-x-c motif) Ligand 12

DAVID	the Database for Annotation, Visualization and Integrated Discovery
DMEM	Dulbecco's Modified Eagle Medium
DNMT	DNA Methyltransferase
ECM	Extracellular Matrix
EED	Embryonic Ectoderm Development
EGF	Epidermal Growth Factor
EGFR	Epidermal Growth Factor Receptor
EID	EED-Interaction Domain
ERK1/2	Extracellular signal-Regulated Kinase
EZH1	Enhancer of Zeste Homolog 1
EZH2	Enhancer of Zeste Homolog 2
FBS	Fetal Bovine Serum
FGF	Fibroblast Growth Factor
GAP	GTPase-Activating Protein
GDP	Guanosine Diphosphate
GEF	Guanine nucleotide Exchange Factor
GO	Gene Ontology
GTP	Guanosine Triphosphate
HA	Hyaluronic Acid
HAT	Histone Acetylases
HDAC	Histone Deacetylases
HDM	Histone Demethylase
HE	Hematoxylin & Eosin
HEPES	4-(2-Hydroxyethyl)-1-Piperazineethanesulfonic acid

HKMT	Histone Lysine Methyltransferase
HMT	Histone Methyltransferase
iCAF	Inflammatory Cancer-Associated Fibroblast
IFP	Interstitial Fluid Pressure
IHC	Immunohistochemistry
IL	Interleukin
IP	Intraperitoneal
KMT	Lysine Methyltransferase
KRAS	Kirsten Rat Sarcoma viral oncogene homolog
LPS	Lipopolysaccharides
LSL	Lox-Stop-Lox
MAPK	Mitogen-Activated Protein Kinase
MEK1/2	Mitogen-Activated Protein Kinase Kinase
MHC II	Major Histocompatibility Complex class ii
MIST1	Muscle, Intestine and Stomach expression 1
MPC	Multipotent Progenitor Cells
mTOR	Mammalian Target of Rapamycin
MUC1	Mucin 1
MVD	Microvascular Density
myCAF	Myofibroblast Cancer-Associated Fibroblast
NADPH	Nicotinamide Adenine Dinucleotide Phosphate
NF-κB	Nuclear Factor Kappa-light-chain-enhancer of activated B cells
NFATc1	Nuclear Factor of Activated T cell
NK	Natural Killer

NSF	N-ethylmaleimide Sensitive Fusion protein
OncomiRs	Oncogenic miRNA
PanIN	Pancreatic Intraepithelial Neoplasia
PAS	Periodic Acid–Schiff
PBS	Phosphate Buffered Saline
PBST	Phosphate-Buffered Saline/Tween
PcG	Polycomb Group
PCR	Polymerase Chain Reaction
PDAC	Pancreatic Ductal Adenocarcinoma
PDX1	Pancreatic and Duodenal homeobox 1
PI3K	Phosphatidyl Inositol 3 Kinase
PRC1	Polycomb Repressive Complex 1
PRC2	Polycomb Repressive Complex 2
PSC	Pancreatic Stellate Cell
PTF1A	Pancreatic Transcription Factor 1A
RBBP4/7	Retinoblastoma-Binding Protein 4/7
Ser21	Serine 21
SEM	Standard Error of the Mean
SET	The suppressor of variegation 3-9 (Su(var)3-9), the enhancer of zeste (E(z)), and the trithorax-group chromatin regulator trithorax (Trx)
SMAD4	Mothers Against Decapentaplegic homolog 4
SNARE	Soluble N-ethylmaleimide sensitive fusion protein Attachment Receptor
SOX9	Sry-related high-mobility group box 9
STAT3	Signal Transducer and Activator of Transcription 3

STI	Soybean Trypsin Inhibitor
SUZ12	Suppressor of Zeste 12 homolog
TAA	Tumor-Associated Antigens
TAM	Tumor-Associated Macrophage
TGFβ	Transforming Growth Factor-β
TIL	Tumor-Infiltrating Lymphocyte
TME	Tumor Microenvironment
TP53	Tumor Protein p53
TSmiR	Tumor Suppressor miRNA
VEGF	Vascular Endothelial Growth Factor
WT	Wild-Type
α-SMA	α -Amooth Muscle Actin

1 CHAPTER 1: INTRODUCTION

1.1 PANCREATIC DUCTAL ADENOCARCINOMA

Pancreatic ductal adenocarcinoma (PDAC) constitutes 95% of all pancreatic cancers and is predicted to be the second leading cause of death related to cancer in Canada by 2030 (Haeberle & Esposito, 2019). The overall five-year survival rate for PDAC is less than 9% due to the lack of early detection methods and effective treatments (Sarantis et al., 2020). PDAC is highly malignant and the prognosis is the poorest of any common solid tumour. PDAC often remains asymptomatic until the tumor becomes advanced. Common symptoms include abdominal pain, weight loss, and jaundice. The majority of patients are diagnosed at late stages when PDAC has already metastasized (Zhang et al., 2019), likely due to the pancreas being located deep in the abdomen and often lacking early symptoms until the tumor spreads to other organs. In 60-70% cases, PDAC develops from the head of the pancreas (Corbo et al., 2012). These cases are often diagnosed earlier because the head of the pancreas contains the pancreatic duct that joins the lower part of the common bile duct, which is responsible for carrying bile through the pancreas into the duodenum. In contrast, PDAC arising from the body and tail of the pancreas usually has a poor prognosis (Sarantis et al., 2020).

The high mortality rate of PDAC is also due to the resistance these tumours show to most current cancer treatments. Most traditional cancer therapies, such as chemotherapy, radiotherapy, and surgery, have limited effects on improving survival. Surgical resection and chemotherapy with gemcitabine are considered the most effective treatments to improve the survival rate of early-stage PDAC patients with resectable and locally advanced tumors, respectively. However, these treatments are not sufficient for late-stage patients (Sarantis et al., 2020) and have relapse rate up to 80% (Low et al., 2011). For these reasons, it is essential to elucidate factors that affect the initiation and progression of PDAC and discover methods of detection and stratification of PDAC. To identify novel targets for treatment, there is a critical need in identifying and understanding mechanisms that

underlie the initiation events in PDAC, as well as the potential to increase patient's survival rate after diagnosis.

1.1.1 ORIGIN OF PDAC

PDAC originates in the exocrine part of the pancreas. The pancreas is a long-flattened gland located in the abdomen surrounded by the spleen, liver and small intestine. The pancreas has two functional components - the exocrine pancreas that produces, stores and delivers digestive enzymes, and the endocrine islets that regulate blood sugar levels (Zhou et al., 2018). The exocrine pancreas is composed of acinar cells, which are responsible for producing and secreting digestive enzymes, and duct cells, which form interposed conduits that transport enzymes into the small intestine (Backx et al., 2022).

PDAC can originate from acinar cells or duct cells with similar phenotypes but different modes of tumor progression (Ferreira et al., 2017). Due to the high expression of duct cell markers and duct morphology, PDAC was originally thought to arise exclusively from duct cells. However, recent studies show evidence of acinar cells adopting duct cell features, with acinar cells the most common cell of origin for PDAC (De La et al., 2008; Ferreira et al., 2017; Xu et al., 2019). Acinar-derived PDAC usually develops via pre-neoplastic precursors called pancreatic intraepithelial neoplasia (PanINs), which is one of the precursor lesions in PDAC. Studies also show acinar cells are more sensitive to pancreatic tumor driver mutations and are more likely to develop into PanIN and PDAC effectively. Duct cells are more resistant to oncogenic drivers and are less likely to develop to PDAC (Brembeck et al., 2003; Guerra et al., 2007; Ray et al., 2011), therefore, our models have focused on expressing oncogenic KRAS within acinar cells.

1.1.2 PDAC PROGRESSION AND MORPHOLOGY

1.1.2.1 ACINAR-TO-DUCT CELL METAPLASIA (ADM)

A key event that can increase the risk of PDAC is a common and reversible process called acinar-to-duct cell metaplasia (ADM), which can be induced by the pancreatic inflammation that occurs in pancreatitis (Liu et al., 2016). ADM is a process in which

pancreatic acinar cells dedifferentiate into progenitor-like cells and then re-differentiate into duct-like cells with duct cell traits. An ADM lesion is characterized by a lobular structure consisting of mainly metaplastic duct-like cells, which are proliferative and replenish the tissue after damage (McDonald, 2022; **Fig 1.1**). ADM facilitates acinar cell regeneration and reverses loss of pancreatic tissue due to injury, showing the ability of acinar cells to adapt to pressures caused by environmental and/or genetic stress (Wang et al., 2019). However, when oncogenic genetic mutations are acquired and/or environmental stress is persistent, ADM may become irreversible and lead to low-grade PanINs, increasing the risk of further progressing to PDAC (Andrew et al., 2020; Storz, 2017).

Multiple genetic and environmental factors have been implicated in regulating the formation of ADM, including oncogenic *KRAS* (Hingorani et al., 2003), persistent stress signalling (Liou et al., 2016), inflammatory cytokines (Liou et al., 2013), loss of cell-cell and cell-matrix contacts (Greer et al., 2013; Sawey et al., 2007), loss of cell polarity (Direnzo et al., 2012), and the presence of growth factors that activate epidermal growth factor receptor (EGFR) (Liou et al., 2016; Storz, 2017). Studies from both human (Liu et al., 2016; Huang et al., 2021) and mouse models (Collins et al., 2012; Habbe et al., 2008) identified the essential role of oncogenic $KRAS^{G12D}$ in the induction of ADM-like change in cell culture and *in vivo*. In mouse acinar cells, oncogenic *KRAS* changes gene expression profiles, which results in suppression of acinar-specific genes including *carboxypeptidase A1* (*Cpa1*) (Livshits et al., 2018) and *Amylase* (Liou et al., 2013), and activation of duct-specific genes such as *cytokeratin 19* (*CK19*) (Liou et al., 2013), mucin 1 (*Muc1*) (Zhu et al., 2007), and *Sry-related high-mobility group box 9* (*Sox9*) (Zhou et al., 2018).

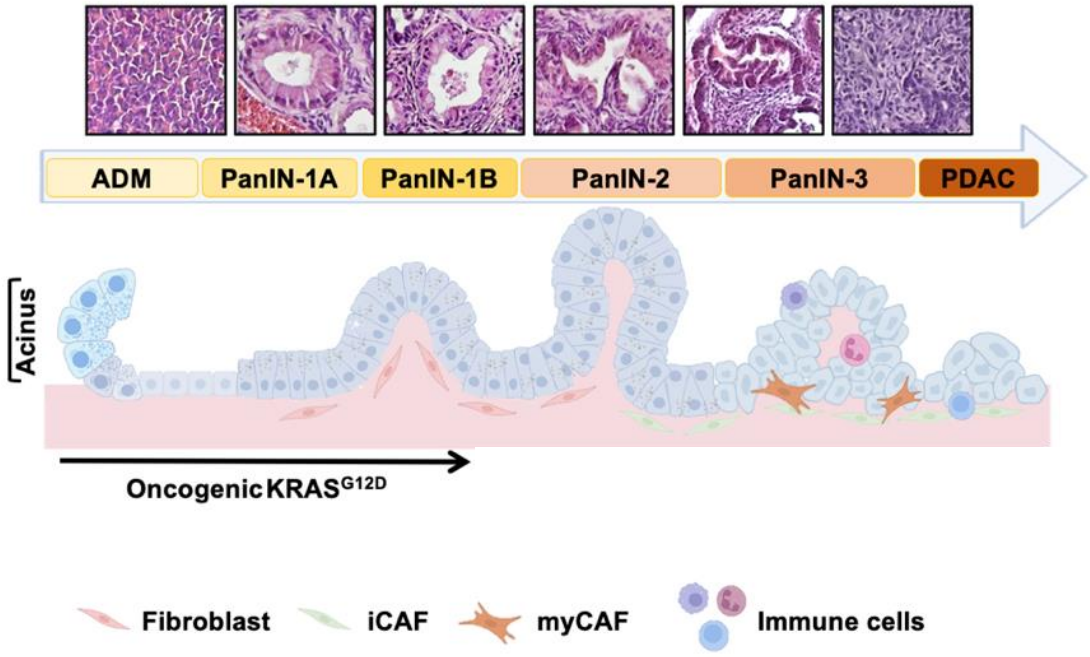
ADM
PanIN-1A
PanIN-1B
PanIN-2
PanIN-3
PDAC
Acinus
Oncogenic KRAS^{G12D}
Fibroblast
iCAF
myCAF
Immune cells

Figure 1.1 Schematic model of the progression of normal pancreatic acinar cells to PanIN lesions to PDAC. Oncogenic $KRAS^{G12D}$ expression in acinar cells promotes acinar to duct cell metaplasia (ADM) and pancreatic intraepithelial neoplasia (PanIN). This eventually results in PDAC observed in PDAC mice models. PDAC cells release factors that stimulate surrounding residential fibroblasts into activated myofibroblasts (myCAFs) and inflammatory fibroblasts (iCAFs). During tumorigenesis, immune cell populations including T cells, NK cells, and macrophages infiltrate the tumor microenvironment (TME).

1.1.2.2 PANCREATIC INTRAEPITHELIAL NEOPLASIA (PANIN)

PanINs are the most common type of non-invasive precursor lesion that leads to invasive PDAC. Generally, PanIN are asymptomatic and microscopic lesions that measure less than 5 mm in diameter (Distler et al., 2014). The progression from PanIN to PDAC is classified into three different stages according to the level of morphologic dysplasia and accumulation of genetic alterations: low grade (PanIN-1A and PanIN-1B), intermediate grade (PanIN-2), and high grade (PanIN-3). Significant genetic and molecular changes take place in each stage that drive metastasis of PDAC cells, including mutations in *KRAS*, *p53*, and *SMAD4* (Guo et al., 2016; **Figure 1.1**).

Low-grade PanINs arise in metaplastic ductal epithelium and can be observed in healthy pancreatic tissue (Habbe et al., 2008). PanIN-1A lesions are flat lesions characterized by simple columnar epithelium with no nuclear dysplasia (Distler et al., 2014). PanIN-1B lesions are papillary epithelial lesions that are similar to PanIN-1A but show nuclear atypia and undulating architecture. PanIN-2 are mucinous epithelial lesions that show loss of cell polarity, with enlarged nuclei that vary in size and shape and have a pseudostratified appearance. Cytologically, PanIN-2 show moderate architectural atypia, which includes nuclear crowding, and nuclear hyperchromasia. PanIN-3 exhibit the most severe dysplasia, which is characterized by extensive loss of nuclear polarity, papillae and cribriform structure formation, poorly oriented nuclei, and cell clusters bud from the papilla into the lumen of the duct. PanIN-3 lesions are stratified, predominantly papillary and rarely flat (Guo et al., 2016; Distler et al., 2014; Hruban et al., 2008; Seeley et al., 2010; **Figure 1.1**). The accumulation of genetic alterations is often correlated with the histological progression of pancreatic carcinogenesis.

1.1.2.3 PDAC

Grossly, PDAC presents as a solid white-yellowish mass with abnormal contours, most frequently located at the pancreatic head. At diagnosis, PDAC tumors have usually developed beyond the pancreatic anatomical boundary and infiltrated into neighboring structures including associated blood vessels, peripancreatic fat tissue, duodenum, or

stomach (Esposito et al., 2019). PDAC tumors often reach a size between 2-4 cm if localized in the proximal pancreas, or even larger if localized in the body and tail (Haeberle and Esposito, 2019). Microscopically, PDAC lesions appear as irregular small pancreatic ducts consisting of atypical ductal units lined by one or two layers of cuboidal duct cells, embedding in dense desmoplastic stroma (Korc, 2007). Based on transcriptomic analysis of PDAC epithelial cells, Moffitt et al. (2015) identified four subtypes of tumors by separating tumor and stromal gene expression profile. Two tumor-specific subtypes include classical and basal-like PDAC. Patients with classical PDAC have significantly higher survival rate and better diagnosis, while basal-like PDAC is associated with poor diagnosis and clinical outcomes (Moffitt et al., 2015; Shinkawa et al., 2022). The classical PDAC is characterized by the expression of epithelial markers and higher level of differentiation, with the presence of fibrosis and inflammation in pancreatic tissues. Basal-like PDAC is characterized by the expression of mesenchymal markers and poor differentiation (Juiz et al., 2020; Shinkawa et al., 2022). Two stromal-specific subtypes are identified as normal and activated stromal PDAC. Activated stromal PDAC is characterized by two factors that demonstrated gene expression specifically from the stromal area. Patients with activated stromal PDAC have worse diagnosis compared to patients with normal subtype (Moffitt et al., 2015).

1.1.3 GENETIC FACTORS

PDAC tumorigenesis involves progressive accumulation of diverse genetic alterations including point mutations, insertions, deletions, and amplifications in more than 500 genes (Lucito et al., 2007). However, genome-wide sequencing studies identified only four signature genetic mutations for PDAC, including the *KRAS* oncogene, and tumour suppressor genes *TP53*, *CDKN2A/p16*, and *SMAD4* (Waddell et al., 2015). These genetic alterations are the main cause of the histological changes that occur in different stages of PDAC progression (Hruban et al., 2008). The majority of PDAC patients carry *KRAS* and *TP53* mutations. Almost 95% PDAC patients carry at least two out of four mutations, while *KRAS* mutations alone was found in 93% patients. It is reported that patients with less mutations survived significantly longer than patients with more mutations, and that patients

carrying wild-type *KRAS* or *CDKN2A/p16* also survived significantly longer than those with oncogenic *KRAS* (Schlitter et al., 2017).

1.1.3.1 ONCOGENE KRAS

Kirsten rat sarcoma viral oncogene homolog (KRAS) mutations are the most common driver genes of PDAC that occur in early preneoplastic lesions (Waddell et al., 2015; Guo et al., 2016). Approximately 95% of all PDAC patients are found to carry an oncogenic *KRAS* mutation (Guo et al., 2016). *KRAS* is located at chromosome 12p12.1 and encodes for a small plasma membrane bound GTPase protein called KRAS (21 kDa), which acts as a molecular switch for multiple downstream signaling pathways. KRAS protein comprises two functional domains, one of which called the G domain that is responsible for binding and hydrolysing guanosine triphosphate (GTP). The second domain is the membrane targeting domain that anchors to the cell membrane and is necessary for the bioactivity of KRAS. The function of KRAS as a molecular switch is controlled by the intrinsic guanosine triphosphate (GTP)- guanosine diphosphate (GDP) cycling (Vigil et al., 2010). In the quiescent state, KRAS is predominantly bound to GDP and is inactive. Extracellular stimulations such as epidermal growth factor (EGF) bind to the epidermal growth factor receptor (EGFR) and activate tyrosine kinases (Ardito et al., 2012). This leads to rapid transition of KRAS from the GDP-bound inactive state to the GTP-bound active state mediated by guanine nucleotide exchange factors (GEFs) (Vigil et al., 2010). Active KRAS is capable of recruiting effector proteins and, therefore, regulates more than 80 downstream intracellular signalling pathways (Buscail et al., 2020). The deactivation of KRAS is mainly mediated by GTPase-activating proteins (GAPs), which accelerate the hydrolysis of GTP (**Figure 1.2**). In general, KRAS couples growth factor receptors on the cell membrane to intracellular signalling pathways and eventually promotes cell proliferation, differentiation, migration, and survival by activating various signaling pathways and transcription factors (Buscail et al., 2020).

Common *KRAS* variants include G12D, G12V, and G12R, while some less common *KRAS* variants include G12C, Q61H, Q61R, representing different types of amino acid changes due to mutations (Bournet et al., 2016). These are gain-of-function mutations in KRAS that

cause hyperactivation. Among all the PDAC-associated variants in KRAS, G12D is the most frequent type of point mutation that accounts for nearly 40% of all KRAS mutations (Waters and Der, 2018). Two mutational hot spots, G12D and G12V, involve single nucleotide mutations that induce replacement of the GGT (glycine) sequence by the GAT (aspartic acid) sequence and by the GGT (valine), respectively (Bournet et al., 2016). These mutations permanently impair the GTPase activity of KRAS and prevent the conversion of GTP to GDP, resulting in persistent activation of KRAS independent of extracellular stimulation (di Magliano and Logsdon, 2013; Jonckheere et al., 2017). The KRAS protein is therefore capable of constitutively activating various downstream signalling pathways, leading to cancer cell proliferation, invasion and survival.

Numerous studies revealed that *KRAS* mutations are the main genetic driver that initiates the development of PDAC. However, this progression from normal pancreatic tissue to invasive metastatic PDAC requires additional genetic aberrations and has a long latency period of 10 to 12 years (Iacobuzio-Donahue et al., 2012; Kanji et al., 2013). Several major signaling pathways modulated by aberrant KRAS activation include canonical mitogen-activated protein kinase (MAPK), NF-κB, and PI3K-AKT-mTOR signalling pathways (**Figure 1.2;** Collisson et al., 2012; Collins, et al., 2014; Jazirehi et al., 2012; Hassan et al., 2018; Prabhu et al., 2014). The KRAS/MAPK cascade (**Figure 1.2**) is the best-studied effector pathway normally activated by EGF, which is the main activating protein for KRAS signaling. Constitutively active KRAS first binds to and activates the serine/threonine kinase Raf, which in turn phosphorylates and activates the mitogen-activated protein kinase kinase (MEK1/2). Subsequently, MEK1/2 phosphorylates extracellular signal-regulated kinase (ERK1/2), which eventually translocates to the nucleus where it phosphorylates transcription factors and promotes gene expression involved in cell-cycle progression, cell proliferation and differentiation (Collison et al., 2012; Cargnello et al., 2011). Constitutive up-regulation of the MAPK pathway by $KRAS^{G12D}$ promotes acinar cell dedifferentiation and is essential for the maintenance of PanIN lesions (Collins et al., 2014).

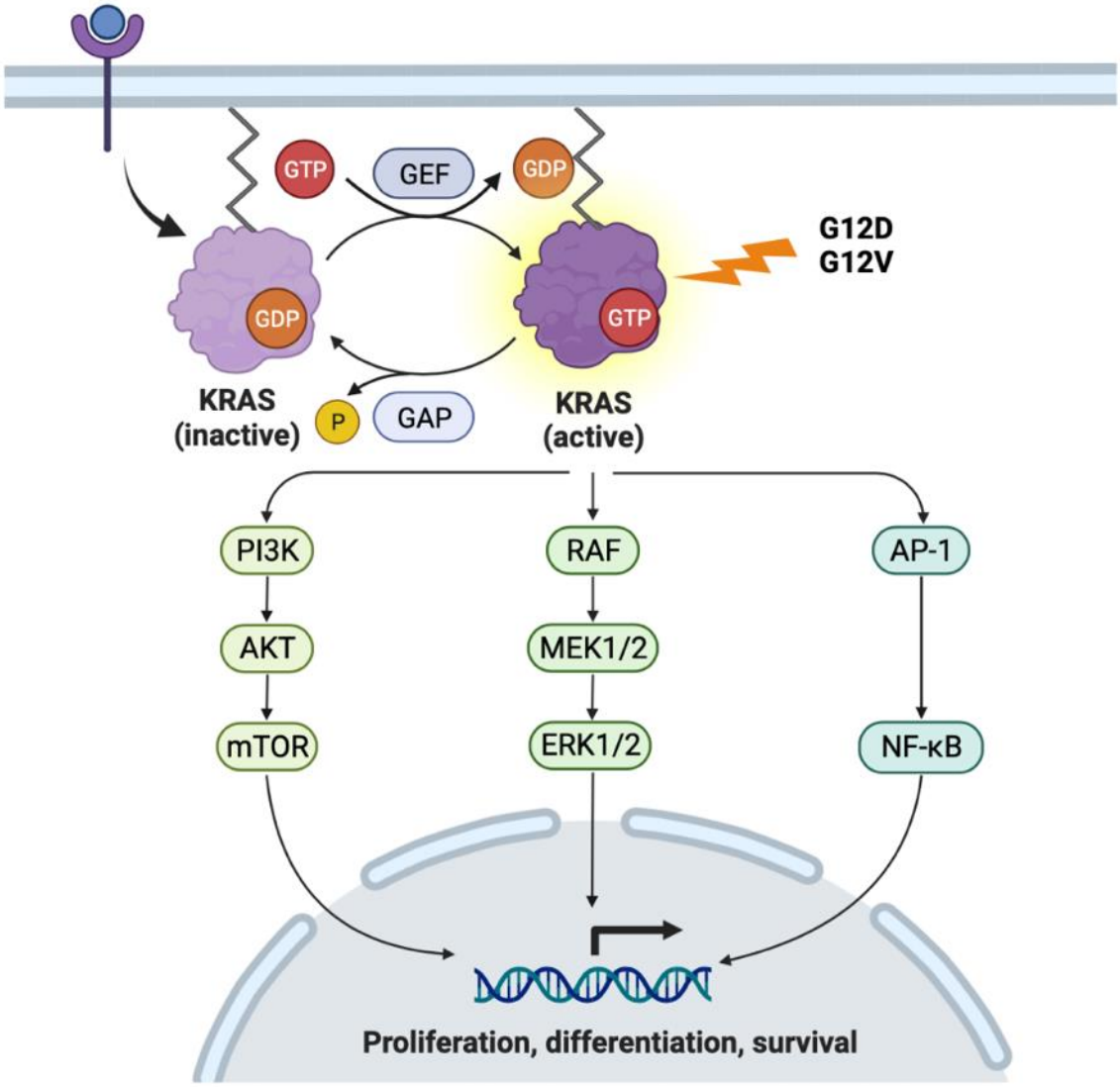
GTP
GEF
GDP
G12D
G12V
GDP
GTP
KRAS
(inactive)
P
GAP
KRAS
(active)
PI3K
RAF
AP-1
AKT
MEK1/2
mTOR
ERK1/2
NF-κB
Proliferation, differentiation, survival

Figure 1.2 Activation of KRAS protein and downstream intracellular signaling pathways. Extracellular ligands such as epidermal growth factor (EGF) which are bound to the epidermal growth factor receptor (EGFR) and leads to interaction with KRAS protein. The KRAS protein is attached to the cell membrane in order to be activated. KRAS is activated when bound to GTP and is deactivated when bound to GDP. Intrinsic GTP–GDP cycling is controlled by guanine nucleotide exchange factors (GEFs) that can convert GDP to GTP, and by GTPase-activating proteins (GAPs) that can accelerate GTP hydrolysis. Point mutations (e.g., G12D, G12V) impair the GTPase activity of KRAS and prevents deactivation. KRAS is therefore constitutively active and is able to upregulate multiple downstream signaling pathways and nuclear transcription factors, leading to cell proliferation, differentiation, and survival.

PI3K-AKT-mTOR is the second major intrinsic intracellular signalling pathway that contributes to cell cycle regulation (Hassan et al., 2018). $KRAS^{G12D}$ constitutively activates downstream effector Phosphatidyl inositol 3 kinase (PI3K), which in turn phosphorylates protein kinase B (AKT). AKT can activate multiple downstream transcription factors, one of which is mammalian target of rapamycin (mTOR), a serine/threonine protein kinase mainly regulating growth and proliferation of cells. As a master switch of many downstream effectors, AKT predominantly functions to promote cell survival mediated by growth factors and to restrict apoptosis (Jazirehi et al., 2012; Hassan et al., 2018). Overactivation of this pathway in PDAC results in limited cell apoptosis, which therefore allows cancer cell proliferation and enhanced PDAC aggressiveness (Jazirehi et al., 2012). The PI3K-AKT-mTOR pathway also plays a role in modulating crosstalk between tumor cells and the stromal immune cells, which eventually promotes tumor growth and therapy resistance (Yuan et al., 2008). The third intrinsic signaling pathway is the Nuclear factor kappa-light-chain-enhancer of activated B cells (NF-κB). NF-κB is the "matchmaker" of cancer and cancer-associated inflammation in PDAC (Kabacaoglu et al., 2019). By activating a transcription factor called activator protein 1 (AP-1), oncogenic KRAS promotes the production of interleukin-1α (IL-1α), which stimulates constitutive activation of the NF-κB signaling (Ling et al., 2012). This not only results in the activation of multiple target genes responsible for proinflammatory and antiapoptotic responses in PDAC, but also leads to overexpression of sequestosome-1, also known as ubiquitin-binding protein p62, which positively regulates the feedback loop and further increases NF-κB levels (Prabhu et al., 2014).

By activating numerous major intrinsic signaling pathways, $\textit{KRAS}^{G12D}$ is able to promote irreversible ADM and initiate progression to PDAC. However, additional genetic or environmental factors are required along with *KRAS* oncogene to promote more progressive PanIN lesions.

1.1.3.2 TUMOR SUPPRESSOR GENES

In addition to *KRAS*, *TP53*, *CDKN2A/p16*, and *SMAD4* tumor suppressor genes are mutated in many PDAC cases, with a prevalence of 70%, 21% and 17%, respectively (Waters and Der, 2018; Maddalena et al., 2021). The presence of additional mutational burden in tumor suppressor genes can dramatically accelerate the progression of $KRAS^{G12D}$-mediated PDAC (Hingorani et al., 2005). In contrast to *KRAS*, *TP53*, *CDKN2A/p16*, and *SMAD4* are inactivated in most of PDAC cases, while KRAS is activated (Hahn & Schmiegel, 1998).

The majority of mutations in *tumor protein p53* (*TP53*) are missense mutations, leading to excessive production of mutant p53 in tumor cells (Maddalena et al., 2021). Mutations in *TP53* essentially promote metastasis of PDAC by preventing growth arrest or senescence of cancer cells (Morton et al., 2010). Cyclin dependent kinase inhibitor 2A (*CDKN2A*) encodes for the p16 protein, which can negatively regulate the progression of cell cycle (Zhao et al., 2016). Mutations in *CDKN2A* result in functional inactivation and uncontrolled cell growth and differentiation (Zhao et al., 2016). Mothers against decapentaplegic homolog 4 (*SMAD4*) mutations are rare in PDAC, but the combination of *SMAD4* mutations with other genetic mutations increase the risk of PDAC. It encodes for the SMAD4 protein, which acts as an effector protein that activates the transforming growth factor-β (TGFβ) pathway (Dardare et al., 2020). Given TGFβ primarily plays a role in cell cycle regulation as a tumor suppressor, alterations in the *SMAD4* gene contribute to promoting the progression of PDAC (Waddell et al., 2015). However, TGFβ can promote tumour progression at later stages of PDAC, suggesting an opposing role of *SMAD4*. In contrast to *KRAS*, which occur early in the disease, *CDKN2A* and *SMAD4* genes usually appear in later stages of PDAC such as PanIN-3, when lesions are histologically recognizable (Kubiczkova et al., 2012; Zhao et al., 2016).

1.1.3.3 GENETIC MODELS OF PDAC

Given the well-known role of oncogenic *KRAS* in initiating multiple genetic events for PDAC, studying *KRAS* mutations has been important in improving our knowledge on the

transformation process in PDAC and to develop effective treatments. In the past few decades, transgenic animal models, especially a *KRAS*^{G12D} mouse model, has been widely used for pathophysiological studies of PDAC (Löhr et al., 2005; Hingorani et al., 2003; Siveke et al., 2007; Jonckheere et al., 2017). Some commonly used mouse lines were developed in which KRAS^{G12D} was conditionally activated by cre recombinase expressed from pancreas-specific genes such as *pancreatic and duodenal homeobox 1* (*Pdx1*), *Ptf1a/P48*, and *Mist1* (Hingorani et al., 2005; Herreros et al., 2012). These models are named *Pdx1*$^{cre/+}$/lox-stop-lox (LSL)-*KRAS*^{G12D}, *Ptf1a*(*P48*)$^{cre/+}$/LSL-*KRAS*^{G12D}, and *Mist1*$^{cre/+}$/LSL-*KRAS*^{G12D} (Herreros et al., 2012). In general, these genetically engineered mice have cre recombinase targeted to the specific genes to ensure spatially restricted expression. The cre recombinase then promotes deletion of the LSL region located within the *KRAS* gene, but upstream of a mutated, constitutively activate *KRAS*^{G12D}.

Pdx1$^{cre/+}$/LSL-*KRAS*^{G12D} mice are also known as the KC mouse model. PDX1 is a critical transcription factor involved in the development of the pancreas. Specifically, PDX1 facilitates growth and lineage specification of pancreatic multipotent progenitor cells (MPC) during embryogenesis (Kawaguchi et al., 2002; Hingorani et al., 2005). Therefore, KC mice express pancreas wide oncogenic KRAS^{G12D} from early embryonic development (Guerra et al., 2013). Pancreatic transcription factor 1a (*Ptf1a*) and MIST1 are two of the basic helix-loop-helix (bHLH) transcription factors, whose downregulation is often associated with acinar cell dedifferentiation and loss of acinar cell identity during ADM (Pin et al., 2001; Johnson et al., 2004; Rodolosse et al., 2004). They coordinate to maintain the highly differentiated status of acinar cells and prevent the pancreas from undergoing carcinogenesis (Jakubison et al., 2018). Silencing of *Ptf1a* and *Mist1* genes make acinar cells more prone to undergo irreversible ADM in the context of KRAS^{G12D} hyperactivation (Adell et al., 2000). Transgenic mouse models using *Ptf1a* and *Mist1* as cre driver genes, termed *Ptf1a*$^{cre/+}$*KRAS*^{G12D} (PK model) and *Mist1*$^{cre/+}$*KRAS*^{G12D} (MK model), respectively, induce acinar-specific activation of *KRAS*^{G12D} as they are specifically expressed in acinar cells to coordinate transcription network. Notably, when PK model is used without an inducible cre-recombinase, non-specific gene deletion will occur in the pancreas because *Ptf1a* is originally express in all pancreatic cells (Jakubison et al., 2018; Azizi et al., 2021).

Interestingly, many studies reported pancreas-wide hyperactivation of oncogenic *KRAS* in adult mice using an inducible Cre/loxP system, resulted in limited spontaneous ADM and PanIN formation, suggesting $KRAS^{G12D}$ alone works inefficiently in driving tumorigenesis (Guerra et al., 2011). KRAS works more effectively when chronic pancreatitis, a major risk factor for PDAC, coexists (Carrière et al., 2009; Guerra et al., 2011). $KRAS^{G12D}$ activation, along with an inflammatory environment, can effectively induce formation of ADM formation and early PanIN lesions (Ferreira et al., 2017).

1.1.4 ENVIRONMENTAL FACTORS

In addition to contributions of genetic and epigenetic alterations, there are many known modifiable environmental risk factors for pancreatic cancer including tobacco smoking, alcohol abuse, obesity, diabetes, diet, inactivity, infections, pancreatitis, and certain abdominal surgeries (Boursi et al., 2017). Many studies have indicated that alcohol consumption and tobacco smoking are the strongest risk factors at this time, as they are linked to 60-90% of chronic pancreatitis cases (Pandol & Raraty, 2007; Tsai & Chang, 2019). In addition, international variation and gender differences in the prevalence of PDAC may be attributed to exposure to environmental risk factors related to different lifestyles or cultures (Parkin et al., 2010; Bosettin et al., 2012).

1.1.4.1 PANCREATITIS

Pancreatitis is one of most common pathologies in the exocrine pancreas resulting from inflammation of the pancreas due to premature activity of digestive enzymes inside acinar cells. In general, enzymes produced by the pancreas are activated after they are transported into the small intestine to help with digestion and glucose homeostasis in the body. If these enzymes become activated while still in the pancreas, they cause irritation of pancreatic cells and result in pancreatitis. The pathophysiology of pancreatitis is characterized by extracellular fluid that causes swelling of tissues, separation of lobule and acini, loss of acinar cell zymogen granules, and enlarged acinar lumen (Magana-Gomez et al., 2006). The most common causes of pancreatitis are alcohol abuse and gall stones. Ethanol mainly induces the initiation of pancreatitis by improper activation of digestive zymogens within

acinar cells and soluble N-ethylmaleimide sensitive fusion protein (NSF) attachment receptor (SNARE) proteins that are required for the fusion of zymogen granules (Clemens et al., 2014). During pancreatitis, the tissue usually displays histological features such as immune cell infiltration and fibrosis (Yadav and Lowenfels, 2013). Pancreatitis can be acute, which happens suddenly and lasts for a few days, or chronic, which occurs over years. Chronic pancreatitis (CP) are the major risk factors for human PDAC (Guerra et al., 2007; Vujasinovic et al., 2020). A large nationwide study conducted by Kirkegard et al. revealed that AP can also promote PanIN formation, while the relationship between AP and PDAC is still debatable. However, CP is proposed to be the most common cause of PDAC initiation as nearly 60% patients with CP appear to develop PanINs to different extents, with 4% of which had high-grade PanIN (Hruban et al., 2008). People with hereditary pancreatitis have a 40-55% possibility of developing PDAC in their lifespan (Yadav and Lowenfels, 2013). For these reasons, pancreatitis models using the cholecystokinin agonist cerulein are widely used in research involving PanINs and PDAC.

1.1.4.2 EXPERIMENTAL MODEL OF PANCREATITIS

Pancreatitis induced in the mouse model by cerulein is currently the most widely used experimental model to study PDAC (Hyun and Lee, 2014). This method is based on the mechanism that cerulein activates high levels of nicotinamide adenine dinucleotide phosphate (NADPH) oxidase, the most abundant reactive oxygen species in acinar cells during inflammation and apoptosis, and causes oxidative stress in cells (Kim, 2008). Oxidative stress is linked to pancreatic inflammation and is the major pathogenic factor contributing to pancreatitis (Vaziri, 2004). In brief, cerulein causes pancreatic tissue damage by inducing necrosis, inflammation, and ADM transition. Cerulein-induced pancreatic injury usually allows full recovery within 7 days (Mallen St. Clair et al., 2012). However, in the presence of oncogenic KRAS, pancreatitis-induced ADM rapidly progresses to PanIN and PDAC instead of re-differentiating back into acinar cells for tissue recovery (Ferreira et al., 2017). Cerulein-induced pancreatitis can be either chronic (with repeated dosing over up to 5 weeks) or acute (Huang et al., 2013). Alternative methods to induce chronic or acute pancreatitis (AP) in mouse models include continued alcohol consumption that causes lipopolysaccharides (LPS)-induced pancreatic injury (Vonlaufen

et al., 2011), group B coxsackieviruses (CVB)-induced pancreatitis (Tracy et al., 2000), and intake of choline deficient ethionine-supplemented (CDE) diet (Ida et al., 2010).

1.2 TUMOR MICROENVIRONMENT (TME)

As PDAC develops, tumor cells accumulate genetic and epigenetic alterations and result in significant dysregulation of signaling pathways that cause histological changes in the progression of PDAC, but also reprogram the surrounding microenvironment (Sousa, 2014; Tiomsland et al., 2011; Whatcott et al., 2015). These alterations eventually alter normal physiological function of the stroma, which normally supports tissue regeneration and restrains tumor growth with its component of connective tissues, immune cells, fibroblasts, and vasculature, and generate a favorable tumor microenvironment (TME) (Dunne & Hezel, 2015; Foster et al., 2018). Unlike most other tumors, the PDAC TME can make up the ~90% of the tumor volume, while it could also be as low as 20% depending on high and low cellularity (Karagiannis et al., 2012). Generally, the TME provide cancer cells with innate chemoresistance through the dense stromal compartment, which acts like a physical barrier that prevents successful drug delivery and immune cell infiltration (Provenzano et al., 2012). As an important feature of PDAC, the heterogenous TME is an ecosystem mainly characterized by infiltration of immune cells, dense stroma, and proliferating cancer-associated fibroblasts (CAFs) (Öhlund et al., 2017). It also contains extracellular matrix (ECM) proteins and soluble proteins (cytokines, growth factors) that are believed to contribute to the aggressiveness and drug resistance of PDAC tumor (**Figure 1.3**). The interactions between TME components and cancer cells are essential for tumor cell survival, proliferation, and development.

1.2.1 CANCER-ASSOCIATED FIBROBLAST (CAF)

Fibroblasts are spindle-shaped cells responsible for secreting extracellular matrix proteins and collagen and build the structural framework in tissues. Fibroblasts play an important role in inflammation and cancer formation by modifying the microenvironment. Cancer cells can stimulate surrounding fibroblasts by releasing stimulating factors, such as TGFβ, that give rise to CAFs (Dvorak, 1986; Yu et al., 2014). A major source of CAFs is activated

pancreatic stellate cells (PSCs), which primarily derive from bone marrow mesenchymal stem cell (Öhlund et al., 2017; Haber et al., 1999). PSCs are the predominant type of fibroblast cell located in exocrine pancreas. In healthy pancreas, PSCs are quiescent star-shaped cells and control the production of ECM proteins during the wound healing process (Tomasek et al., 2002). However, in PDAC, PSCs are activated by stimulating factors released by cancer cells and become high in abundance with myofibroblast-like phenotypes (Murray et al., 2022). Activated PSCs constitute almost half of the stromal area and can produce a large amount of the ECM components, including fibronectin, hyaluronic acid (HA), and collagen I and III, which significantly promote desmoplasia (Binkley et al., 2004). The dense ECM is the main cause of high interstitial fluid pressure (IFP) within the stroma, which limits drug infusion and promotes chemotherapy and radiotherapy resistance (Provenzano et al., 2012). Excessive deposits of ECM and collagen fibers also contribute to the development of pancreatic fibrosis, resulting in stiffness of pancreatic tissue (Ferdek & Jakubowska, 2017). The abilities of PSCs to interact with PDAC cells and form a dense fibrotic stroma facilitate are usually related to the aggressiveness of PDAC and therapy resistance.

PSCs can differentiate into at least two CAF subpopulations with diverse phenotypes and functions. Myofibroblastic CAFs (myCAFs) are located in close proximity to tumor cells, while inflammatory CAFs (iCAFs) are located more distantly from tumor cells (Öhlund et al., 2017) (**Figure 1.3**). myCAFs are characterized by high expression level of α-smooth muscle actin (α-SMA), an activated fibroblast marker, and are responsible for remodelling of ECM. myCAFs can be both anti-tumor and pro-tumor (Ozdemir et al., 2014). Previous studies revealed that specific deletion of myCAFs in the stroma restricted the development of desmoplasia and tumor aggressiveness (Ozdemir et al., 2014) and high myCAF levels are often associated with poor PDAC diagnosis (Hu et al., 2022). In contrast to myCAFs, iCAFs lack α-SMA expression and are characterized by high expression of interleukin 6 (IL-6). iCAFs play a significant role in the immune regulation by interacting with immune cells, which contribute to immunotherapy resistance of cancer cells. Cancer cells release interleukin 1 (IL-1) that can reprogram iCAFs to produce cytokines and chemokines, such as IL-6, chemokine (C-X-C motif) ligand 1 (CXCL1), chemokine (C-X-C motif) ligand 12 (CXCL12), and chemokine (C-C motif) ligand 2 (CCL2), which enhance immune cell

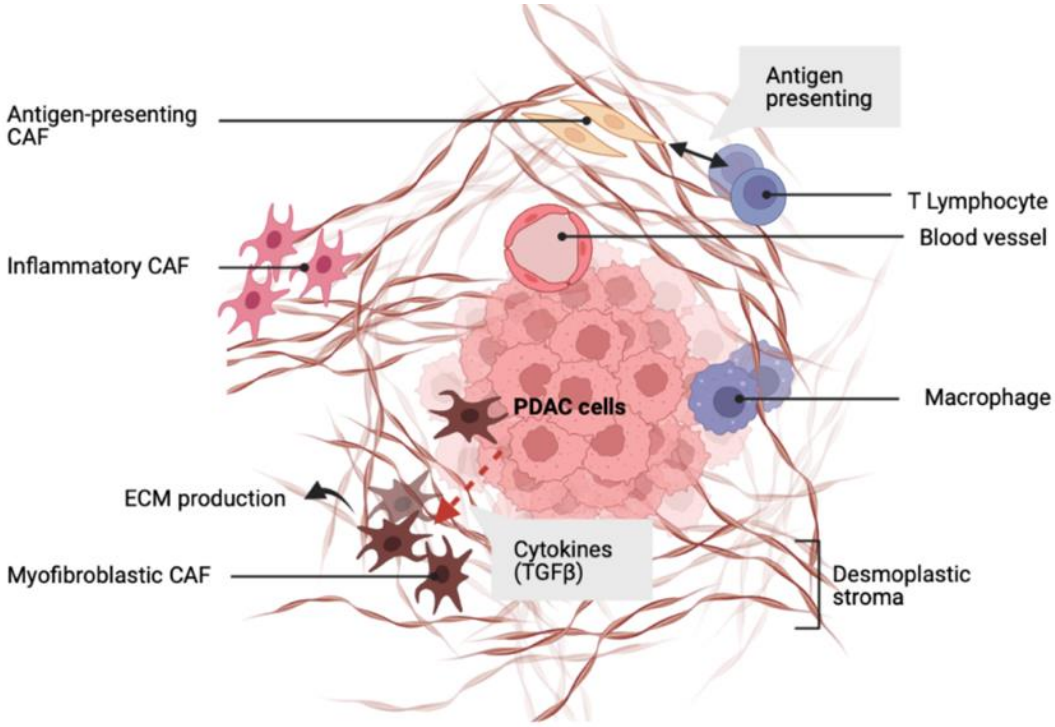
Antigen-presenting CAF
Antigen presenting
T Lymphocyte
Blood vessel
Inflammatory CAF
PDAC cells
Macrophage
ECM production
Cytokines (TGFβ)
Myofibroblastic CAF
Desmoplastic stroma

Figure 1.3 The tumor microenvironment in PDAC is composed of several different cell types. The TME is composed of PDAC tumor cells, inflammatory, myofibroblastic and antigen-presenting CAFs, T lymphocytes, macrophages, vasculature, and desmoplastic stroma. Cancer cells release cytokines and chemokines and interact with surrounding stromal cells through paracrine interaction to promote a microenvironment that favors the growth of tumor cells. ECM, extracellular matrix.

activation through paracrine interactions (Ohlund et al., 2014). PDAC with a higher iCAF abundance is often linked to more reprogrammed metabolism and a higher inflammatory state, suggesting a better response to immunotherapy (Hu et al., 2022). Most studies consider iCAFs as a protective factor against PDAC growth because high iCAF numbers are associated with better diagnosis. However, other studies suggest iCAFs favor cancer progression by synthesizing enzymes responsible for the production of hyaluronan (HA), a major component of the ECM that produces solid stress in PDAC tumor (Elyada et al., 2019).

Recently, genome-wide studies have identified a third CAF subtype termed antigen-presenting CAFs (apCAFs) based on single-cell RNA-seq (scRNA-seq) analysis. apCAFs are capable of expressing high level of major histocompatibility complex class II molecules (MHC II complex), which is able to present antigens to specific T cells (Huang et al., 2022). Therefore, apCAFs are hypothesized to induce immune suppression by inducing specific T cells into regulatory cells (Treg), which can inhibit the immune response in PDAC and contribute to tumorigenesis (Elyada et al., 2019; Huang et al., 2022).

CAFs are also responsible for promoting angiogenesis in PDAC. PDAC is a solid tumor with high interstitial fluid pressure and low microvascular density (MVD), resulting in hypoxic microenvironment. For aggressive tumorigenesis to occur, CAFs secrete angiogenic factors, including vascular endothelial growth factor (VEGF) and fibroblast growth factor (FGF), to induce formation of new blood vessels that provide more oxygen and nutrients and remove metabolic waste for better growth of cancer cells (Longo et al., 2016). In summary, CAFs play a role in tumorigenesis, metastasis, drug resistance, angiogenesis, and immunosuppressive phenotypes of PDAC, which can either be pro-tumorigenic or anti-tumor.

1.2.2 IMMUNE CELLS

Immune cells are essential components of the TME and affect the progression of PDAC (Mahajan et al., 2018). While PDAC develops, cancer cells are recognized as foreign by the immune system, resulting in immune cells infiltration and accumulation within the stroma. The crosstalk between immune cells and the TME is complicated, as immune cells

can supress or promote tumor growth depending on the context. The immune system generally has two types of cells: innate immune cells and adaptive immune cells. The innate immune response is a non-specific defence mechanism that detects and destroys tumor cells. Innate immune cells include macrophages, neutrophils, dendritic cells. The adaptive immune response involves cancer cell detection and destruction with specialized immune cells and antibodies. Adaptive immune cells include predominantly T cells, B cells, and natural killer (NK) cells.

The infiltration of tumor-associated macrophages (TAMs) is observed very early in the PDAC development (Feig et al., 2012). Cancer cells can reprogram macrophages by releasing cytokines, such as interleukin 4 (IL-4), and switch them from inflammatory M1 subtype to immune-suppressive M2 subtype, which has tumorigenic functions. TAMs support PDAC cell invasion and aggressiveness mainly by stimulating angiogenesis and inhibiting activation of anti-tumor T effector cells and NK cells (Borrego et al., 1998). Tumor-associated antigens (TAAs) activate T cells via MHC complex and, therefore, trigger enhanced anti-tumor immune responses. In the initial stages of PDAC, T lymphocytes are carried through blood vessels and migrate to small ducts to eliminate the abnormal PanIN cells. When the amount of activated T cells reaches a threshold, the regulatory T cells, or Tregs, become activated to negatively regulate the action of T cells (Tanaka, 2017). $CD8^+$ cytotoxic T cells are one of the subpopulations of T cells responsible for detecting abnormal TAAs and target cancer cells for destruction (Zamora et al., 2018). Cytotoxic T cells also contribute to tumor suppression by inhibiting angiogenic process. Therefore, the presence of cytotoxic T cells in the TME usually represent positive prognosis in PDAC patients (Tanaka, 2017). However, it is reported that $CD8^+$ tumor-infiltrating lymphocytes (TIL) can be inhibited by TAMs (Etzerodt et al., 2019). Cancer cells release TGF-β that promotes the proliferation of Tregs, which secrete immune-suppressive cytokines and result in fewer T effector cells infiltration in the TME. In this manner, Tregs restrict the immune response and is often associated with adverse prognosis (Tanaka, 2017).

1.3 EPIGENETICS

Research into the epigenomics of PDAC has revealed that PDAC initiation and progression is associated not only with genetic alterations, but also epigenetic changes that may play a critical role in cancer metastasis by regulating the expression of genes associated with tumor progression and survival (Thompson et al., 2015; Abukiwan et al., 2018). Three identified types of epigenetic regulations include DNA methylation, histone modifications, and noncoding RNAs (Ennis, 2014). These epigenetic processes result in reversible and heritable modifications to the chromatin, or within the DNA itself, which affects the expression of genes without changing the DNA sequence.

This is achieved by changing the chromatin structure surrounding genes and regulating accessibility to the promoter region (Shen & Laird, 2013). The crosstalk between epigenetic factors and major signaling pathways associated with cell proliferation and apoptotic control may have implications in the development of PDAC (Lomberk et al., 2015). There is evidence suggesting dysregulation of epigenetic pathways normally contributes to the tumorigenesis of cancer (Paradise et al., 2018). PDAC usually involves deregulation of several epigenetic regulators, including methyltransferases, Enhancer of Zeste Homolog 2 (EZH2), and histone deacetylases (HDACs) (Chan-Seng-Yue et al., 2020). Understanding the epigenomics of PDAC and its extensive control over cancer-related genes may help broaden anti-cancer therapeutic options in PDAC.

1.3.1 DNA METHYLATION

DNA methylation is the addition of a methyl group to the 5' carbon of cytosines mediated by DNA methyltransferases (DNMTs), forming 5-methylcytosine (5mC) (Abukiwan & Berger, 2018). This epigenetic reaction occurs mainly at CpG islands, which are genomic regions where C and G bases appear at a higher frequency than predicted and are usually located in the gene promoter regions. Methylation of CpG islands at promoter region interferes with the transcription of the gene, reducing access and, therefore, suppressing gene expression (Antequera & Bird, 1999). DNA methyltransferase 1 (DNMT1), DNMT3A and DNMT3B are major enzymes catalyzing methylation of DNA. DNMT3A

and DNMT3B facilitate de novo DNA methylation, while DNMT1 is responsible for the maintenance of parental methylation patterns (Cheng et al., 2008; Abukiwan & Berger, 2018). Excessive DNA methylation of several genes due to DNMT1 overexpression was detected in 81% of PDAC patients, while less than 4% of healthy individuals presented DNA methylation on these genes in the pancreas (Brancaccio et al., 2019). Silencing of key tumor suppressor genes as a result of DNA methylation is believed to contribute to tumorigenesis of PDAC (Tan et al., 2009). Interestingly, a recent study revealed that not only cancer-associated genes, but also DNMTs themselves are differentially methylated in PDAC (Vincent et al., 2011).

1.3.2 MICRORNA

MicroRNAs (miRNA) are small noncoding, single strand-RNA molecules consisting of 20-23 nucleotides. One of the major mechanisms by which miRNAs regulate gene expression is by binding to the untranslated region of mRNAs and lead to its degradation of reduced translation (Ambro, 2004). In healthy cells, miRNAs are responsible for regulating the expression of about 60% protein coding genes involved in cell differentiation, proliferation, and apoptosis (Winter et al., 2009). The machinery of miRNA has been implicated in physiological and pathological development of various cancers (Abukiwan & Berger, 2018). Many PDAC studies have revealed that miRNAs are dysregulated in the presence of oncogenic KRAS, resulting in increased expression of pro-oncogenes or prohibited expression of tumor suppressor genes (Yonemori et al., 2017). In general, miRNAs mainly have two distinct roles in PDAC, one as tumor suppressors (TSmiRs), and the other as oncogenes (OncomiRs) (Kunej et al., 2012; Abukiwan & Berger, 2018). On the other hand, mutant tumor suppressor genes such as *p53* can also downregulate miRNA transcription, resulting in increased cancer cell proliferation and survival (Sohn et al., 1997; Zhang et al., 2010).

1.3.3 HISTONE MODIFICATIONS

Histone modifications regulate gene transcription by affecting the structure of chromatin, whose basic unit is the nucleosomes (Abukiwan & Berger, 2018). Each nucleosome

consists of a small region of DNA (147 base pairs) wrapped around an octamer of eight histone proteins – two each of H2A, H2B, H3, and H4 (Audia & Campbell, 2016). There are many histone modifications including methylation, acetylation, phosphorylation, and ubiquitination, all of which correlate to specific outcomes on gene expression.

Histone methylation is a reversible modification of chromatin where methyl groups are added to the histone tail by histone methyltransferases (HMTs) or removed by histone demethylase (HDMs) (Hyun et al., 2017). Histone methylation usually occurs on the residues of arginine, lysine, and histidine, while lysine alterations are the most common modification in PDAC (Abukiwan & Berger, 2018). Methylation of lysine residue is coordinated by histone lysine methyltransferases (KMTs), which can either be associated with transcriptional repression (H3K9, H3K27, and H3K20 trimethylation) or activation (H3K4, H3K36, and H3K79 trimethylation) of genes (Abukiwan & Berger, 2018). Among KMTs, one of the subfamilies termed EZH2 is a H3K27me3-specific histone lysine methyltransferase (HKMT), able to transfer up to three methyl groups to this residue (Black et al., 2012). Increased expression of EZH2 occurs in many solid cancers, including PDAC, and is believed to have effects on the malignancy of PDAC (Wang et al., 2015; Abukiwan & Berger, 2018).

Histone acetylation is a process by which the lysine residues from the histone are acetylated with an acetyl group by histone acetylases (HATs) or deacetylated by histone deacetylases (HDAC) (Abukiwan & Berger, 2018). Lysine acetylation results in relaxation of chromatin structure and make the DNA accessible to transcription factors (Grunstein, 1997). The balance between histone acetylation and deacetylation is a key in regulating critical gene expression in cells, and unbalanced activity of these enzymes may result in malignant transformation and tumorigenesis in PDAC (Schneider et al., 2011). Recent studies showed a role of HDACs/HATs in the activation of expression of many tumor suppression genes, and the hyperactivation of HDACs is associated with cancer cell proliferation and impaired cell apoptosis regulation (Sato et al., 2004; Haefner et al., 2008).

1.4 ENHANCER OF ZESTE HOMOLOGUE 2 (EZH2)

Numerous studies have revealed that in addition to genetic alterations, abnormal epigenetic regulation is also a determinant of tumorigenesis of various cancers (Thompson et al., 2015; Abukiwan et al., 2018). The aberrant expression of a widely known epigenetic regulator, enhancer of zeste homologue 2 (EZH2), has been implicated in the tumorigenesis of PDAC using transgenic mouse model and human PDAC samples (Patil et al., 2020).

EZH2 is a histone methyltransferase encoded by the *EZH2* gene, located at chromosome 7q35 in human genome, and contains 20 exons with 746 amino acid residues (Cardoso et al., 2000). EZH2 is a key member of the polycomb group (PcG) protein family. PcG is a group of proteins that determine cell fate mainly by epigenetically repressing transcription of genes involved in differentiation and proliferation. PcG proteins form two core complexes, polycomb repressive complexes 1 and 2 (PRC1 and PRC2) (Sauvageau & Sauvageau, 2010). They both play a crucial role in transcriptional suppression of genes through histone tail modification and subsequent chromatin compaction (Duan et al., 2020). Specifically, PRC2 is responsible for mono-, di- and tri-methylation of histone 3 at lysine 27 (H3K27me2/3), while PRC1 monoubiquitylates lysine 119 of histone H2A (H2AK119ub) (Cao et al., 2002; Pengelly et al., 2013). PRC2 is highly conserved in various animals and plants in terms of its function (Chica et al., 2017). PRC2 composed of four main subunits including EZH2, embryonic ectoderm development (EED), suppressor of zeste 12 homolog (SUZ12), and retinoblastoma-binding protein 4/7 (RBBP4/7) (O'Meara, 2012; **Figure 1.4**). PRC2 performs its function mainly through the core enzymatic subunit EZH2, which catalyzes trimethylation of H3K27 in the cell nucleus and leads to transcriptional silencing of target genes (Völkel et al., 2015). The EZH2 protein has five domains, EED-interaction domain (EID), homologous domain I, homologous domain II, cysteine-rich domain (CXC domain), and SET domain (Laible et al., 1997). The evolutionally conserved SET domain consists of 130-140 amino acids and was initially recognized in and derived from three *Drosophila* proteins: the suppressor of variegation 3-9 (**S**u(var)3-9), the Enhancer of zeste (**E**(z)), and the trithorax-group chromatin regulator trithorax (**T**rx) (Yao et al. 2016; Nutt et al., 2020). The SET domain maintains histone methyltransferase activity of EZH2, and this enzymatic process is facilitated by the CXC

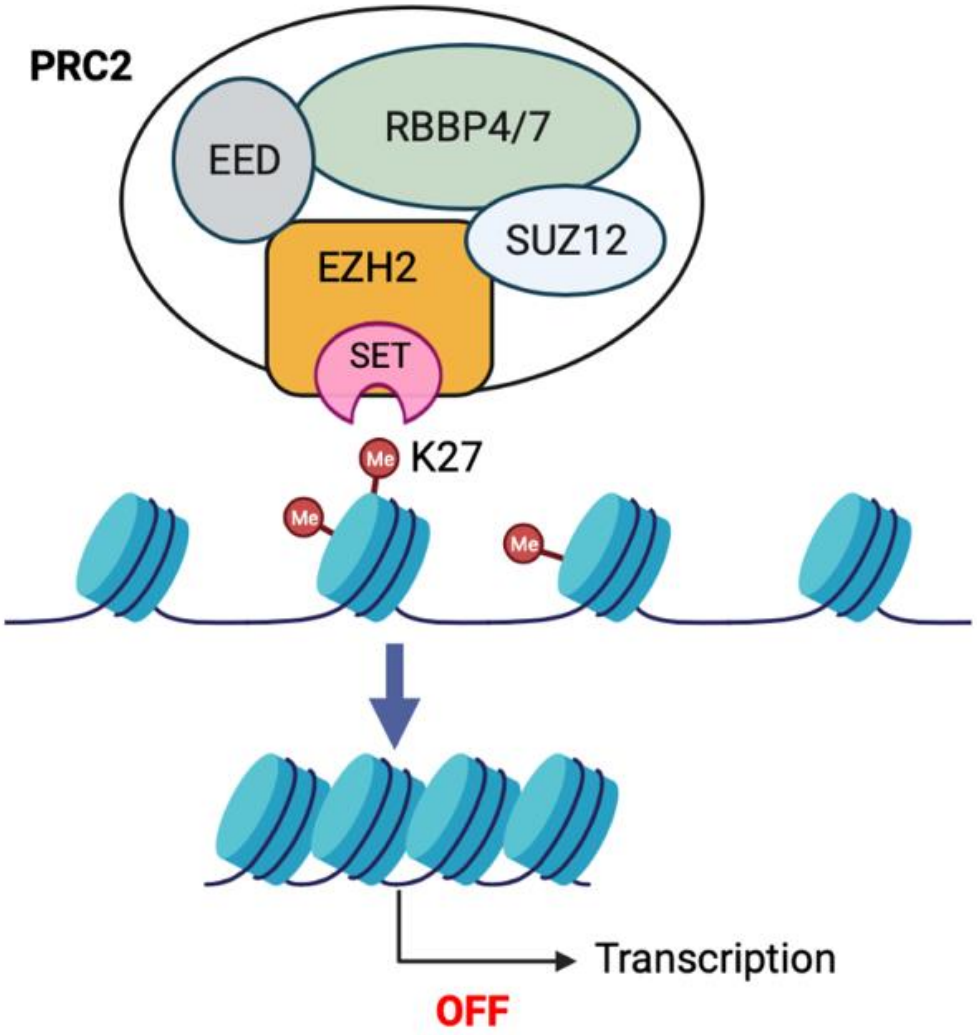
PRC2
EED
RBBP4/7
SUZ12
EZH2
SET
Me
K27
Me
Me
Transcription
OFF

Figure 1.4 Model of the PRC2 complex. Enhancer of Zeste Homologue 2 (EZH2) interacts with Suppressor of Zeste 12 (SUZ12) and embryonic ectoderm development (EED) to form the Polycomb repressive complex 2 (PRC2). EZH2 has a SET domain which serves as the methyltransferase for PRC.

domain N-terminal that helps assemble all subunits for proper PRC2 function (Simon et al., 2008). EZH2 has a close homolog, EZH1, which also acts as a methyltransferase of H3K27 and forms an alternative PRC2 with EED and SUZ12. Despite the similarities between EZH1 and EZH2, they function independently of each other and have distinct activities and expression patterns. EZH1 expression is detected in both normal cells and cancer cell lines, while EZH2 is primarily highly expressed in proliferating cells. The PRC2 complex with EZH2 shows considerably higher methyltransferase activity compared to the EZH1-containing PRC2 complex (Margueron et al., 2008).

1.4.1 MECHANISMS OF EZH2

EZH2 has both canonical and non-canonical roles in supressing transcription of target genes. PRC2-dependent H3K27me3 is the major canonical pathway of gene silencing mediated by EZH2 (Patil et al., 2020). In normal condition, the methyltransferase function of EZH2 is facilitated by EED and SUZ12, the other two core subunits of PRC2. When the PRC2 complex is assembled, EED can recruit PRC2 to H3K27 sites at promoter regions of target genes and stimulate the methyltransferase activity of EZH2. SUZ12 helps maintain the integrity of the PRC2 complex and stabilizes EZH2 activity (Cao & Zhang., 2004). Once PRC2 is recruited to the chromatin, the SET domain catalyzes successive methyl transfers that yield mono-, di- or trimethylated lysine, each has distinct functions (Zee et al., 2010).

Most H3K27 residues are dimethylated in cells, while only 15% regions are trimethylated. Although H3K27me2 mainly serves as a substrate for further EZH2-mediated trimethylation, it also prevents histone tails from being acetylated, which normally antagonizes the silencing effect of EZH2 (Tie et al., 2009). H3K27me3 is a stable chromatin mark associated with repression of gene expression, normally associated with cell fate determination and development (Yin et al., 2019). H3K27me3 acts as a docking site for recruiting chromosomal regulators that results in changes in chromatin structure, which facilitate chromatin compaction and eventually promote transcriptional silencing of downstream genes (Wang et al., 2016). Recent studies revealed that polymerase (Pol) II is found in H2K27me enriched promoters with a low transcription level detected, suggesting

RNA Pol II-mediated transcription elongation could be paused due to chromatin structure changes (Stock et al., 2007; Zhao et al., 20017). In general, the major role of EZH2 in cells is to repress tumor suppressor genes through H3K27me3 and regulate cell proliferation, apoptosis, and cell cycle (Huang et al., 2021).

Numerous studies have also revealed non-canonical roles of EZH2 (He et al., 2012; Lee et al., 2012). This includes non-histone protein methylation, which can either be performed in a PRC-dependent or -independent fashion (He et al., 2012). Increasing evidence suggests EZH2 can induce methylation on multiple non-histone substrates, including transcription factors and chromatin-associated proteins. Specifically, proteins with a similar sequence to the methylated domain of H3K27, which is termed the amino acid sequence R-K-S, can be directly methylated on the lysine residue by EZH2 (Lee et al., 2012). However, the biological consequences of non-histone methylation by EZH2 are context dependent.

EZH2 can also mediate PRC2-independent gene transactivation. Protein kinase B phosphorylates EZH2 in serine 21 (Ser21). Phosphorylated EZH2 directly methylates multiple transcriptional factors independently of the PRC2 complex. For instance, EZH2 activates the signal transducer and activator of transcription 3 (STAT3) signaling pathway by methylating STAT3 (Kim et al., 2013). In castration-resistant prostate cancer (CRPC), EZH2 is capable of methylating androgen receptor (AR) and promoting downstream gene transcription and tumor growth (Xu et al., 2012). EZH2 can directly bind to the promoter region of target genes as a transcription factor. For example, EZH2 can bind to the promoter of transcription factor RelB and activate expression, which helps maintain the self-renewal of breast cancer tumor-initiating cells (Laurence et al., 2016). However, evidence suggest noncanonical EZH2 activities are more evident in cancers, especially when EZH2 is overexpressed (Xu et al., 2015)

Through the three distinct mechanisms mentioned above, EZH2 is capable of regulating various signaling pathways involved in cell cycle, apoptosis, DNA damage repair, and cell fate determination (Nutt et al., 2020; He, 2016). Due to the dramatic functions of EZH2 in various biological processes within the cell, alterations in EZH2 activity can be related to

many cancers, including PDAC. Hence, elucidating the role of EZH2 in the initiation and development of PDAC becomes important for potential therapy development.

1.4.2 IMMUNE MODULATORY FUNCTION OF EZH2

In vitro studies revealed that EZH2 enhances PDAC cancer cell proliferation in cell culture. However, EZH2 plays an opposing role as a suppressor of pancreatic carcinogenesis in mouse models in vivo, indicating that tumor microenvironment may affect the role of EZH2 (Ougolkov et al. 2008; Mallen-St Clair et al., 2012). Oncogenic activation of EZH2 mediates aberrant epigenetic changes not only in pancreatic tumor cells but also immune cell populations, leading to alterations in expression of critical genes involved in cell fate determination and immune dysfunction in the PDAC TME (Chiappinelli et al., 2016). Increasing evidence suggest that, in addition to regulating pancreatic cell plasticity, EZH2 plays an important role in mediating cellular pathways involved in immune invasion and resistance of PDAC cells (Chiappinelli et al., 2016; Jones et al., 2019). Dysregulation of EZH2 function has been observed in many tumor-infiltrating immune cells in the TME including T cells, Tregs, and TAMs and chronic changes in the epigenetic landscape due to EZH2 were widely demonstrated in $CD8^+$ and $CD4^+$ T cells (He et al., 2017). EZH2 promotes the survival and proliferation of effector T cells, while low EZH2 levels in T cells normally leads to poor prognosis (Karantanos et al., 2016). In the PDAC TME, however, the percentage of T cells expressing EZH2 is much lower than in normal tissues, suggesting cancer cells may block the expression of EZH2 in T cells to restrict T cell-mediated immunity (He et al., 2017). Inhibition of EZH2 activity caused repressed function of tumor-specific effector T cells and therefore favors immune suppression and tumor metastasis (Zhao et al., 2016). Tregs are known to negatively affect anti-tumor immunity in PDAC by controlling effector T cell activity (Adeegbe & Nishikawa, 2013). Tumor cells can release factors that convert $CD4^+$ T cells into Tregs. EZH2 is upregulated in activated Tregs (Wang et al., 2018). Epigenetic changes mediated by EZH2 is found essential for the recruitment of tumor-infiltrating Tregs and the repression of immune-mediated tumor control (Wang et al., 2018; Curiel et al., 2004). Taken together, these results demonstrate that EZH2 may have various effects on immune cell populations and associated tumor progression and the consequences are context dependent.

1.4.3 ALTERATIONS OF EZH2 IN PDAC

EZH2 plays a critical role in mediating H3K27me3 through the canonical pathway, inducing transcriptional silencing of regulatory genes involved in cell differentiation, lineage specification, and tissue renewal (Mallen-St Clair et al., 2012). Therefore, alterations of EZH2 activity and function have been implicated in various cancer pathologies, including PDAC (Völkel et al., 2015). In particular, overexpression of EZH2 is frequently correlated with advanced human PDAC progression and poor prognosis, making EZH2 a potential target for anti-cancer therapy (Kim et al., 2015). In PDAC, EZH2 is important in regulating acinar cell reprogramming and tumorigenesis. EZH2 is regularly overexpressed in about 68% of human PDAC cases, while almost 90% progressive PDAC cells accumulate EZH2 in the nucleus (Ougolkov et al., 2008).

Although pancreatic regeneration from injury is largely dependent on acinar cell re-differentiation promoted by EZH2-mediated transcriptional silencing of various genes, overexpression of EZH2 can switch tumor suppressor genes off, thus promoting oncogenic factors for cell proliferation and metastasis. Therefore, excessive EZH2 expression and activity in the pancreas is often linked to advanced stages of pancreatic tumorigenesis and progression toward invasive PDAC (Versemann et al., 2022). In the initial stages of the carcinogenesis, however, EZH2 is transiently upregulated to facilitate pancreatic tissue regeneration. Loss of EZH2 at early stage leads to uncontrolled expansion of proliferative acinar cells and acceleration of *KRAS*-driven PDAC progression (Mallen-St Clair et al., 2012). In addition to acinar cells, human embryonic stem cells with EZH2 deficiency showed compromised self-regeneration and lack of cell differentiation (Collinson et al., 2016). Chen et al (2017) demonstrated EZH2 can transcriptionally repress the calcium/calcineurin-responsive *nuclear factor of activated T cell* (*NFATc1*) gene, which encodes for a key transcription factor responsible for malignant transformation of cells and enable redifferentiation and regeneration of acinar cells. However, constitutive activation of *KRAS* oncogene can invert EZH2-mediated effects on many intracellular signaling pathways, which serves to transcriptionally activate instead of repressing genes associated with cell differentiation and proliferation (Chen et al., 2017).

KRAS-signaling has been shown to have profound effects on EZH2 function and activity (Mallen-St Clair et al., 2012; Chen et al., 2017). *KRAS*-mediated PDAC is often accelerated by deletion of EZH2. In previous studies, Chen et al. (2017) suggested the presence of EZH2 resulted in a slight decrease in the level of pancreatic lesions in pancreas of 2-3 months old mice in the context of $KRAS^{G12D}$ hyperactivation. In 6-month-old mice, however, the loss of EZH2 results in decreased level of pancreatic carcinogenesis and PanIN lesions (Chem et al., 2017). Conversely, Mallen St Clair et al. (2012) showed EZH2 is required for tissue repair by promoting gene expression involved in cell regeneration and proliferation, impaired acinar cell regeneration and enhanced $KRAS^{G12D}$-driven neoplasia (Mallen-St Clair et al., 2012). These contradictory findings may suggest flaws in the mouse models used or distinct, temporal roles for EZH2 in *KRAS*-mediated PDAC progression.

1.5 RATIONALE, HYPOTHESIS AND OBJECTIVES

Rationale: Although progress has been made to understand the role of EZH2 in PDAC progression, the exact molecular mechanisms underlying the effects of EZH2 on *KRAS*-driven PDAC are largely unknown. Therefore, further investigation is required to identify specific roles of EZH2 in the context of *KRAS*-mediated PDAC. In previous studies, EZH2 deletion occurred at early stages of pancreatic development, which may affect the differentiation status of the cells. In addition, the Cre driver used was targeted to the *Ptf1a* locus, which makes these mice haplo-insufficient for PTF1A, which may also affect acinar cell gene expression. In this study, EZH2 will be deleted in adult pancreatic tissues after acinar cells are fully mature.

Hypothesis: *I hypothesize that EZH2 restricts KRAS-driven initiation of PDAC in acinar cells in response to injury.*

Objectives:

1. Determine if loss of EZH2 after acinar cell differentiation enhances *Kras*-driven PanIN formation following pancreatic injury in vivo
2. Determine whether the acinar-specific loss of EZH2 increases KRAS-mediated ADM in an ex vivo culture.

2 CHAPTER 2: MATERIALS AND METHODS

2.1 MOUSE STRAINS AND HANDLING

All procedures and methods of mouse colony maintenance and mouse handling were approved by the University of Western Ontario Animal Care Committee (Protocols 2020-157 and 2020-158). Mice were housed in a pathogen-free facility with abundant food and water supply and exposed to a 12-hour light/dark cycle under guidelines approved by the Canadian Council for Animal Care. Mice carrying *creERT* targeted to the *Mist1* allele (*Mist1*$^{+/creERT}$) were generated to allow for inducible acinar cell-specific gene deletion through the *cre-LoxP* system. *CreERT* is activated by tamoxifen and allows *cre* recombinase to translocate to the nucleus, where it recognizes specific DNA sequences called *loxp* sites and deletes the DNA sequence between *loxp* sites (Johnson et al., 2004). *Mist1*$^{+/creERT}$ mice were bred with mice containing an *EZH2* allele with the SET domain (exons 16-19) flanked by loxP sites (*Ezh2*$^{\Delta SET}$) and/or mice containing a constitutively active KRAS^{G12D} allele downstream of *loxp* sites flanking a stop codon within the endogenous *KRAS* allele (lox-stop-lox; LSL, *KRAS*$^{LSL\text{-}G12D/+}$ mouse). The resulting lines include *Mist1*$^{creERT/+}$*KRAS*$^{LSL\text{-}G12D/+}$*Ezh2*$^{\Delta SET/\Delta SET}$ (referred to as *KRAS*$^{LSL\text{-}G12D/+}$*Ezh2*$^{\Delta SET}$ or KE), *Mist1*$^{creERT/+}$*KRAS*$^{G12D/+}$, and *Mist1*$^{creERT/+}$*Ezh2*$^{\Delta SET/\Delta SET}$ (**Figure 2.1**). Genotypes of mice were determined at time of weaning and confirmed after experiments through PCR (polymerase chain reaction) of DNA obtained from ear punches using gene-specific primers shown in Table 2.1. All experiments were carried out with adult mice (2-4 months) from *Mist1*$^{+/creERT}$*KRAS*$^{G12D/+}$*Ezh2*$^{\Delta SET}$ mouse strain on a C57Bl6 background.

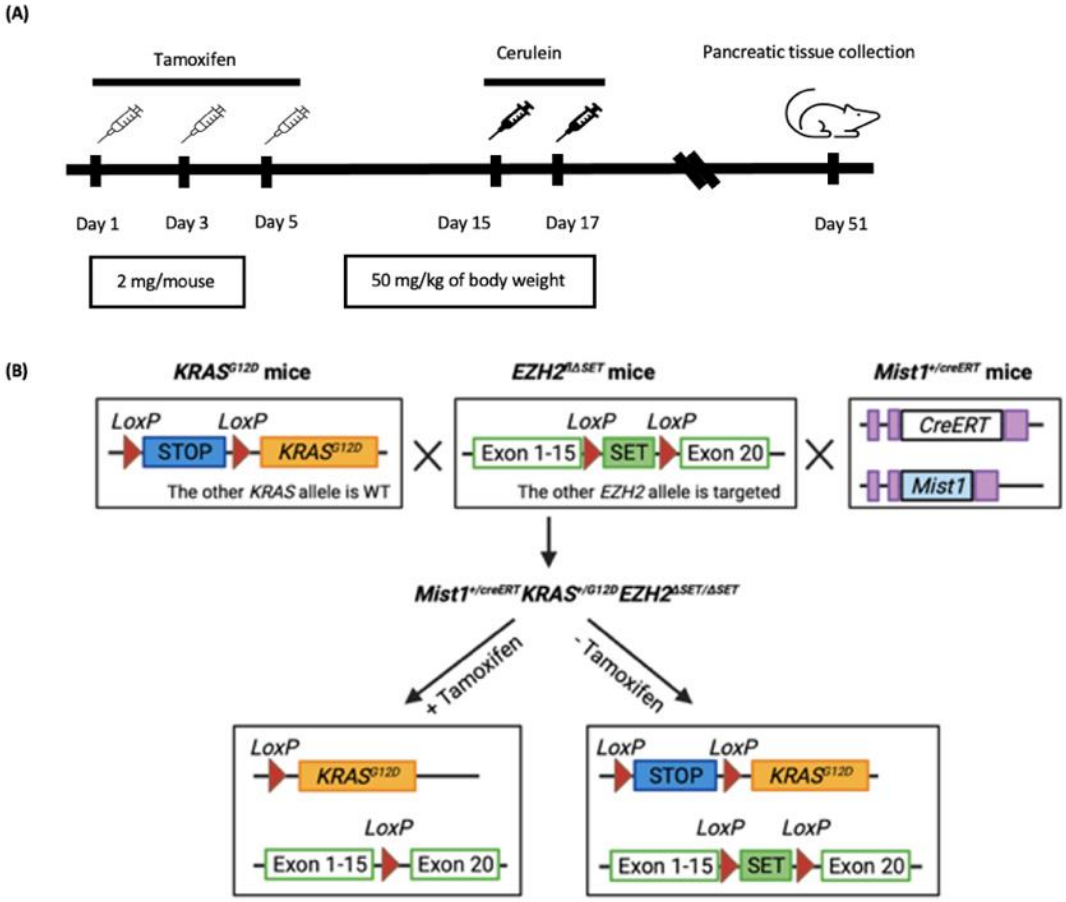
(A)
Tamoxifen
Cerulein
Pancreatic tissue collection
Day 1
Day 3
Day 5
Day 15
Day 17
Day 51
2 mg/mouse
50 mg/kg of body weight
(B)
KRASG12D mice
EZH2flΔSET mice
Mist1+/creERT mice
LoxP
STOP
KRASG12D
The other KRAS allele is WT
Exon 1-15
SET
Exon 20
The other EZH2 allele is targeted
CreERT
Mist1
Mist1+/creERT KRAS+/G12D EZH2ΔSET/ΔSET
+ Tamoxifen
- Tamoxifen

Figure 2.1 Generation of triple-transgenic mice and the experimental timeline. (A) Schematic experimental timeline of cerulein-induced acute pancreatic injury model and time points at which tamoxifen and cerulein were administered. Tamoxifen was given in three doses as indicated in 2 mg per mouse each time. Cerulein was administered through eight hourly intraperitoneal (IP) injections of 50 mg/kg of body weight **(B)** Schematic representation of the transgenic lines and how $KRAS^{G12D}$ and $EZH2^{DSET}$ were generated by expressing an inducible cre recombinase from the Mist1 gene in acinar cells following tamoxifen exposure. The SET domain is encompassed by exons 16-19 on the EZH2 allele.

Table 2.1 DNA primers used for genotyping

Gene	WT/Mutation	Forward	Reverse	Amplicon Length
Mcre	WT	5'-GGTTTAAGCAAATTGTCAAGTACGG 3'	5'-GAAGCATTTTCCAGGTATGCTCAG 3'	720 bp
	Cre-ERT	5'-ATAGTAAGTATGGTGGCGGTCAGCG 3'	5'-GAAGCATTTTCCAGGTATGCTCAG 3'	520 bp
KRAS^{G12D}	WT	5'-GTCTTTCCCCAGCACAGTGC 3'	5'-AGCTAGCCACCATGGCTTGAGTAAGTCTGCA 3'	650 bp
	G12D	5'-CTCTTGCCTACGCCACCAGCTC 3'	5'-AGCTAGCCACCATGGCTTGAGTAAGTCTGCA 3'	550 bp
Ezh2	WT/ΔSET	5'-AGACCCCTGGGGCTTAATCT 3'	5'-CCAAGACAGGCTCTTGAGGG 3'	523 bp (WT) 563 bp (ΔSET)

2.2 TAMOXIFEN ADMINISTRATION AND CERULEIN-INDUCED PANCREATITIS

Tamoxifen (Sigma-Aldrich, St. Louis, MO, #T5648) was prepared in ethanol (Commercial Alcohols) and corn oil (Sigma-Aldrich, St. Louis, MO, #C8267) on the day of the first oral gavage administration. Tamoxifen was re-suspended in 4 ml corn oil and each mouse received one ml (2 mg/mouse/day) every other day over 5 days using a 1 ml syringe and a gavage needle (20G 1''x2.25mm, SIGMA, St. Louis, MO). *Cre*-recombinase efficiency using this methodology is >95% (Johnson et al., 2012).

Cerulein (MedChemExpress, London, UK, #FI-6934) was freshly prepared from powder to reach a final concentration of 10 μg/ml. Stock cerulein was stored at -20 °C. 15 and 17 days after the first dose of tamoxifen, mice received eight hourly intraperitoneal injections of cerulein (50 μg/kg body weight in saline) to induce acute pancreatic injury (Carrière et al., 2009). Control mice received a similar volume of 0.9% saline. Mice were weighed every other day to monitor weight changes and health until sacrificed for the downstream experiments.

2.3 TISSUE FIXATION AND HISTOLOGY

Mice were sacrificed five weeks after the first cerulein injection. The complete pancreas was immediately harvested from each mouse and weighed. The head and tail of the pancreas were placed in tissue cassettes and fixed in 4% formaldehyde for at least 24 hours at 4 °C. Tissues were rinsed in phosphate buffered saline (PBS) post fixation before being dehydrated and embedded in paraffin blocks. Tissue blocks were sectioned at 5 μm thickness on a Microtome (ThermoFisher Scientific, Waltham, MA), and 2-4 sections were mounted onto glass microscope slides to prepare for use in the downstream staining.

Tissue sections were stained using several histological techniques including hematoxylin and eosin stain (H&E), Periodic acid–Schiff (PAS), Alcian Blue stain (AB), and picrosirius red stain. For all staining methods, tissue sections were de-waxed in xylene (3 x 5 min) and rehydrated in a series of ethanol (100% ethanol 2 x 2 min, 90% ethanol 2 x min, 70%

ethanol 2 x 2 min) followed by tap water for 5 min and distilled water for 1 min. After staining, sections were dehydrated in 70% ethanol (2 x 30 sec), 90% ethanol for 1 minute, 100% ethanol (2 x 3 min), and xylene (3 x 5 min). Sections were coverslipped with permount (ThermoFisher Scientific, Waltham, MA, #SP15500) and stored in a slide box at room temperature for the downstream histological analysis.

To assess general histology of mouse pancreatic tissues, sections were subjected to H&E staining. Sections were immersed in CAT Hematoxylin (Biocare Medical, #CATHE-M) for 2 minutes and then washed in running tap water for 30 seconds. Sections were placed in freshly filtered Tacha's Bluing Solution (Biocare Medical, #HTBLU-M) for 30 seconds followed by running tap water for 10 minutes. Finally, sections were dipped in freshly filtered Eosin Y three times, immediately followed by dehydration and mounting. Whole slide scanning and analysis was performed using the Aperio ScanScope (Leica Biosystems Imaging Inc.). Pancreatic lesions were identified and graded based on the extent of acinar cell differentiation, nuclear irregularities, and tissue fibrosis. Scoring of tissue damage such as ADM, PanIN, inflammation and fibrosis was done by Dr. Liena Zhao. The percentage of lesion area verses total tissue area was quantified using Aperio ImageScope software (Leica Biosystems Imaging Inc.). For each genotype, slides obtained from 5-7 different samples that contain the head and tail of the pancreas were assessed, and 10-15 representative images were taken from each sample using a Leica Microscope (Leica Microscope DM5500B, Leica Microsystems, Wetzlar, Germany).

To measure the frequency and grade of preneoplastic lesions, tissue sections were stained using standard Alcian Blue (AB) stain (Abcam Inc., Cambridge, UK, ab150662) for the assessment of acidic mucins. Deparaffinized slides were incubated in acetic acid for 3 minutes and then in Alcian Blue pH 2.5 solution (Abcam Inc., Cambridge, UK, ab150662) for 30 minutes at room temperature. After a few washes, sections were stained in Nuclear Fast Red Solution (Abcam Inc., Cambridge, UK, ab150662) for 5 minutes. To detect glycogen deposits in mucinous structure, Periodic Acid Schiff (PAS) staining (Sigma-Aldrish Inc., St. Louis, MO, #3952) was performed. For each genotype, 5 slides from different samples that contain the head and tail of pancreas were stained. The positive

staining lesions (blue for AB and red for PAS) were identified and quantified as a percent of the total amount of lesions using ImageJ (National Institutes of Health, Maryland, USA).

2.4 IMMUNOHISTOCHEMISTRY

After de-paraffin and rehydration, tissue sections were incubated in antigen retrieval buffer (100X citrate buffer pH 6.0) and put in a steamer for 45 minutes. Sections were cooled to room temperature for 20 minutes. Sections were immersed in 3% H_2O_2 in methanol to remove endogenous peroxidase activity followed by incubation in cell permeation reagent (0.2% Triton-100 in PBS) for 12 minutes and washing in phosphate-buffered saline/tween (PBST) (0.2% Tween-20 in PBS) for 5 minutes. To prevent non-specific binding of antibodies to the tissue, sections were incubated in blocking solution (1.5% sheep serum in PBS) for 1 hour at room temperature in a wet chamber. Sections were incubated in primary antibodies diluted at recommended ratio in blocking solution overnight at 4 °C. Table 2.2 shows information about antibodies used and corresponding dilution ratio, sources, and species. On the second day, sections were incubated in biotinylated secondary antibody (diluted 1:200 in blocking solution) for 30 minutes at room temperature followed by washing in PBST for 6 minutes and PBS for 4X 6 minutes. IHC was developed using VECTASTAIN rabbit ABC staining kit and DAB peroxidase substrate (Vector Laboratories, SK-4105).

Analysis of acinar cell dedifferentiation and transdifferentiation was performed using ImageJ. The expression of biomarker of acinar cells (amylase) and duct cells (CK19) was visualized as brown stain in histologically relevant area of mouse pancreatic tissues. Quantification of DAB signals was done using the threshold method in ImageJ, which can selectively calculate the brown signal as the percent of total tissue area by adjusting the threshold. The extent of immune cell infiltration in the stromal area was determined using the Aperio ImageScope software. Positive immune cells were manually counted and were divided by the total lesion area. Whole tissue images and representative images (10-15 images obtained per sample) of the lesion area were obtained with the Aperio ScanScope and Leica Microscope, respectively.

Table 2.2 Antibodies used for IHC

Antibody	Species	Source	Catalog #	Dilution
CK19	Rabbit	Abcam	Ab15463	1:200
AMYLASE	Rabbit	Cell Signaling	4017	1:400
CD3	Rabbit	BD Biosciences	560591	1:200
CD8	Rabbit	ThermoFisher	98941	1:200
F4/80	Rabbit	Abcam	Ab111101	1:100
VIMENTIN	Rabbit	Cell Signaling	5741S	1:400
α-SMA	Rabbit	Cell Signaling	19245	1:200
C3	Rabbit	ThermoFisher	ab111101	1:200

2.5 ACINAR CELL CULTURE

Mice of each genotype, WT, *Ezh2*$^{\Delta SET}$, *KRAS*^{G12D}, *KRAS*^{G12D}*Ezh2*$^{\Delta SET}$ were sacrificed three weeks after the first tamoxifen injection, and the pancreas was harvested and washed in ~10 ml of 1xPBS in a 15 ml falcon tube on ice. 1 ml of collagenase (1 mg/ml) and ~50 ml of HEPES (4-(2-hydroxyethyl)-1-piperazineethanesulfonic acid) buffer was pre-warmed to 37 °C in a shaking water bath. Pancreatic tissues were transferred into a clean weigh boat without solution. Tissues were injected with 1 ml collagenase using a 1 ml syringe and 25- or 27-gauge needle, then immediately incubated in collagenase solution in 2 ml tubes in 37^{o}C shaking at 75 rpm for 12 minutes. Then tissues were transferred to 50 ml tubes with 6-7 ml DMEM (Dulbecco's Modified Eagle Medium) and vigorously resuspended to break up clumps of tissue into cells. Once clumps were sufficiently dispersed and the solution was cloudy, cell suspensions were gently pipetted through a pre-wetted 70 um nylon mesh into a 50 ml falcon tube. Cells were centrifuged at 200g in centrifuge (Eppendorf Canada, #5804R) for 1 minute and collected at bottom of tube.

Acinar cells were incubated in 48-well plates with freshly made acinar cell culture media containing DMEM/ F12 Medium (Gibco, Invitrogen, Carlsbad, CA), 10% fetal bovine serum (FBS), 0.04 mg/ml Soybean Trypsin Inhibitor (STI), and 0.1% dexamethasone. Collagen type I and acinar cell culture media were mixed at a proportion of 1:1, with a small volume (1:20 dilution) of 0.25 M NaOH to adjust the pH. Approximately 2500 acinar cells were mixed with 100 ul of the mixture and were plated at the bottom of the well. Cells were monitored at a daily basis and media was changed every other day.

2.6 RNA ISOLATION AND RNA -SEQ ANALYSIS

RNA was extracted from mouse pancreatic tissues using Trizol (Invitrogen) following Pure link kit (Invitrogen) manufacturer's protocol. To obtain RNA, tissue samples were mechanically homogenized immediately following dissection. Three replicates were obtained for *KRAS*^{G12D} and *KRAS*^{G12D}*Ezh2*$^{\Delta SET}$ groups. RNA from each sample was subjected to paired-end sequencing with Illumina TruSeq Stranded Total RNA kit.

To perform RNA-seq analysis, reads were aligned to the mouse reference genome mm10 (GRCm38) and sorted by coordinate using STAR v2.7.9a (Dobin et al., 2013). Gene counts were generated using featureCounts function of the Subread v2.0.3 aligner (Liao et al., 2014). Differential expression analysis was performed using edgeR v3.32.1 (Robinson et al., 2010; McCarthy et al., 2012) R Studio package. A 0.05 adjusted p value cut off was used. Pathway analyses was performed using clusterProfiler v3.18.1 R package (Yu, 2012 and 2018) with a 0.05 adjusted p value cut off.

2.7 STATISTICAL ANALYSIS

Statistical analysis of data and graph generation were done using GraphPad Prism 6 software (Graphpad La Jolla, USA). Comparisons between groups and within groups were performed using one-way Anova with a tukey's post hoc test and unpaired two-tailed t-test. Data was expressed as mean ± standard error of mean (SEM), with individual values and error bar presented. Statistical significance level was set at $p < 0.05$.

3 CHAPTER 3: RESULTS

3.1 The absence of EZH2 in the *KRAS*^{G12D} context does not alter the size of premalignant lesions in mice after acute pancreatitis

To determine whether *Ezh2* deletion promotes *KRAS*-driven initiation of PDAC following acute pancreatic injury, a cohort of wild type, *Ezh2*^{DSET}, *KRAS*^{G12D}, and *KRAS*^{G12D}*Ezh2*^{DSET} mice were treated with either saline (control) or cerulein every other day over three days to induce acute pancreatitis (**Figure 2.1**). The body weight of mice was monitored and evaluated three times a week after the first day of injections. A sharp reduction in body weight was observed in all mice post treatment, with a gradual recovery starting at day 5. CIP (cerulein induced pancreatitis)-treated mice showed significant weight loss ($P<0.05$) compared to the saline group from Day 3 to Day 10, but no significant differences ($P>0.05$) in the percent changes in body weight were seen between different genotypes **(Figure 3.1A)**. The overall body weight change (i.e., comparing final to starting weights) were not significantly different ($P>0.05$) between all the genotypes or between saline- and CIP-treated groups **(Figure 3.1B)**. Mice were killed 35 days after the first cerulein injection and pancreatic tissues harvested and weighed. No statistical differences ($P>0.05$) were found in the pancreas to body weight ratios between saline- and cerulein-treated mice or between genotypes **(Figure 3.1C)**. Representative images of the pancreas of CIP-treated mice were obtained upon dissection. The pancreatic tissues all appeared as relatively flat and pinkish white in color **(Figure 3.1D)**. Comparisons of the gross pancreatic morphology revealed no obvious differences among genotypes.

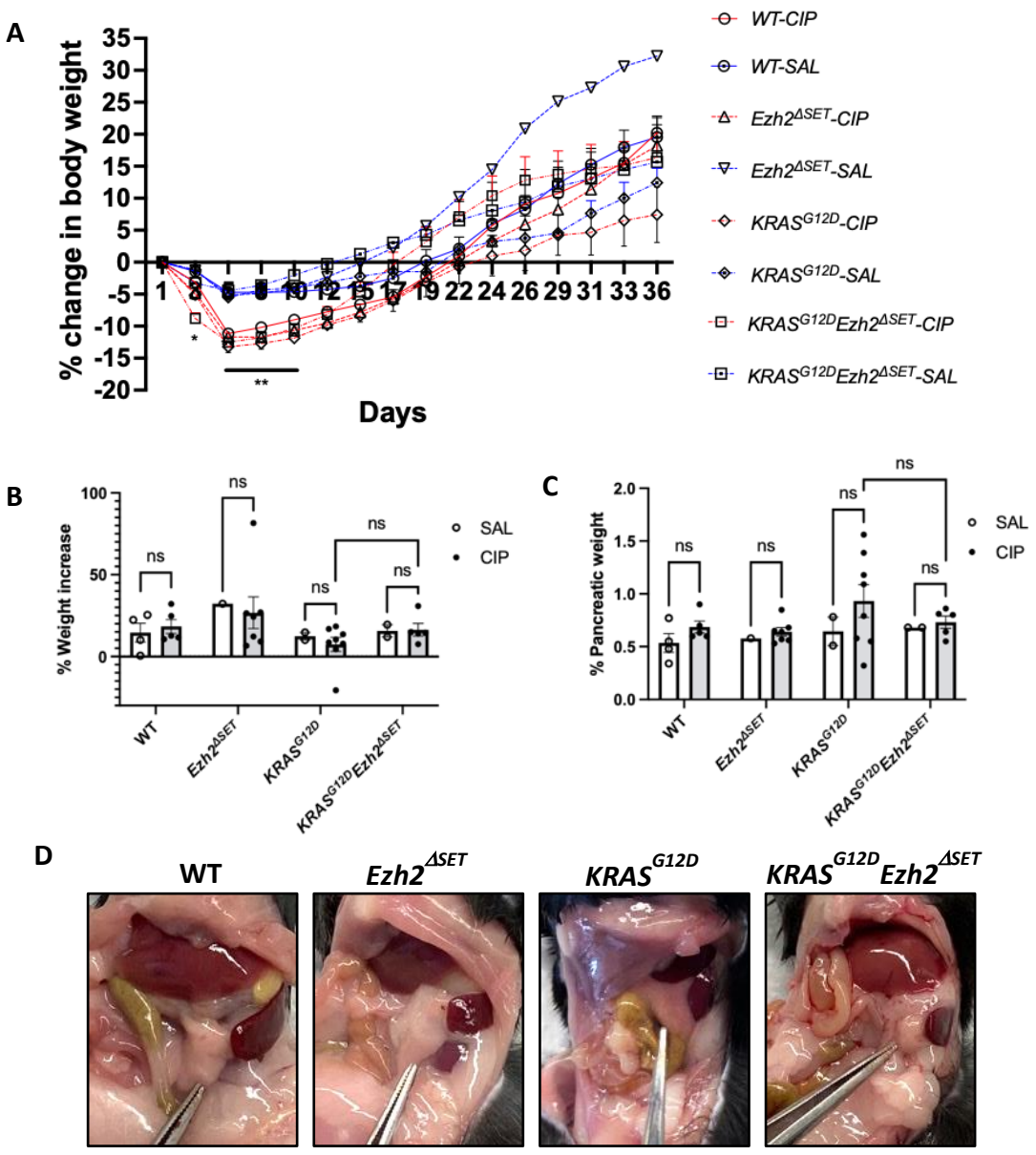
A
% change in body weight
Days
WT-CIP
WT-SAL
Ezh2ΔSET-CIP
Ezh2ΔSET-SAL
KRASG12D-CIP
KRASG12D-SAL
KRASG12DEzh2ΔSET-CIP
KRASG12DEzh2ΔSET-SAL
B
% Weight increase
SAL
CIP
ns
WT
Ezh2ΔSET
KRASG12D
KRASG12DEzh2ΔSET
C
% Pancreatic weight
D
WT
Ezh2ΔSET
KRASG12D
KRASG12DEzh2ΔSET

Figure 3.1 *KRAS^{G12D}* and *KRAS^{G12D}Ezh2$^{\Delta SET}$* mice show no significant difference in body weight gain and pancreatic/body weight ratio compared to WT and *Ezh2$^{\Delta SET}$* mice after acute pancreatic injury. (A) Cerulein-treated mice (CIP; n=25, includes all genotypes) showed significant loss in body weight compared to saline-treated groups (n=9; *P<0.05, **P<0.0001; a repeated measures ANOVA with a Tukey's post hoc test was performed) from day 3-10. No statistical difference in final body weight change **(B)** and pancreatic/body weight ratio **(C)** was observed between genotypes or between cerulein and saline group (P>0.05). The error bar represent mean ± SEM. **(D)** Gross morphology of pancreas in situ. The forceps pointed out the pancreas.

To examine the level of tissue damage in wild-type (WT), *Ezh2*$^{\Delta SET}$, *KRAS*^{G12D}, and *KRAS*^{G12D} *Ezh2*$^{\Delta SET}$ pancreatic tissues, portions of both the head and the tail of the pancreas were embedded and subjected to histological analysis. The assessment of general morphology of pancreatic tissues by H&E staining revealed significantly more PanIN lesions and dense dysplastic stroma in cerulein-treated *KRAS*^{G12D} and *KRAS*^{G12D}*Ezh2*^{DSET} mice compared to saline-treated groups or cerulein-treated WT and *Ezh2*^{DSET} tissues **(Figure 3.2A)**. Interestingly, a large fraction of PanIN lesions is found predominately located in one part of the pancreas, while the other part is relatively normal acinar tissue, which is consistent with previous finding that most PDAC develops from the head of the pancreas (Corbo et al., 2012). Saline-treated *KRAS*^{G12D} and *KRAS*^{G12D}*Ezh2*$^{\Delta SET}$ mice showed only occasional lesions in the pancreas while WT and *Ezh2*$^{\Delta SET}$ pancreas did not. Quantification of the lesion area indicated *KRAS*^{G12D} and *KRAS*^{G12D} *Ezh2*$^{\Delta SET}$ tissues contained significantly more lesion area, including desmoplastic stroma, than WT and *Ezh2*$^{\Delta SET}$ tissues **(**which showed no PanIN lesions or ADM; **Figure 3.2C)** following cerulein treatment. The extent of pancreatic injury varied among *KRAS*^{G12D} and *KRAS*^{G12D}*Ezh2*$^{\Delta SET}$ mice. *KRAS*^{G12D} tissues showed more variation in the percentage of lesion size, with some mice showing occasional focal lesions (1.69% of total pancreatic tissue area) to large majority of the tissue showing lesions (84.18% of total pancreatic tissue area). *KRAS*^{G12D} *Ezh2*$^{\Delta SET}$ tissues showed more consistent lesions to total tissue size ratio. However, *KRAS*^{G12D}*Ezh2*$^{\Delta SET}$ mice showed no differences in the number or extent of PanINs in terms of the size and the area of metaplastic lesions in the pancreas compared to age matched *KRAS*^{G12D} mice **(Figure 3.2C)**. The average lesion to total tissue area ratio was 26.92 ± 10.96% SEM for CIP-treated *KRAS*^{G12D} tissues (n=7), and 15.04 ± 3.51% SEM for *KRAS*^{G12D}*Ezh2*$^{\Delta SET}$ tissues (n=9), which are not statistically different (P>0.05) (**Figure 3.2B**).

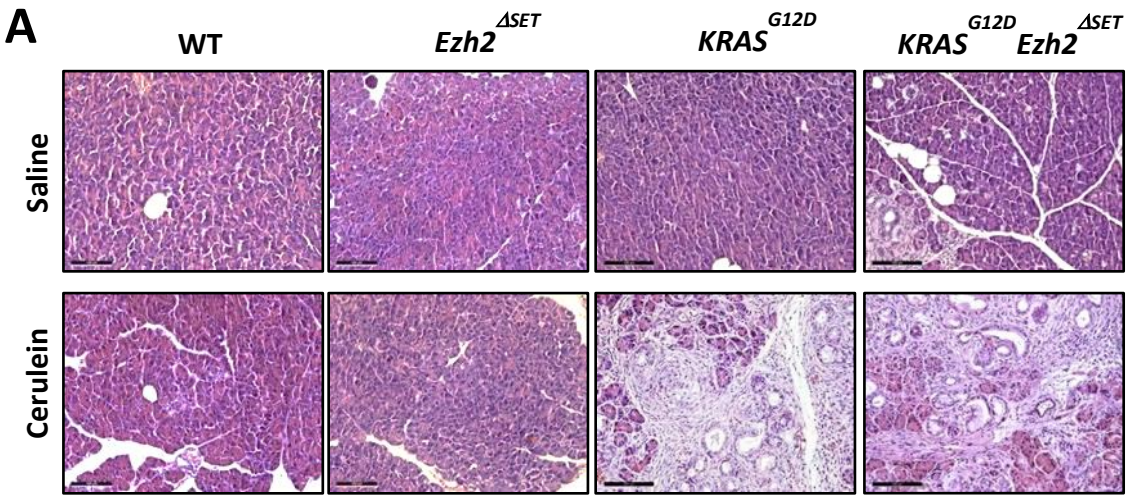
A
WT
Ezh2ΔSET
KRASG12D
KRASG12D Ezh2ΔSET
Saline
Cerulein

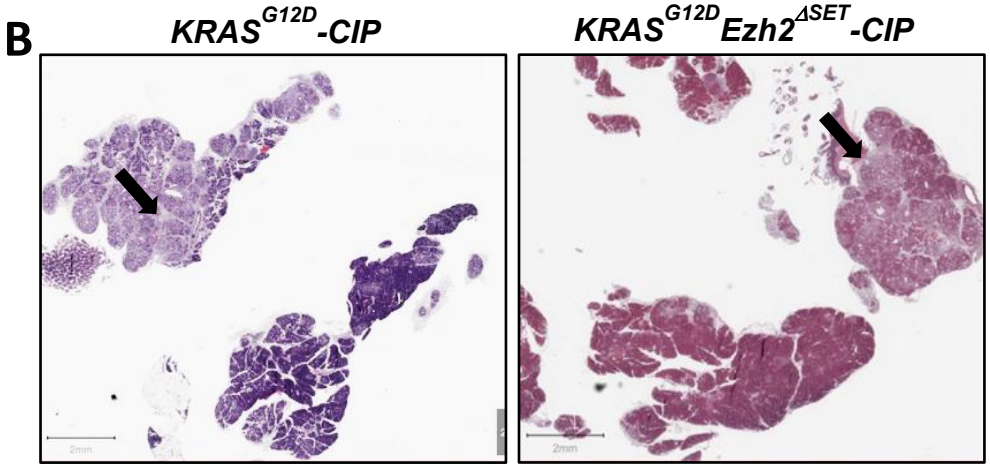
B
KRASG12D-CIP
KRASG12D Ezh2ΔSET-CIP

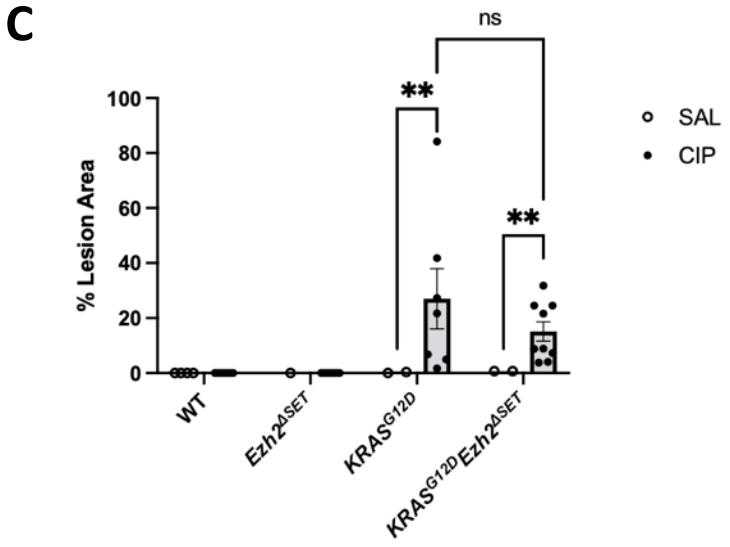
C
ns
**
**
% Lesion Area
100
80
60
40
20
0
SAL
CIP
WT
Ezh2ΔSET
KRASG12D
KRASG12D Ezh2ΔSET

Figure 3.2 The absence of EZH2 does not alter PanIN lesion size. (A) Representative H&E displays occurrence of pancreatic lesions in WT, *Ezh2*$^{\Delta SET}$, *KRAS*^{G12D}, and *KRAS*^{G12D}*Ezh2*$^{\Delta SET}$ mice with (n=7, 7, 7, and 9, respectively) or without cerulein treatment (n=4, 1, 2, and 2, respectively) five weeks after initial cerulein injections. Magnification bar = 100 μm. **(B)** Whole slide H&E images showed regionalization of PanIN lesions (indicated by black arrows). Magnification bar = 2 mm. **(C)** There were no significant differences in the percentage of lesion area between *KRAS*^{G12D} and *KRAS*^{G12D}*Ezh2*$^{\Delta SET}$ tissues cerulein treatment (P>0.05). The error bars represent mean ± SEM. Significantly increased levels of tissue damage were observed between saline- and CIP-treated groups in *KRAS*^{G12D} and *KRAS*^{G12D}*Ezh2*$^{\Delta SET}$ tissues. A two-way ANOVA with a Tukey's post hoc test was performed.

Atrophy of pancreatic acini, lobulated proliferation of ducts with associated stromal fibrosis, and chronic inflammation were observed in both *KRAS*^{G12D} and *KRAS*^{G12D} *Ezh2*$^{\Delta SET}$ tissues treated with cerulein. Cells within some precursor lesions exhibited basally located nuclei and abundant mucinous cytoplasm, suggesting the presence of PanIN with low-grade dysplasia, such as PanIN-1 and PanIN-2. High-grade dysplasia or invasive malignancy was rarely seen in both genotypes (**Figure 3.3**).

To examine ADM in response to acute pancreatic injury, IHC was performed for the duct cell marker, cytokeratin 19 (CK19), and the acinar cell marker, amylase in cerulein-treated mice (**Figure 3.4**). *KRAS*^{G12D} and *KRAS*^{G12D}*Ezh2*$^{\Delta SET}$ pancreata showed a significant decrease in amylase+ to CK19+ tissue compared to WT and *Ezh2*$^{\Delta SET}$ pancreata, indicating gain of ductal identity in both genotypes following injury **(Figure 3.4A)**. In addition, expression of ductal marker CK19 was observed within many acinar cells of *Ezh2*$^{\Delta SET}$ tissues, while amylase was observed in PanIN lesions, supporting an acinar origin for PanINs (Liu et al., 2016). However, the ratio of amylase+/CK19+ tissue was comparable ($P>0.05$) between *KRAS*^{G12D} (27.08±2.04% SEM, n=7) and *KRAS*^{G12D}*Ezh2*$^{\Delta SET}$ pancreata (39.21±5.37% SEM, n=7) **(Figure 3.4B)**. This suggests that acinar cell de-differentiation to duct cells occurs to the same extent in *KRAS*^{G12D} and *KRAS*^{G12D} *Ezh2*$^{\Delta SET}$ tissues following cerulein-induced injury. Interestingly, *Ezh2* deletion does not limit the ability of acinar cells to regenerate in the pancreas after injury with or without the effects of oncogenic *KRAS*.

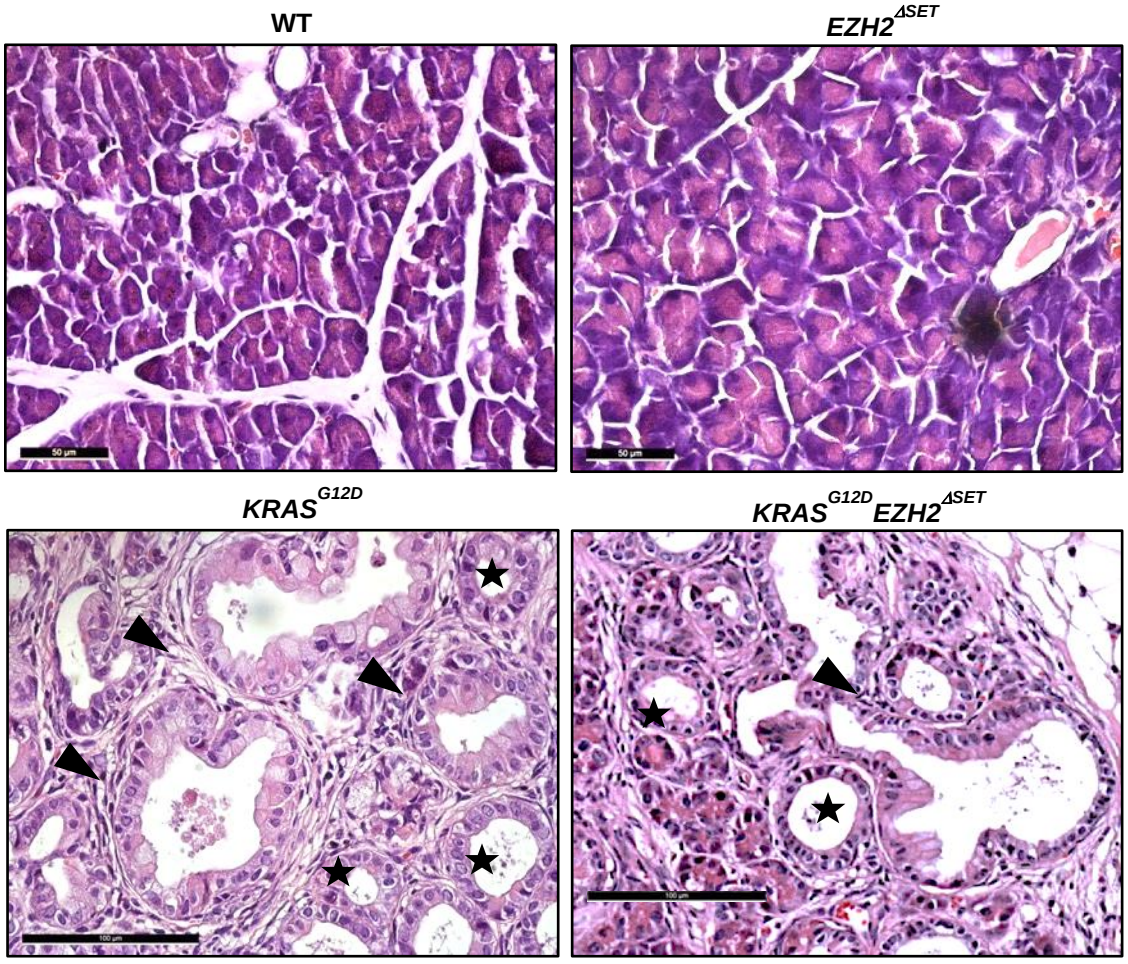
WT
EZH2ΔSET
KRASG12D
KRASG12DEZH2ΔSET

Figure 3.3 Both *KRAS^{G12D}* and *KRAS^{G12D}Ezh2$^{\Delta SET}$* mice show low grade PanIN lesions after acute pancreatic injury. Representative high magnification H&E images showing histological grading of pancreatic lesions in WT, *Ezh2$^{\Delta SET}$*, *KRAS^{G12D}*, and *KRAS^{G12D}Ezh2$^{\Delta SET}$* mice five weeks post-cerulein treatment. The presence of ADM (indicated by stars) and PanIN-1 lesions (indicated by arrows) were identified in both *KRAS^{G12D}* and *KRAS^{G12D}Ezh2$^{\Delta SET}$* tissues. Magnification bar = 100 μm.

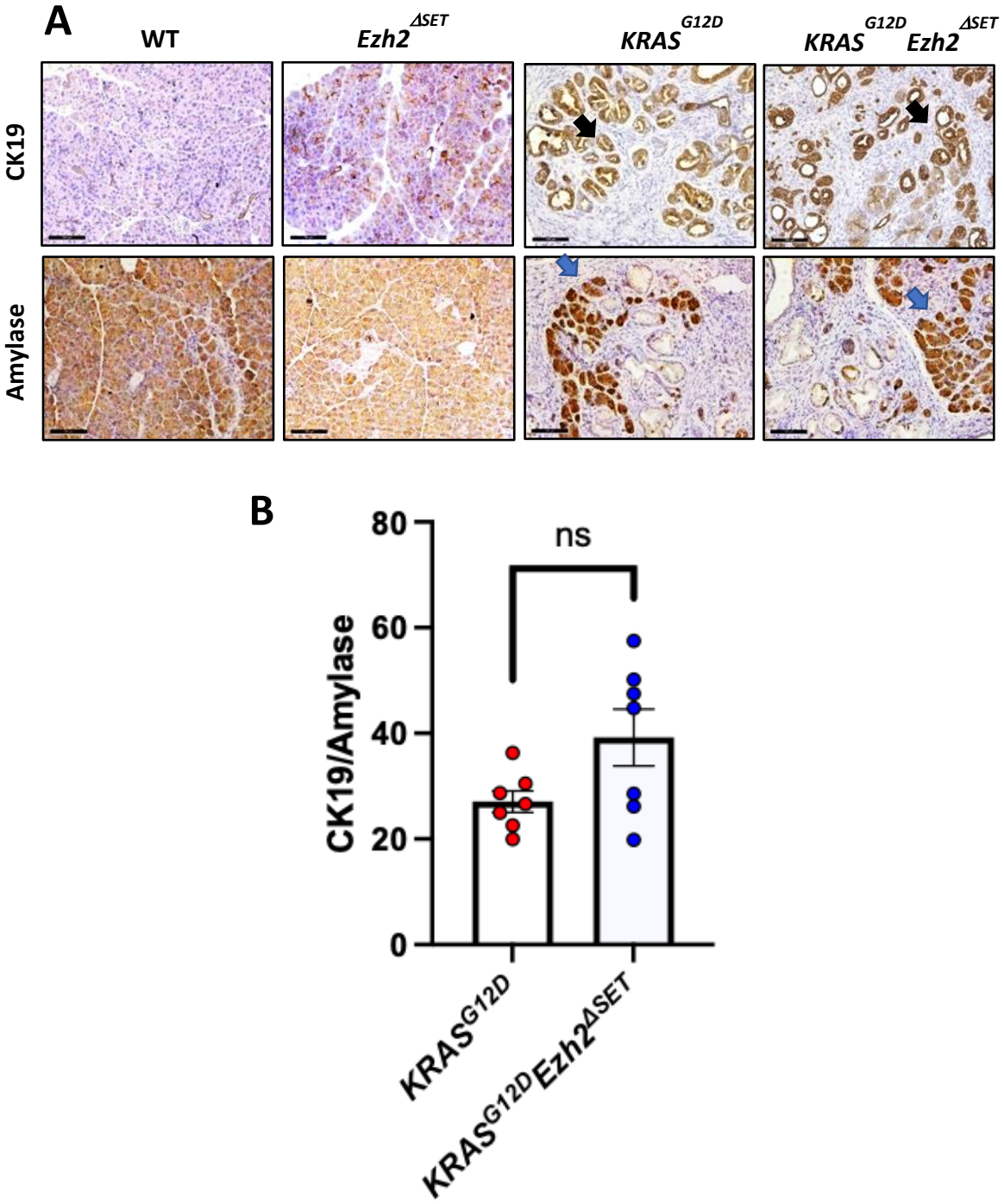
A
WT
Ezh2ΔSET
KRASG12D
KRASG12D Ezh2ΔSET
CK19
Amylase
B
ns
CK19/Amylase
80
60
40
20
0
KRASG12D
KRASG12D Ezh2ΔSET

Figure 3.4 The loss of EZH2 does not affect the amount of acinar/duct tissue. (A) Representative images of IHC staining for CK19 and amylase in WT, $Ezh2^{\Delta SET}$, $KRAS^{G12D}$, and $KRAS^{G12D}Ezh2^{\Delta SET}$ mice following cerulein treatment. Black arrows indicate CK19+ lesions, and blue arrows indicate amylase+ acini. Magnification bar = 100 μm. **(B)** No significant difference was found in the CK19/amylase ratio between $KRAS^{G12D}$, and $KRAS^{G12D}Ezh2^{\Delta SET}$ mice 5 weeks after the last cerulein injection ($P>0.05$). An unpaired two-tailed t test was performed.

3.2 Mice lacking EZH2 methyltransferase activity showed an increased number of higher grade PanIN lesions in the context of *KRAS*^{G12D} activation

Although initial analysis did not show significant differences in the level of *KRAS*^{G12D} -induced PanIN lesions in the absence of EZH2, it is possible that the role of EZH2 in the progression of PanIN lesions is more subtle. To address this possibility, the severity of lesions was examined using two different histological staining methods, Alcian Blue and PAS stain. Alcian Blue stain detects acidic mucin production, which is normally associated with enhanced tumorigenicity and invasiveness of reactive PanIN lesions (Saitou et al., 2005). PAS stains glycogen and is used to accurately measure the extent of PanIN lesions as glycogen deposits are evidence of cancerous cells. Alcian Blue stain revealed no staining in CIP-treated WT or *Ezh2*$^{\Delta SET}$ mice or in saline treated groups. However, by week five following induced injury, a significantly greater ($P<0.005$) percentage of Alcian Blue+ lesions were detected in CIP-treated *KRAS*^{G12D}*Ezh2*$^{\Delta SET}$ mice (55.14 ± 3.26% SEM, n=9) compared to *KRAS*^{G12D} mice (34.14 ± 2.90% SEM, n=7) **(Figure 3.5A-C)**, suggesting *KRAS*^{G12D}*Ezh2*$^{\Delta SET}$ mice treated with cerulein more frequently developed higher grade PanIN lesion compared to *KRAS*^{G12D} mice. This finding was supported by PAS staining, showed significantly fewer ($P<0.05$) glycogen+ PanIN lesions **(Figure 3.6A-C)** in *KRAS*^{G12D} mice (39.86% ± 6.15% SEM) compared to *KRAS*^{G12D}*Ezh2*$^{\Delta SET}$ mice (58.57% ± 3.05% SEM) (**Figure 3.6B**). No accumulation of glycogen was detected in saline-treated *KRAS*^{G12D} and *KRAS*^{G12D}*Ezh2*$^{\Delta SET}$ mice, as well as in CIP-treated control groups. In summary, these combined results show *KRAS*^{G12D}*Ezh2*$^{\Delta SET}$ tissues have more progression PanIN lesions 5 weeks after initial cerulein injections compared to *KRAS*^{G12D} tissues, even though the lesion area percentages between two genotypes were comparable.

Finally, the level of collagen in CIP- and saline-treated mouse pancreas was visualized using picrosirius red staining. Positive stain revealed the presence of collagen deposition in CIP-treated *KRAS*^{G12D} and *KRAS*^{G12D}*Ezh2*$^{\Delta SET}$ mice, specifically in the desmoplastic stromal area **(Figure 3.7)**. In contrast, much less collagen accumulation was observed in

saline treated *KRAS*^{G12D} and *KRAS*^{G12D}*Ezh2*$^{\Delta SET}$ tissues. WT and *Ezh2*$^{\Delta SET}$ tissues showed little collagen expression around lobes, large vessels, and islets. *KRAS*^{G12D} *Ezh2*$^{\Delta SET}$ tissues showed more extensive positive staining compared to *KRAS*^{G12D} tissues, which would indicate a higher degree of pancreatic fibrosis in the presence of oncogenic *KRAS*^{G12D} and pancreatic injury, and that deletion of *Ezh2* could lead to more accumulation of dense collagen fibers in the stroma. Collagen quantification was not performed as sufficient sample sizes were not achieved.

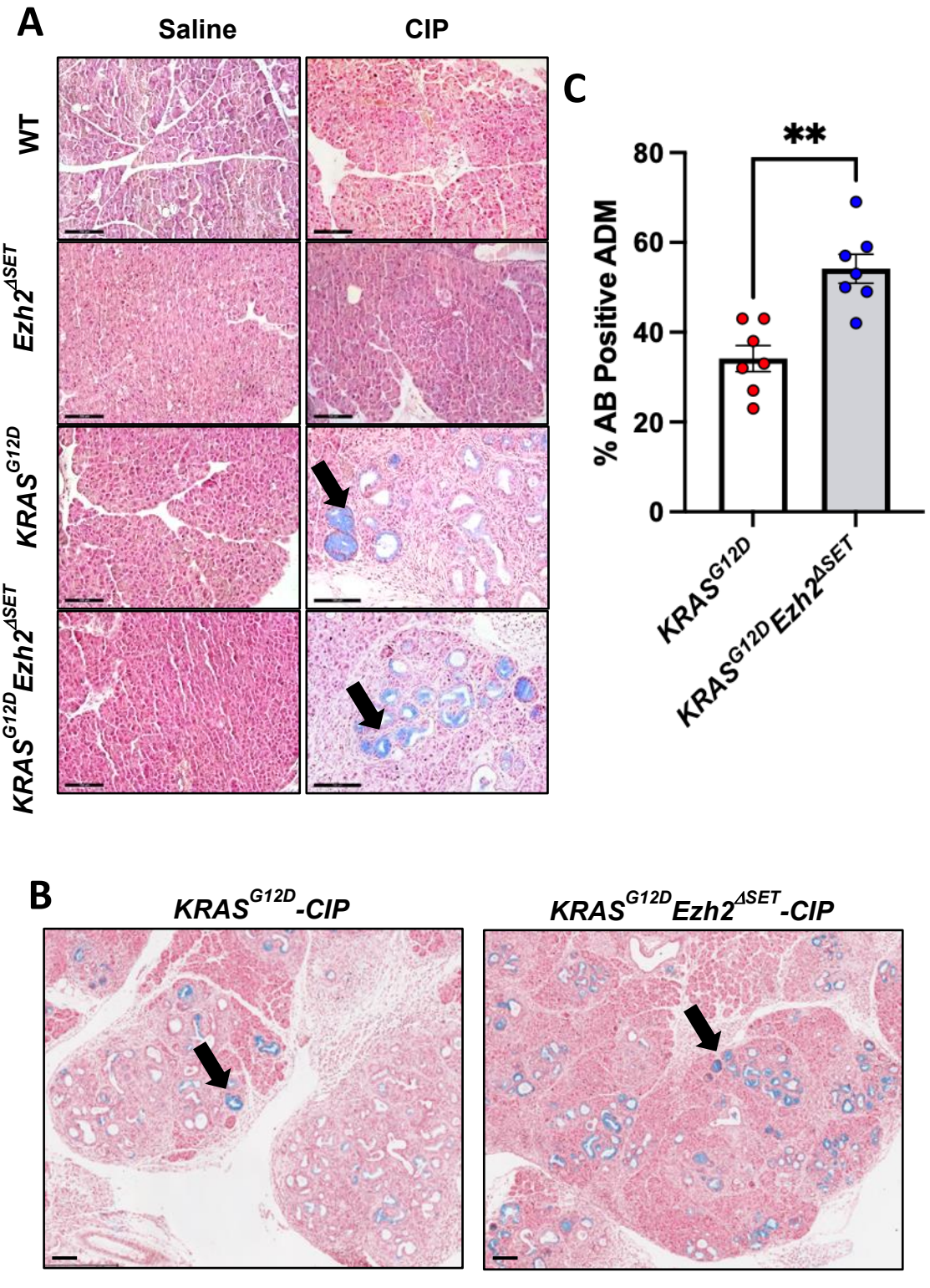
A
Saline
CIP
WT
Ezh2ΔSET
KRASG12D
KRASG12DEzh2ΔSET
C
**
% AB Positive ADM
80
60
40
20
0
KRASG12D
KRASG12DEzh2ΔSET
B
KRASG12D-CIP
KRASG12DEzh2ΔSET-CIP

Figure 3.5 *KRAS^{G12D}Ezh2$^{\Delta SET}$* tissue shows increased expression of acidic mucins. (A) Representative alcian blue images shows an increase in acidic mucins in the absence of Ezh2 in the context of *KRAS^{G12D}* following cerulein treatment. Black arrows point out the positive stain. Magnification bar = 100 μm. **(B)** Low magnification images show a more extensive area of analysis (indicated by black arrows). Magnification bar = 100 μm. **(C)** Quantification of representative images confirms a significant increase (n=7 for both; **P<0.005) in the percentage of AB+ lesions in *KRAS^{G12D} Ezh2$^{\Delta SET}$* mice 5 weeks after the last cerulein injection compared to *KRAS^{G12D}* mice. Mean±SEM is shown. A two-tailed unpaired t test was performed.

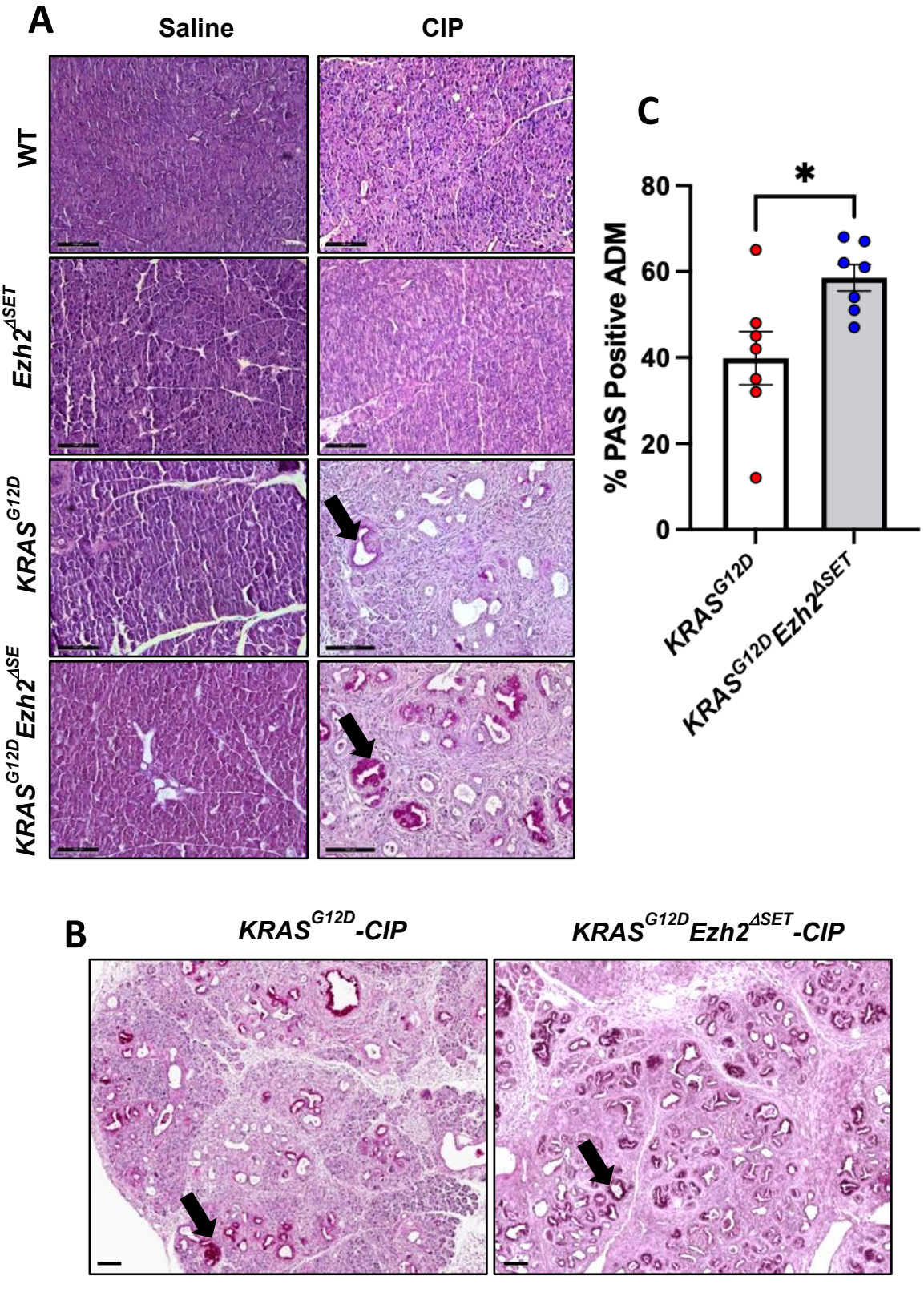
A
Saline
CIP
WT
Ezh2ΔSET
KRASG12D
KRASG12DEzh2ΔSE
C
% PAS Positive ADM
80
60
40
20
0
*
KRASG12D
KRASG12DEzh2ΔSET
B
KRASG12D-CIP
KRASG12DEzh2ΔSET-CIP

Figure 3.6 *KRAS^{G12D}Ezh2$^{\Delta SET}$* tissue shows increased PAS+ stain. (A) Representative PAS images show an increase in PAS+ stain in the absence of *Ezh2* in the context of *KRAS^{G12D}* following cerulein treatment. Black arrows point out the positive stain. Magnification bar = 100 μm. **(B)** Low magnification images show a more extensive area of analysis (indicated by black arrows). (indicated by black arrows). Magnification bar = 100 μm. **(C)** Quantification of representative images confirms a significant increase in the percentage of PAS+ lesions in *KRAS^{G12D}Ezh2$^{\Delta SET}$* mice 5 weeks after the last cerulein injection (n=7 for both; $P<0.05$). A two-tailed unpaired t test was performed.

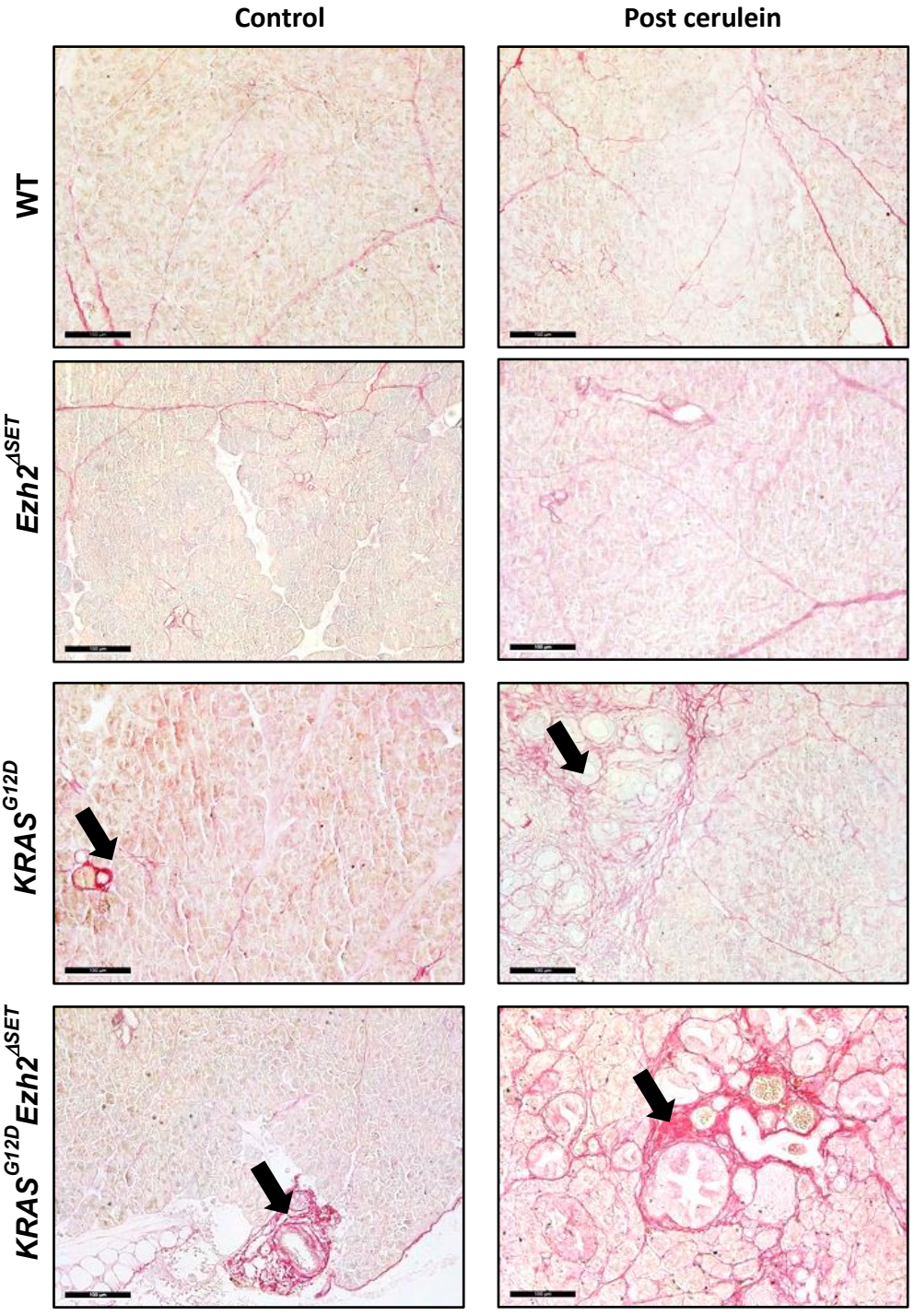
Control
Post cerulein
WT
Ezh2ΔSET
KRASG12D
KRASG12DEzh2ΔSET

Figure 3.7 ***KRAS^{G12D}*** **and** ***KRAS^{G12D}Ezh2$^{\Delta SET}$*** **tissues show increased collagen deposition in the stromal area.** Representative images showing Picrosirius red staining of pancreatic tissues from each group. Black arrows indicate fibrosis. Magnification bar = 100 μm.

3.3 *Ezh2* deletion alters the molecular response to $KRAS^{G12D}$

Next, I examined the effects of *Ezh2* deletion on the molecular profile of acinar cells with or without $KRAS^{G12D}$ activation. WT, $Ezh2^{\Delta SET}$, $KRAS^{G12D}$, and $KRAS^{G12D}Ezh2^{\Delta SET}$ mice of 2-4 months old were administered with tamoxifen to specifically activate creERT, which leads to oncogenic $KRAS^{G12D}$ activation or *Ezh2* deletion. Twenty-two days following tamoxifen treatment, mice of all genotypes were sacrificed. The extent of tissue damage was examined by histological stain. Low power images of H&E staining revealed no obvious difference in general pancreas morphology among all genotypes. Most of the sections showed normal exocrine pancreas - a large number of acini, occasional fat cells, and the islets of Langerhans can be recognized in the tissue sections. No detectable pancreatic lesions are found in all genotypes (**Figure 3.8A**).

RNA-seq was performed on RNA isolated form whole pancreatic tissues from 22 days after tamoxifen gavage without cerulein-induced pancreatic injury. This time point was chosen because no obvious morphological differences were shown, and the cell makeup of the pancreas was relatively similar among genotypes. RNA-seq analysis of $KRAS^{G12D}$ and $KRAS^{G12D}Ezh2^{\Delta SET}$ mouse acinar cells revealed 315 genes significantly dysregulated in the absence of EZH2, with 237 genes upregulated and 78 genes downregulated **(Figure 3.8B)**. To examine the molecular mechanisms involved in the loss of *Ezh2*, pathway analysis was performed with these genes using The Database for Annotation, Visualization and Integrated Discovery (DAVID) Bioinformatics Resources (2021 update) to investigate the functions of the selected 96 genes. Gene Ontology (GO) enrichment analysis identified 49 pathways significantly dysregulated between $KRAS^{G12D}$ and $KRAS^{G12D}Ezh2^{\Delta SET}$ genotypes. The results were ranked by the enrichment score and the top-ranked 20 signaling pathways are shown in **Figure 3.8C**. Many of the top-ranked pathways are related to inflammatory and immune responses, including the top five enriched pathways: adaptive immune response (GO:0002250), antigen processing and presentation of exogenous peptide antigen (GO:0002478), adaptive immune response based on somatic recombination of immune receptors built from immunoglobulin superfamily domains (GO:0002460), antigen processing and presentation of exogenous peptide antigen via MHC class II (GO:0019886),

and antigen processing and presentation of exogenous antigen (GO:0019884) (**Figure 3.8C**).

Among the differentially expressed genes, the *C3* gene appeared in the top five pathways dysregulated in the absence of EZH2. RNA-seq data noted indicated significantly higher levels of C3 expression in $KRAS^{G12D}Ezh2^{\Delta SET}$ compared to $KRAS^{G12D}$ tissues. IHC staining for C3 in mouse pancreas indicated that C3 is solely expressed in $KRAS^{G12D}Ezh2^{\Delta SET}$ tissues, specifically in columnar epithelial cells within the lesion area, while no positive signals were found in $KRAS^{G12D}$ lesions. To be noted that the gene expression analysis was done in mouse tissues 22 days after tamoxifen without cerulein-induced injury, while histological analysis of C3 was done in tissues that were injured five weeks before dissection **(Fig 3.9B)**.

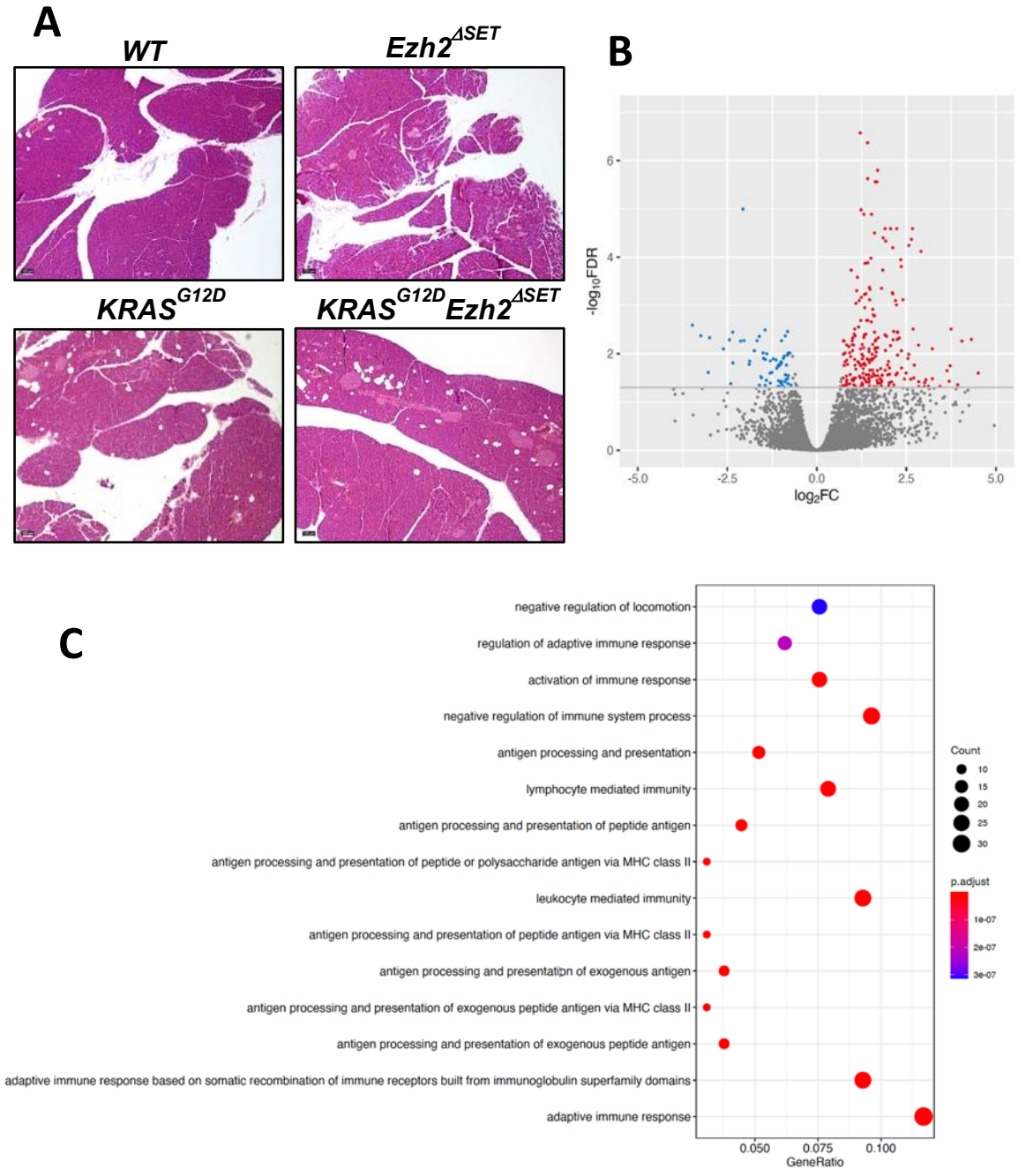
A
WT
Ezh2ΔSET
KRASG12D
KRASG12DEzh2ΔSET
B
-log10FDR
log2FC
C
negative regulation of locomotion
regulation of adaptive immune response
activation of immune response
negative regulation of immune system process
antigen processing and presentation
lymphocyte mediated immunity
antigen processing and presentation of peptide antigen
antigen processing and presentation of peptide or polysaccharide antigen via MHC class II
leukocyte mediated immunity
antigen processing and presentation of peptide antigen via MHC class II
antigen processing and presentation of exogenous antigen
antigen processing and presentation of exogenous peptide antigen via MHC class II
antigen processing and presentation of exogenous peptide antigen
adaptive immune response based on somatic recombination of immune receptors built from immunoglobulin superfamily domains
adaptive immune response
GeneRatio
Count
p.adjust

Figure 3.8 The loss of *Ezh2* leads to dysregulation of inflammatory response pathways in the absence of significant damage to the pancreas. (A) H&E histology of WT, $Ezh2^{\Delta SET}$, $KRAS^{G12D}$, and $KRAS^{G12D}Ezh2^{\Delta SET}$ pancreatic tissues. Magnification bar = 100 μm. **(B)** Volcano plot with log2 FC indicating the mean expression level for each gene. Each dot represents a gene. Black dots represent no significant differentially expressed genes between $KRAS^{G12D}$ and $KRAS^{G12D}Ezh2^{\Delta SET}$ groups. Blue and red dots represent significant differentially expressed genes (blue is $p_{adj}< 0.05$, red is $p_{adj}<0.05$ and Log2foldchange >2; n=3 for each group). **(C)** GO pathway analysis of the differentially expressed genes (p_{adj} <0.05, Log2foldchange >2) between $KRAS^{G12D}$ and $KRAS^{G12D}Ezh2^{\Delta SET}$ groups (n=3 for each group). Figure 3.8B and C courtesy of Fatemeh Mousavi.

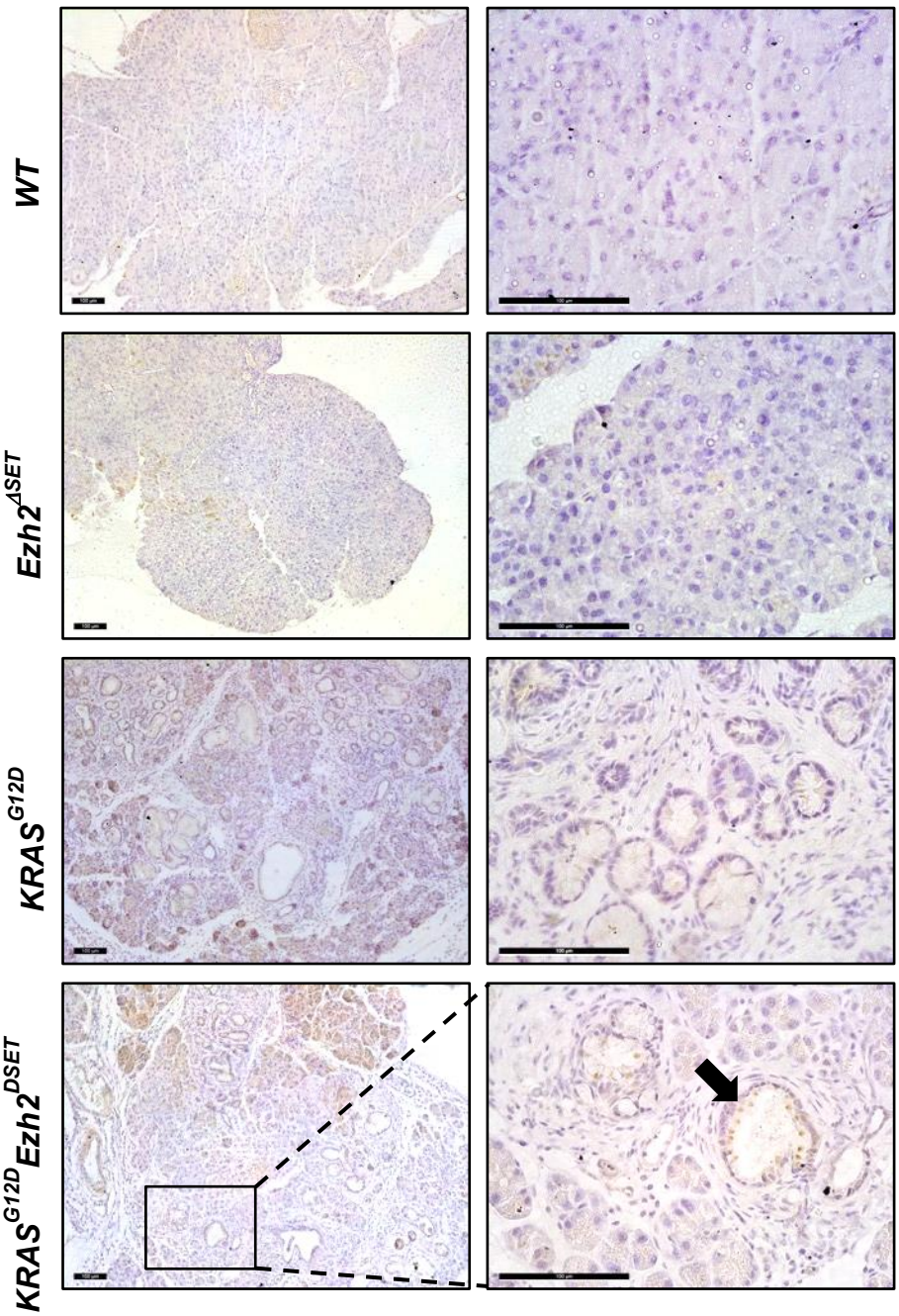
WT
Ezh2ΔSET
KRASG12D
KRASG12DEzh2DSET

Figure 3.9 The absence of EZH2 affects the expression of complement C3 in PanIN cells. Representative high (right) and low (left) power IHC images showed that the expression of complement C3 was observed in the columnar epithelial cells of *KRAS*^{G12D}*Ezh2*$^{\Delta SET}$ tissue at week five post CIP. WT, *Ezh2*$^{\Delta SET}$ and *KRAS*^{G12D} does not show positive signal for C3 in PanIN cells. in Black arrows point out C3-positive cells. Magnification bar = 100 μm.

3.4 *Ezh2* deletion in the context of *KRAS^{G12D}* induces tumor microenvironment modulation in PanIN progression

Previous results indicated that loss of *EZH2* activity enhanced PanIN lesion progression in the presence of *KRAS^{G12D}*. The analysis of RNA-seq in *KRAS^{G12D}Ezh2$^{\Delta SET}$* and *KRAS^{G12D}* suggested the absence of EZH2 leads to dysregulation of multiple inflammatory pathways. To confirm the relationship between *Ezh2* deletion and the immune response in the pancreas, I examined the presence of immune cells and cancer-associated fibroblasts (CAFs) in the tumor microenvironment of CIP-treated mice by IHC staining. Infiltration of cytotoxic T lymphocytes was detected by IHC for CD8, while CD3 measures total intratumoral T lymphocytes (Andrew et al., 2016). The presence of macrophages was marked by the expression of F4/80. High expression of vimentin and aSMA was used as markers for pancreatic CAF (panCAF) and myCAF, respectively.

I first looked at the infiltration of cytotoxic CD8+ T cells. As expected, CIP-treated WT and *Ezh2$^{\Delta SET}$* mice showed no accumulation of CD8 (**Figure 3.10**). In CIP-treated *KRAS^{G12D}Ezh2$^{\Delta SET}$* and *KRAS^{G12D}* mice, however, CD8+ cytotoxic T lymphocytes were detected in the desmoplastic stroma, suggesting the occurrence of inflammation in the TME. Although the difference is not significant (P=0.069), *KRAS^{G12D}* tissues showed a trend towards increased numbers of CD8+ cells (26.91 ± 3.57 cell/mm^2 SEM, n=5) compared to *KRAS^{G12D}Ezh2$^{\Delta SET}$* tissues (14.30 ± 4.75 cell/mm^2 SEM, n=5) (**Figure 3.10**). Similar to CD8, IHC staining for CD3 revealed negligible T cells in *KRAS^{G12D} Ezh2$^{\Delta SET}$* and *KRAS^{G12D}* mice in response to cerulein-induced injury, while *KRAS^{G12D}Ezh2$^{\Delta SET}$* and *KRAS^{G12D}* mice showed T cell infiltration in the TME. The average density of CD3+ T cells was slightly, but not significantly (P>0.05), higher in *KRAS^{G12D}* (153.8 ± 26.08 cell/mm^2 SEM, n=5) compared to *KRAS^{G12D}Ezh2$^{\Delta SET}$* tissues (113.3 ± 18.99 cell/mm^2 SEM, n=5) **(Figure 3.11)**. Next, I tracked macrophage infiltration in all four genotypes by staining for F4/80. IHC revealed no infiltration of macrophages in pancreatic tissues of CIP-treated WT and *Ezh2$^{\Delta SET}$* mice. There was a significantly (P<0.005) increased infiltration of F4/80 positive macrophages in the stromal area of *KRAS^{G12D}* (1.33 ± 0.34% SEM, n=5) compared to *KRAS^{G12D}Ezh2$^{\Delta SET}$* tissues (0.08 ± 0.03% SEM, n=5) (**Figure**

3.12). The amount of macrophage recruitment in the stroma largely varies in *KRAS*^{G12D} samples, which essentially ranges from 0.20% to 2.25% positive stain verses the total lesion area. These results suggested that the absence of EZH2 in the presence of oncogenic *KRAS*^{G12D} slightly reduces the recruitment of T lymphocytes and macrophages into the TME surrounding PanIN lesions.

To determine whether other non-acinar cell types of the TME are affected by the deletion of *EZH2* in the *KRAS*^{G12D} context, I examined if the absence of EZH2 caused altered accumulation of CAFs in the TME of WT, *Ezh2*$^{\Delta SET}$, *Mist1*$^{creERT/+}$*KRAS*^{G12D} and *KRAS*^{G12D}*Ezh2*$^{\Delta SET}$ mice. myCAFs, as marked by aSMA positive signals, was comparably abundant in both *KRAS*^{G12D} and *KRAS*^{G12D}*Ezh2*$^{\Delta SET}$ tissues, while negligible amount of myCAF accumulation can be detected in WT and *Mist1*$^{creERT/+}$*EZH2*$^{\Delta SET}$ tissues (**Fig. 3.13**). MyCAFs were predominantly located at the center of the injured area adjacent to PanIN lesions, and not at the peripheral edges of the TME. Similar analysis for the marker of panCAF, vimentin, revealed no accumulation in WT and *Ezh2*$^{\Delta SET}$, and high amounts of expression in *KRAS*^{G12D} and *KRAS*^{G12D}*Ezh2*$^{\Delta SET}$ mice. No obvious differences in terms of the levels of myCAF and panCAF accumulation was detected between *KRAS*^{G12D} and *KRAS*^{G12D}*Ezh2*$^{\Delta SET}$ tissues. Combined, these data suggest the loss of EZH2 in the context of oncogenic KRAS^{G12D} may play a role in the modulation of the TME, especially the recruitment of immune cells. This difference may be correlated with the more progressive phenotype of PanIN lesions.

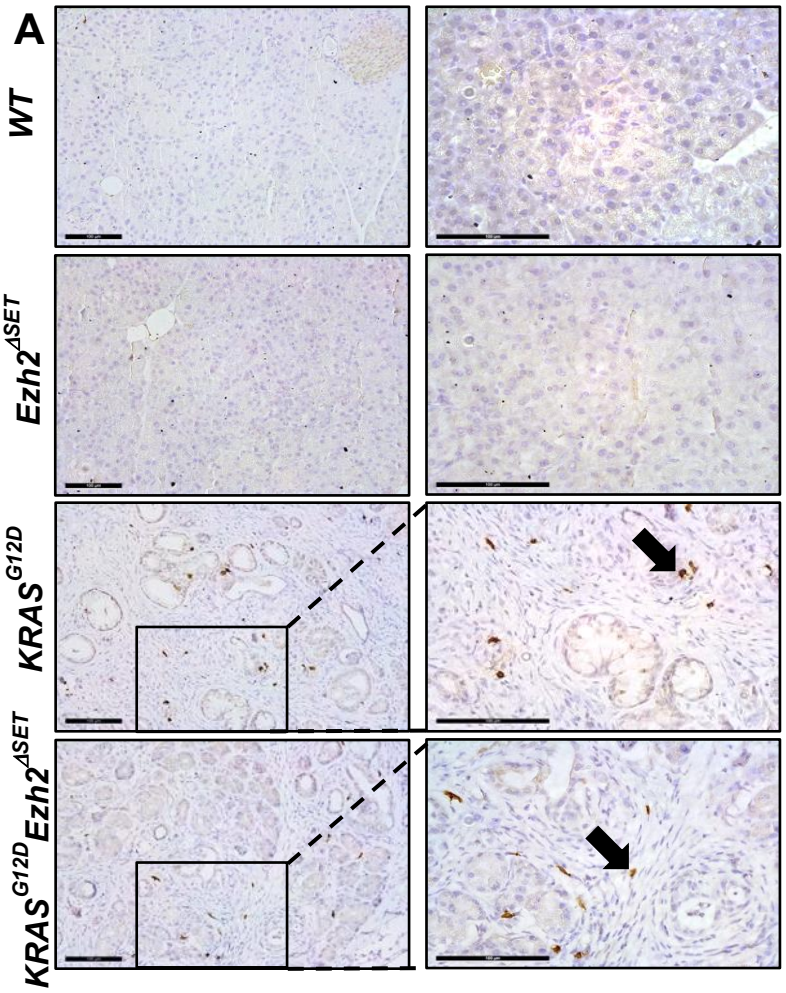
A
WT
Ezh2ΔSET
KRASG12D
KRASG12DEzh2ΔSET

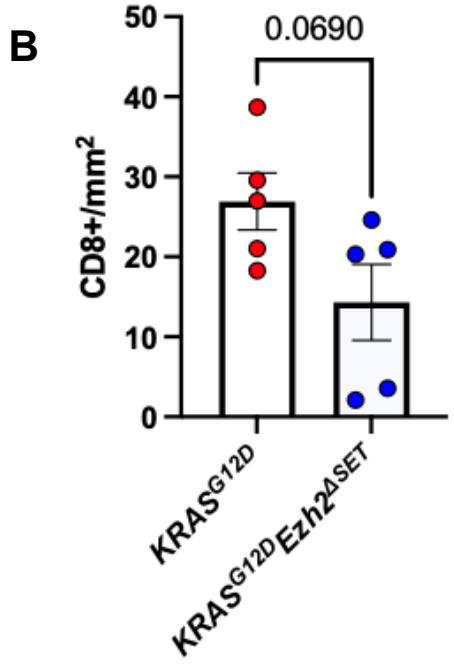
B
0.0690
CD8+/mm2
50
40
30
20
10
0
KRASG12D
KRASG12DEzh2ΔSET

Figure 3.10 Infiltration of CD8+ lymphocytes after CIP show a decreased trend in the absence of EZH2. Representative high (right) and low (left) power IHC images showed that the number of CD8+ lymphocytes marker was lower in *KRAS*^{G12D}*Ezh2*$^{\Delta SET}$ tissues compared to *KRAS*^{G12D}. CD8 infiltration was not observed in WT and Ezh2$^{\Delta SET}$ tissues. Black arrow pointed out the positive stain. Magnification bar = 100 μm. **(B)** Quantification of CD3 confirmed a trend that was not statistically significant in CD8+ cells in *KRAS*^{G12D} tissues post injury (cells/mm^2 mean ± SEM, n = 5; P=0.0690; unpaired two-tail student's t test was performed)

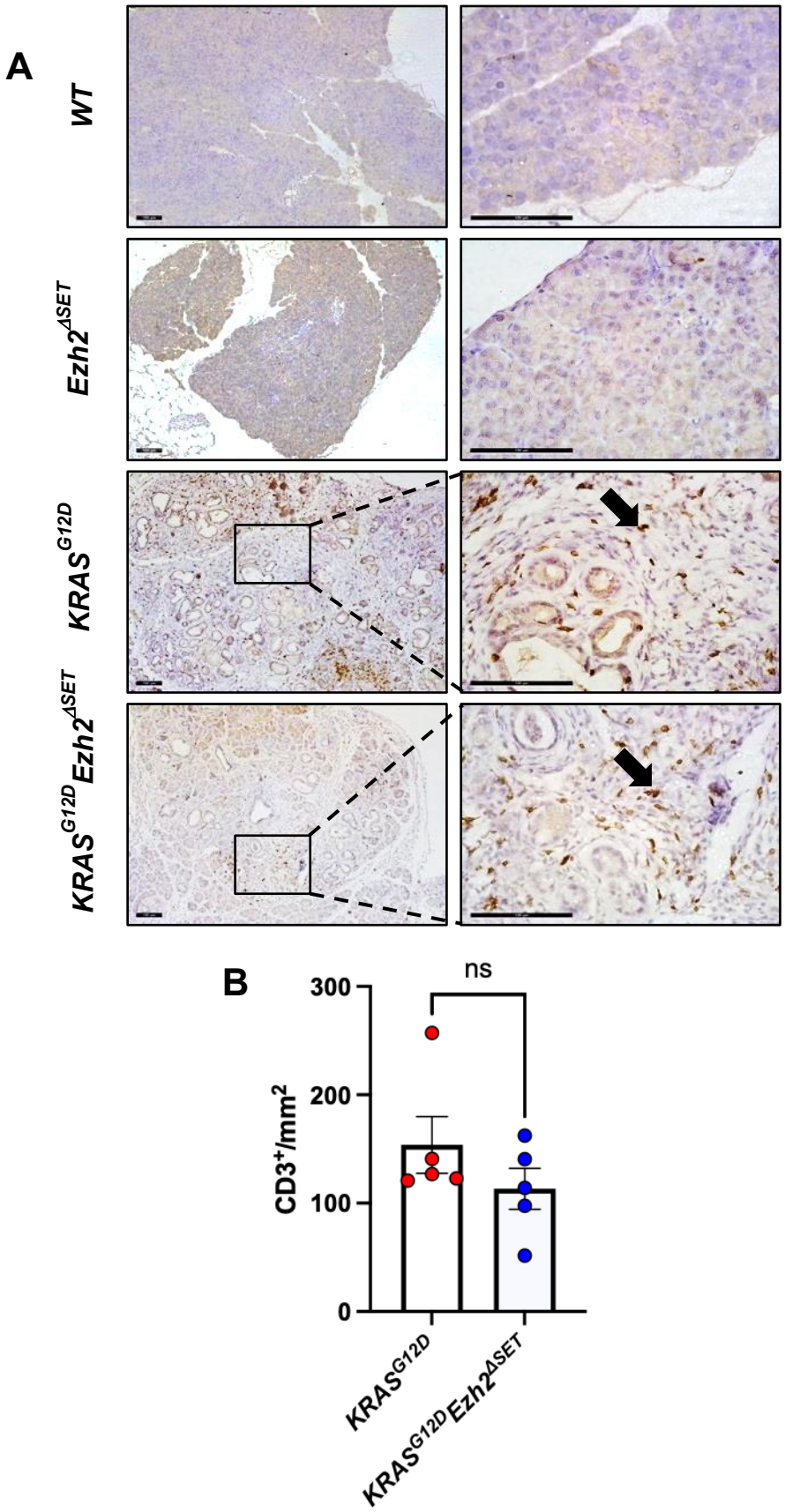
A
WT
Ezh2ΔSET
KRASG12D
KRASG12DEzh2ΔSET
B
ns
300
200
100
0
CD3+/mm2
KRASG12D
KRASG12DEzh2ΔSET

Figure 3.11 EZH2 deletion does not affect the total amount of lymphocyte infiltration into the pancreas the stroma. Representative high (right) and low (left) power IHC images showed that the number of CD3+ lymphocytes marker was not statistically different between *KRAS*^{G12D} tissues compared to *KRAS*^{G12D}*Ezh2*$^{\Delta SET}$. Black arrows indicate positive stain. Magnification bar = 100. **(B)** Quantification of CD3+ cells showed higher numbers in *KRAS*^{G12D} tissue but was not statistically significant that the number of CD3+ cells in *KRAS*^{G12D} tissue post injury (cells/mm^2 mean ± SEM; n = 5; P>0.05; unpaired two-tail student's t test was performed).

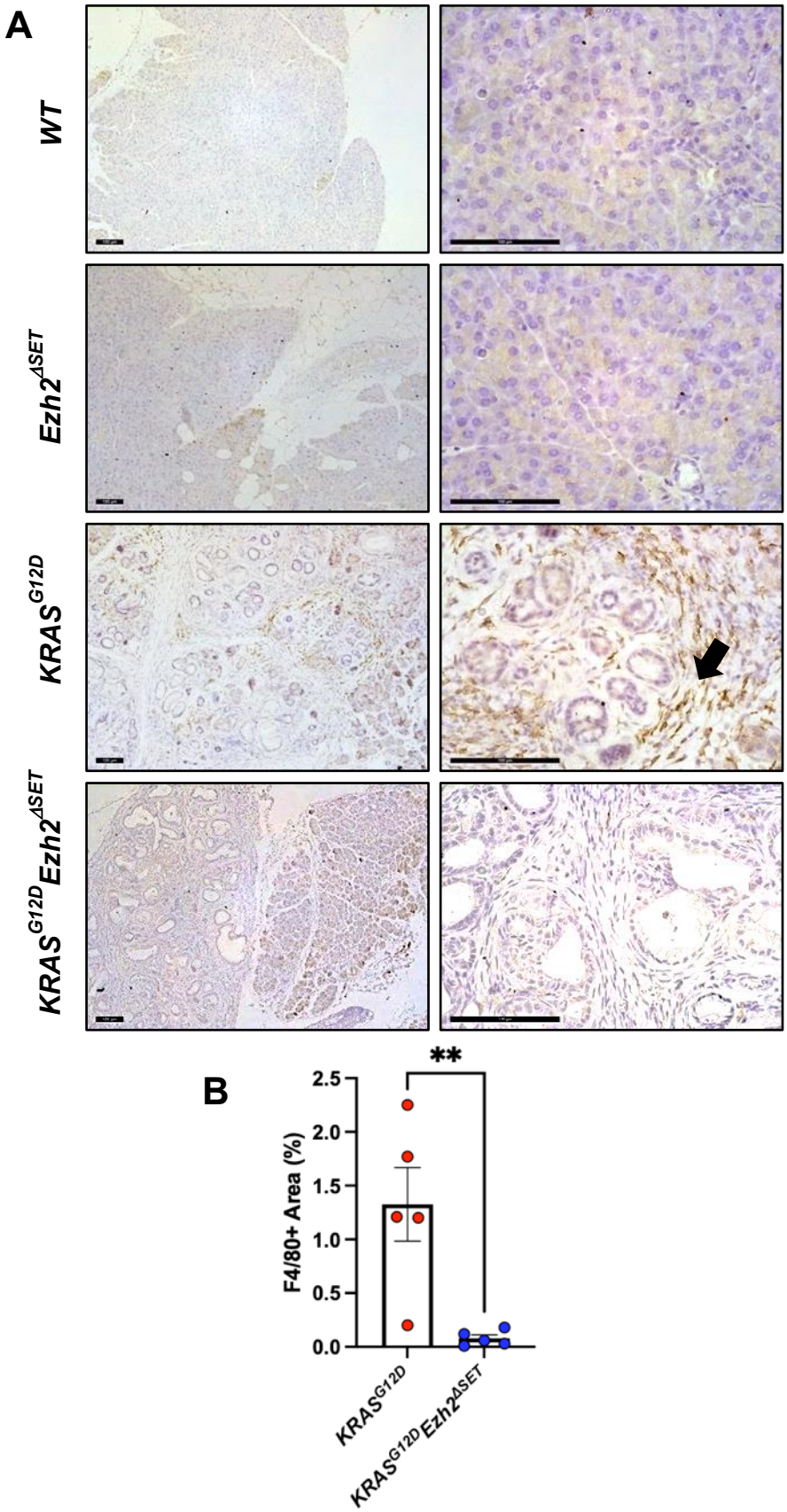
A
WT
Ezh2ΔSET
KRASG12D
KRASG12DEzh2ΔSET
B
**
F4/80+ Area (%)
2.5
2.0
1.5
1.0
0.5
0.0
KRASG12D
KRASG12DEzh2ΔSET

Figure 3.12 EZH2 deletion reduces macrophage infiltration into the stroma. (A) Representative high (right) and low (left) power IHC images of macrophage marker F4/80 showed no accumulation of macrophages in WT and *Ezh2*$^{\Delta SET}$ pancreas. *KRAS*^{G12D}*Ezh2*$^{\Delta SET}$ showed remarkably more positive stain compared to *KRAS*^{G12D} tissue samples. Black arrows indicate the positive stain. Magnification bar = 100 μm. **(B)** The quantification of F4/80 confirmed a significantly increased macrophage accumulation in KRAS^{G12D} tissues post injury (% mean ± SEM; n = 5; **P<0.005; unpaired two-tail student's t test was performed).

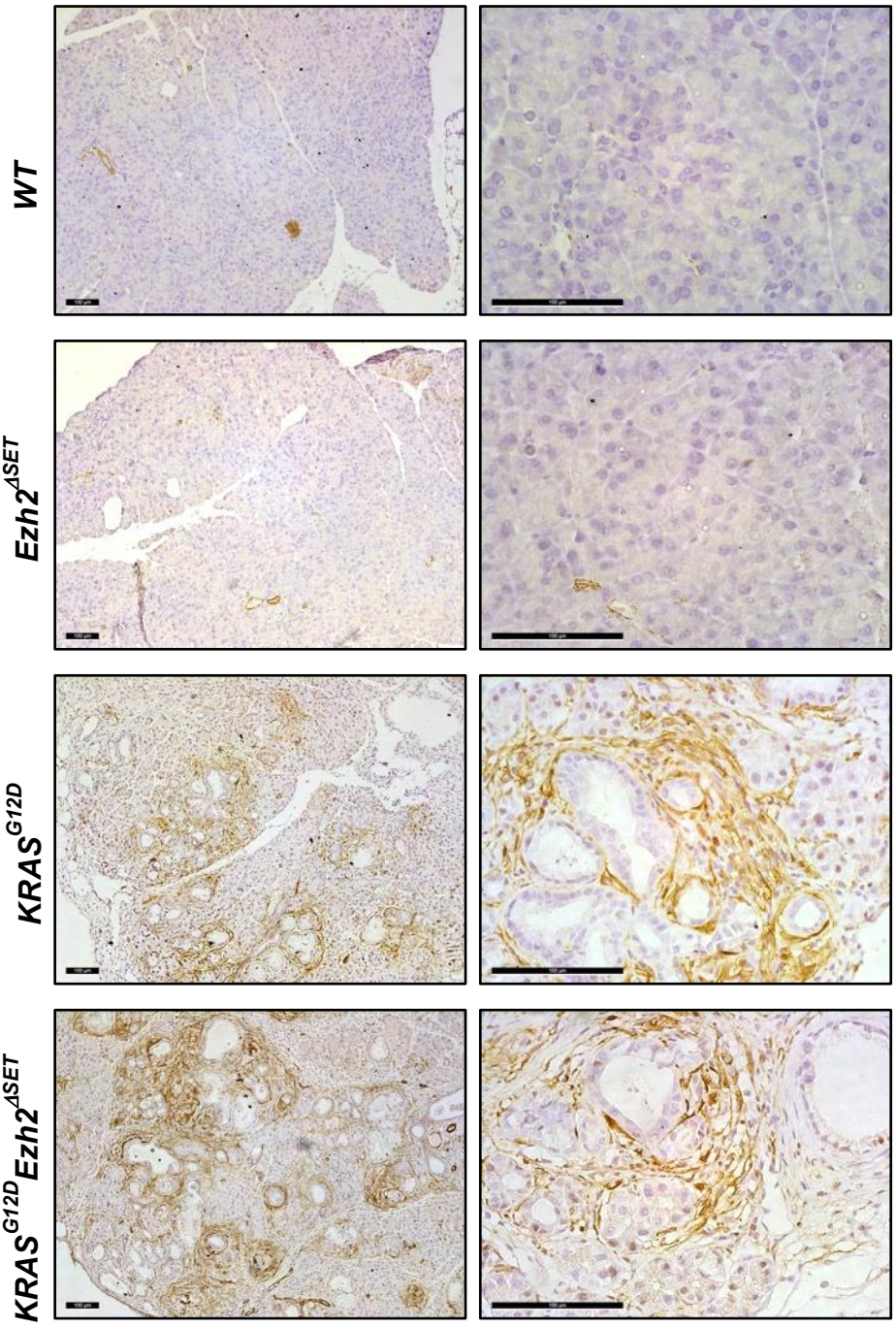
WT
Ezh2ΔSET
KRASG12D
KRASG12DEzh2ΔSET

Figure 3.13 EZH2 deletion does not alter the total number of myCAFs in the tumor microenvironment. Representative high (right) and low (left) power IHC images of myCAF marker smooth muscle actin in $KRAS^{G12D}Ezh2^{\Delta SET}$ and $KRAS^{G12D}$ tissue samples showed no overall difference in the expression level. Magnification bar = 100 μm.

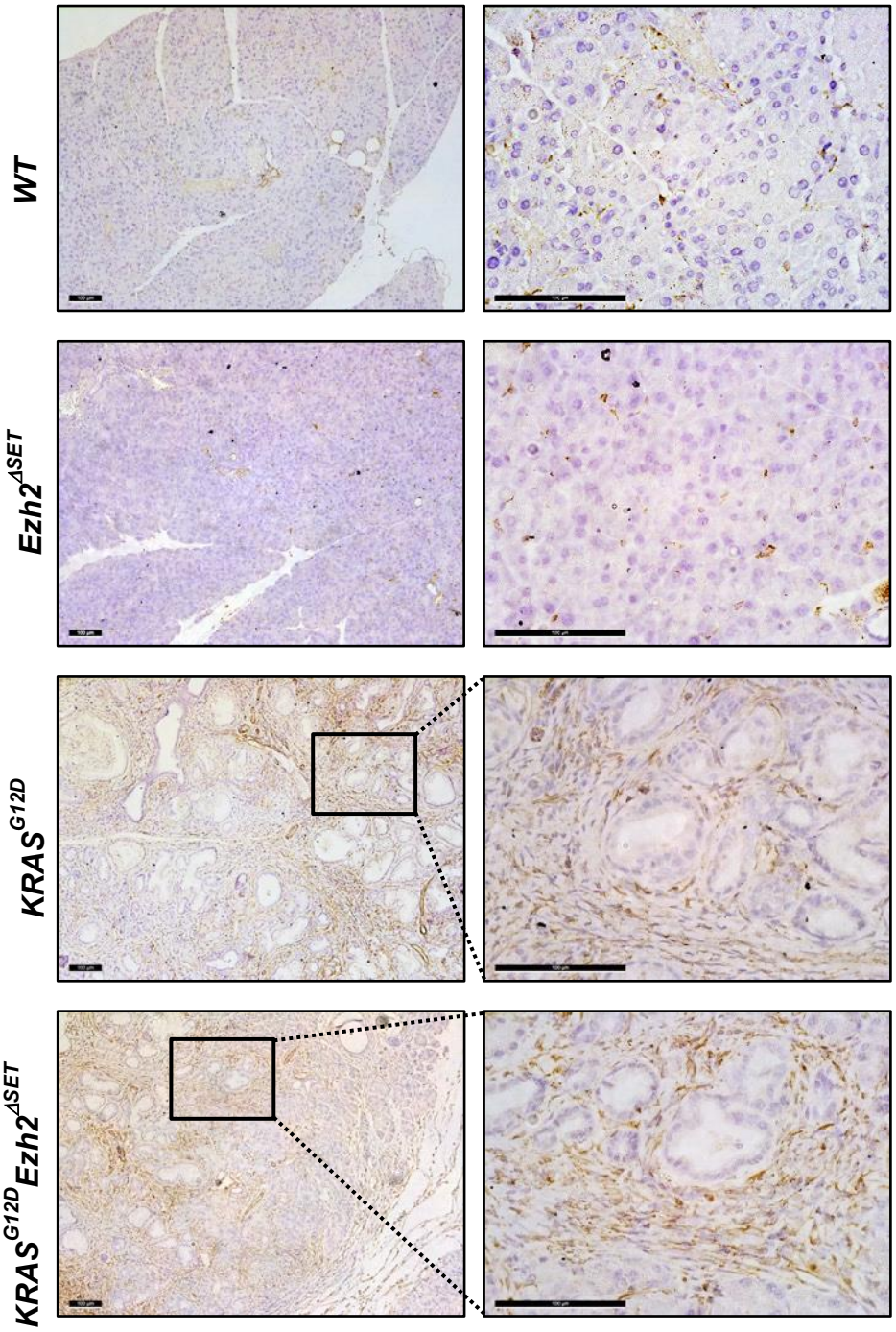
WT
Ezh2ΔSET
KRASG12D
KRASG12DEzh2ΔSET

Figure 3.14 EZH2 deletion does not alter the total amount of CAFs in the tumor microenvironment. Representative high (right) and low (left) power IHC images of panCAF marker vimentin in *KRAS*^{G12D}*Ezh2*$^{\Delta SET}$ and *KRAS*^{G12D} tissue samples showed no overall difference in the expression level. Magnification bar = 100 μm.

3.5 The loss of EZH2 does not affect *KRAS*-mediated ADM in cell culture

Based on *in vivo* experiments, the loss of *EZH2* appeared to promote the progression of PDAC in the $KRAS^{G12D}$ context and reduce immune cell recruitment into the TME. To determine if acinar expression of $KRAS^{G12D}$ along with *EZH2* deletion increased ADM without the effects of the TME, acinar cells from WT, $Ezh2^{\Delta SET}$, $KRAS^{G12D}$ and $KRAS^{G12D}$ $Ezh2^{\Delta SET}$ pancreata were isolated 22 days after tamoxifen injections and embedded in 3D collagen culture. Acinar cells were maintained and monitored for five days in the culture post-isolation. The development of cysts (putative ADM) was measured by calculating the number of cysts formed as a percentage of total clusters of cells, which represent individual acini. The size of ADM was measured for 10-20 clusters. WT and $Ezh2^{\Delta SET}$ cells formed cysts in less than 10% of the total acinar clusters by day 2, while $KRAS^{G12D}$ and $KRAS^{G12D}Ezh2^{\Delta SET}$ acinar cells clusters formed cysts in the majority of clusters examined, reaching up to 95% of the total cell clusters. From day 2 to day 5, significantly more cysts were formed in $KRAS^{G12D}$ and $KRAS^{G12D}Ezh2^{\Delta SET}$ cultures than in WT and $Ezh2^{\Delta SET}$ cells ($P<0.05$) (**Figure 3.15A-B**). However, from the third experimental day, ADM did not change in size and appeared to undergo apoptosis or necrosis, leading to a decrease in the percentage of cysts observed (**Figure 3.15A-B**). Analysis of cyst formation in culture showed no significant differences between $KRAS^{G12D}$ and $KRAS^{G12D}Ezh2^{\Delta SET}$ acini, suggesting *EZH2* does not overtly affect cyst formation, consistent with in vivo data. Next, I examine changes in the size of the cysts throughout experimental days. Morphologically, cysts developed from WT, $Ezh2^{\Delta SET}$, $KRAS^{G12D}$ and $KRAS^{G12D}$ $Ezh2^{\Delta SET}$ all increased their size to different extent during growth in the collagen culture in the beginning. Started from the second day in culture, $KRAS^{G12D}$ and $KRAS^{G12D}$ $Ezh2^{\Delta SET}$ acinar cell clusters formed cysts that became spherical and exhibited hollow lumens. These cysts reached a final size of ~40,000 μm^2, while only ~5,000 μm^2 in WT and $Ezh2^{\Delta SET}$ cultures. (**Figure 3.15C**). The percentage and size of cysts was comparable between $KRAS^{G12D}$ and $KRAS^{G12D}Ezh2^{\Delta SET}$ cells, indicating that knockout of *Ezh2* alone did not affect the growth of KRAS-mediated ADM in culture in an overt fashion.

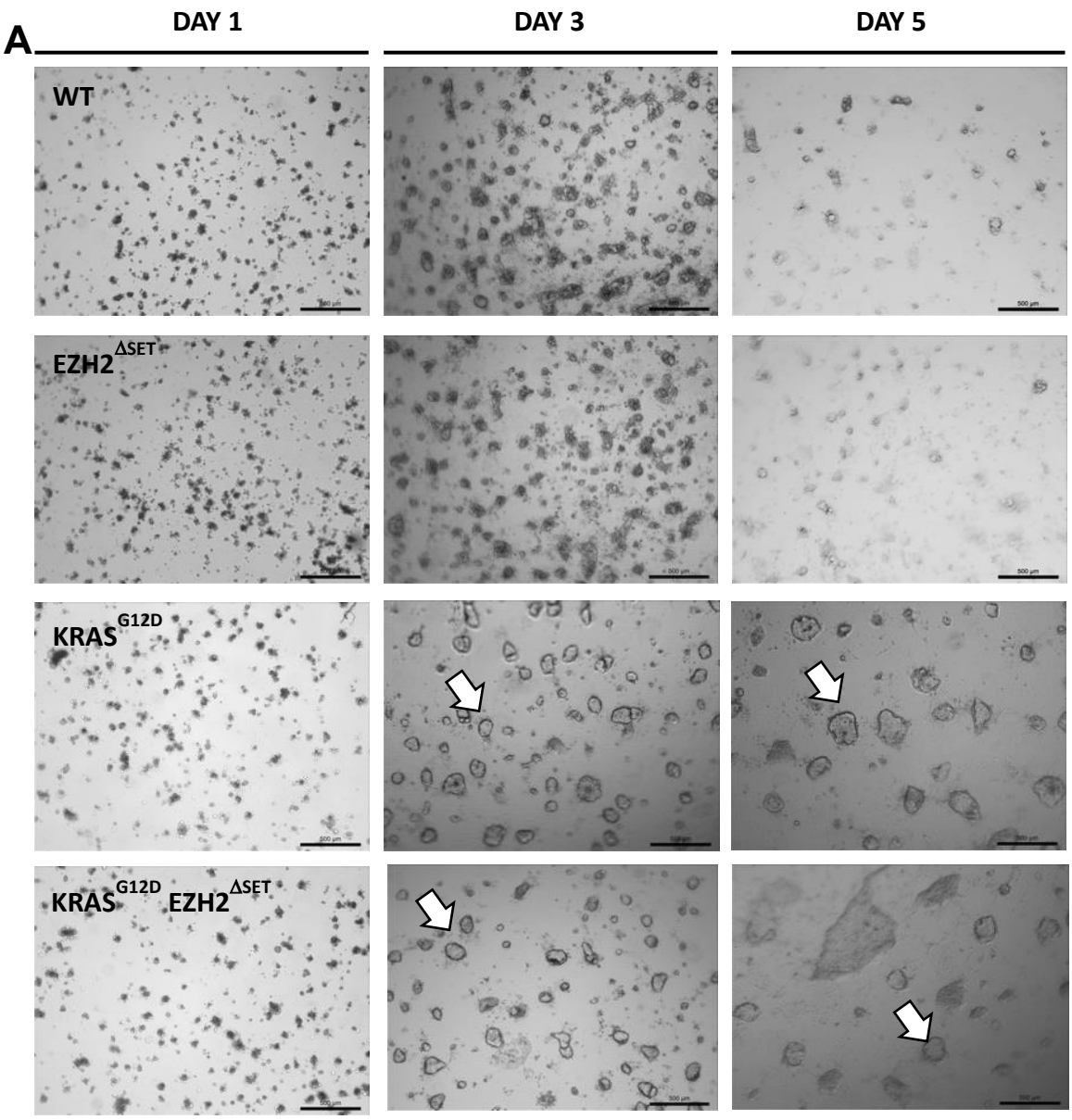
A
DAY 1
DAY 3
DAY 5
WT
EZH2ΔSET
KRASG12D
KRASG12D EZH2ΔSET

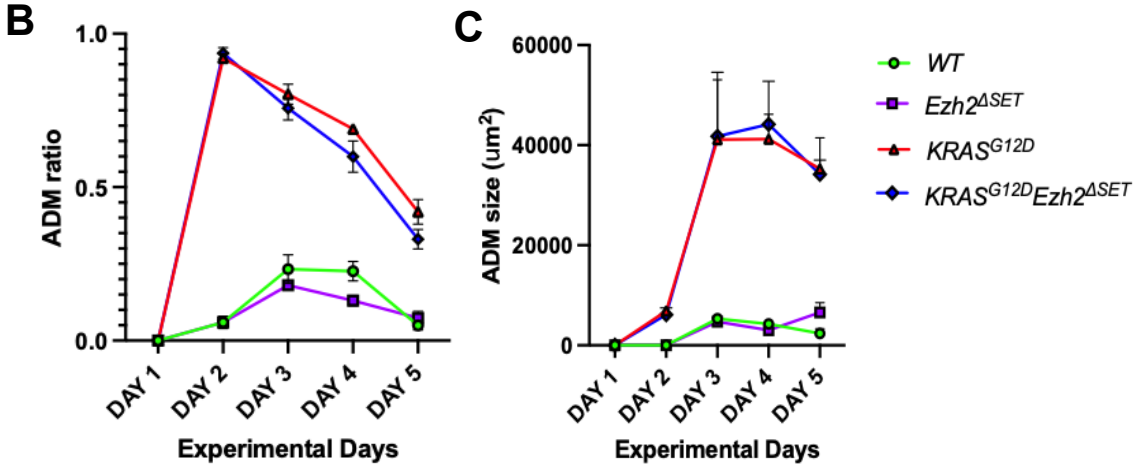
B
ADM ratio
1.0
0.5
0.0
DAY 1
DAY 2
DAY 3
DAY 4
DAY 5
Experimental Days
C
ADM size (um2)
60000
40000
20000
0
DAY 1
DAY 2
DAY 3
DAY 4
DAY 5
Experimental Days
WT
Ezh2ΔSET
KRASG12D
KRASG12DEzh2ΔSET

Figure 3.15 Loss of EZH2 does not affect the amount of KRAS^{G12D}-mediated ADM.

(A) Phase contrast microscopy of acinar cells derived from WT, EZH2$^{\Delta SET}$, KRAS^{G12D}, and KRAS^{G12D}EZH2$^{\Delta SET}$ mice two weeks after tamoxifen administration. Images were taken one, three, and five days in culture. White arrows indicate the presence of cysts (putative ADM). Magnification bar = 100 μm. **(B)** Quantification of the percentage of ADM (% mean ± SEM; n=3) formation showed significant differences between cells with and without *KRAS^{G12D}* activation ($P<0.05$) from day 2-5, but no significant difference found between cells with and without EZH2 ($P>0.05$). **(C)** Quantification of the size of ADM (mm^2 mean ± SD; n=3) from day 1 to day 5. Significant difference was observed between cells with and without *KRAS^{G12D}* activation ($P<0.05$). No significant difference was found between cells with and without EZH2 ($P>0.05$). A repeated measure Two-way ANOVA with a Tukey's Post hoc test was performed.

4 CHAPTER 4: DISCUSSION

4.1 Conclusions

In this thesis, I examined the role of EZH2 in *KRAS*^{G12D}-driven PDAC in response to acute pancreatitis and in *KRAS*^{G12D}-mediated ADM formation in ex vivo cultures. I showed that the absence of EZH2 in adult acinar cells resulted in more progressive PanIN lesions following pancreatic injury and KRAS^{G12D} activation. RNA-seq analysis showed loss of *EZH2* altered the molecular response to KRAS^{G12D} in mouse pancreatic acinar cells, but only a small number of genes were differentially expressed between acinar cells expressing EZH2 or not expressing EZH2. The majority of significantly affected genes were associated with inflammatory signaling pathways. These findings were supported in the context of KRAS^{G12D} expression in the presence of pancreatic injury. The absence of EZH2 methyltransferase activity resulted in reduced immune cell infiltration in the tumor microenvironment, especially macrophages. Interestingly, EZH2 deletion did not affect the development of *KRAS*-driven ADM in cell culture, as the rate of ADM formation and size were unaffected by the absence of EZH2. These findings suggest the effects of EZH2 may be through the tumor microenvironment. Taken together, these data suggest EZH2 modulates inflammatory infiltration and results in higher grade of PanIN lesions following acute pancreatic injury. The findings highlight the potential of *EZH2* as a direct therapeutic target to prevent tumor growth in PDAC patients.

4.2 Overview

Despite extensive research efforts, PDAC continues to be a leading cause of death in Canada due to the lack of early detection methods and effective treatments. The *KRAS* gene is mutated in 95% of all PDAC cases (Guo et al., 2016) and plays a role in the initiation of PDAC by promoting irreversible acinar-to-ductal metaplasia (ADM) process. This leads to low-grade PanINs and increases the risk of further progressing to PDAC (Andrew et al., 2020). Previous research showed the epigenetic regulator EZH2 played a key role in the development of KRAS^{G12D}-driven PDAC. For example, Mallen St. Clair et al. (2012) showed *Ezh2* deletion in mouse embryos accelerated KRAS^{G12D}-mediated PDAC and

prevented pancreatic regeneration. Conversely, Chen et al. (2017) found during late stages of PDAC development, EZH2 deficiency reduced tumor expansion. Both human research and studies on mouse models revealed high levels of EZH2 often correlated to more aggressive and invasive PDAC phenotype and reduced sensitivity to *KRAS* oncogene (Kim et al., 2015; Patil et al., 2020).

In this thesis, I specifically looked at the effects of *Ezh2* deletion on *KRAS*-driven PDAC progression in the context of acinar cells from adult transgenic mice and addressed the hypothesis in early neoplasia in the pancreas before the development of invasive PDAC, which is distinct from the other studies and is not well-addressed before.

4.3 EZH2 restricts the progression of $KRAS^{G12D}$-driven PDAC following acute pancreatic injury without limiting PanIN lesion expansion

A previous study from our lab that examined the effects of EZH2 deficiency in *KRAS*-mediated PDAC that developed spontaneously in adult mice revealed no significant differences in morphological and histological changes in the pancreas. Conversely, EZH2 appeared to dramatically enhance *KRAS*-mediated ADM and PDAC when combined with events that trigger acinar cell dedifferentiation such as *Mist1* deficiency (Shi et al, 2013). Therefore, the work presented in this study utilized methodology that induced acute pancreatic injury, which increases the susceptibility to PDAC, five weeks prior to histological analysis to investigate in detail whether EZH2 deletion affects the progression of PDAC in the context of $KRAS^{G12D}$.

My results showed no evident histological changes in overall lesion formation, which contradicts previous findings (Mallen St. Clair et al, 2012). The lesion size and level of fibrosis of the tumor microenvironment was similar in the absence of EZH2 and constitutive activation of $KRAS^{G12D}$, suggesting loss of EZH2 does not significantly promote or restrict *KRAS*-driven PanIN lesion expansion in response to acute injury. However, significantly more mucin+ PanIN lesions were observed in $KRAS^{G12D}Ezh2^{\Delta SET}$ tissues, suggesting more higher-grade lesions in $KRAS^{G12D}Ezh2^{\Delta SET}$ compared to $KRAS^{G12D}$

tissues. Similar to Mallen St. Clair et al. (2012) whose findings support a model that *KRAS*-mediated PDAC is accelerated by deletion of EZH2. In contradiction with that same study, which demonstrated a vital role of EZH2 in tissue regeneration in response to pancreatic injury (Mallen St. Clair et al., 2012), the loss of EZH2 alone without the effects of oncogenic KRAS did not affect pancreatic regeneration and repair.

The contradictory findings may be explained by differences in the mouse models used and distinct roles for EZH2 at different stages of PDAC progression. Our model focussed on induced deletion of EZH2 and activation of $KRAS^{G12D}$ in adult mice instead of mouse embryos, which is a better predictor of PDAC in humans since most people accumulate mutations and develop cancers later in life. Another explanation for the inconsistency is that different Cre recombinase drivers were used in this project vs. previous studies. Most studies utilize the *Ptf1a* locus as a Cre driver to induce genetic recombination specifically in mouse pancreas, including constitutive $KRAS^{G12D}$ activation and *Ezh2* deletion. Since *Ptf1a* is a crucial gene for pancreatic organogenesis and is expressed in pancreatic multipotent pancreatic cells (MPCs) during development, it may lead to a recombined allele in all cell types in mouse pancreas. However, Ptf1a expression is restricted to acinar cells in adult mice (Kawaguchi et al., 2002). In my thesis, *Mist1* was used as a driver gene to induce acinar-specific deletion. While it is reported that *Ptf1a* and *Mist1* are both essential for maintaining mature acinar identity and restricting *KRAS*-mediated tumorigenesis (Jiang et al., 2016), our preliminary lab data demonstrated a significant difference in the progression of PanIN lesions between PK ($Ptf1a^{creERT/+}KRAS^{G12D}$) and MK ($Mist1^{creERT/+}KRAS^{G12D}$) (unpublished data; Mousavi and Lau).

As previously mentioned, Mallen St. Clair et al. (2012) demonstrated the loss of EZH2 function promotes neoplastic progression during early stage of PDAC, while Chen et al. (2017) stated at late stages of pancreatic regeneration after injury, the loss of EZH2 allows acinar cell redifferentiation and pancreatic tissue recovery. Accumulating evidence suggests EZH2 might have distinct roles at different stages of PDAC progression, and the activation of KRAS oncogene may play a role in modulating the effects of EZH2 in a temporal manner. Therefore, it is possible that the inconsistency between studies is due to different experimental timing that reflect different outcomes, meaning that EZH2 caused

more progressed PanIN lesions in the context of $KRAS^{G12D}$ at the beginning, but trending toward a decreased level of lesions at later stage.

Overall, my data suggest that EZH2 restricts *KRAS*-mediated early PanIN progression in mouse models without limiting PanIN expansion, which raises the question of whether the absence of EZH2 caused genetic alterations that can explain the more progressive phenotype and what intracellular signalling pathways are involved.

4.4 EZH2 dysregulation affects inflammatory response pathways in response to $KRAS^{G12D}$

EZH2 normally functions to suppress gene expression and transcriptional silencing of genes mediated by aberrant EZH2 function has been implicated in cancer cell metastasis. To understand how EZH2 deletion enhances PDAC progression, I examined RNA-seq analysis 22 days after tamoxifen induction and see whether the absence of EZH2 altered the molecular response to $KRAS^{G12D}$ hyperactivation in mouse acinar cells without cerulein-induced injury. RNA-seq analysis identified 315 genes that were differentially expressed between $KRAS^{G12D}$ and $KRAS^{G12D}Ezh2^{\Delta SET}$ cells, at a time when there were no phenotypic differences between the two lines. 237 genes were significantly upregulated and 78 were significantly downregulated in $KRAS^{G12D}Ezh2^{\Delta SET}$ relative to $KRAS^{G12D}$ cells. Consistent with the well-known role of EZH2 as an epigenetic suppressor, more genes seemed to have increased expression levels in the absence of EZH2. GO analysis identified five pathways specifically linked to immune related functions, suggesting an effect on the TME. One immunity related pathway is the adaptive immune response pathway, which predominantly involves the function of T lymphocytes (Slack, 2020). It is reported, however, that EZH2 is overexpressed in many typical cancers and functions by suppressing the activation of the adaptive immune response pathway (Zhao et al., 2016). This specifically affects the anti-tumor effects of the cytotoxic or pro-inflammatory immune response in the pancreas. Other affected pathways include leukocyte mediated immunity pathway, negative regulation of immune system process, and lymphocyte mediated immunity. These findings suggest the deletion of EZH2 alters many intrinsic, immune-

related pathways that may affect the TME, which may explain the higher grade PanIN lesions observed in *KRAS^{G12D}Ezh2$^{\Delta SET}$* mice.

The complement *C3*, one of the genes significantly differentially expressed between *KRAS^{G12D}* and *KRAS^{G12D}Ezh2$^{\Delta SET}$*, is specifically studied in this project because it is involved in most of the top ranked pathways. The *C3* gene encodes the protein complement component 3, which plays a key role in the complement system as part of the immune response (Zhang et al., 2020). The complement system is a group of proteins that collaborate to prevent and destroy foreign invaders and trigger inflammation. Previous studies identified the prognostic role of complement C3 in early stage of acute pancreatitis (Zhang et al., 2020), and revealed that the complement system can interact with cancer cells to contribute to proliferation, migration, and invasion of tumor cells (Zhang et al., 2019). C3 can be used as an effective marker for the diagnosis of PDAC at early stages (Peterson et al., 2017). According to the RNA-seq data, C3 is significantly expressed at higher level (1.5-fold) in *KRAS^{G12D}Ezh2$^{\Delta SET}$* compared to *KRAS^{G12D}* cells. Consistent with these data, C3 was expressed in *KRAS^{G12D}Ezh2$^{\Delta SET}$* tissues in the mouse model that received cerulein treatment five weeks before dissection. Positive C3 signals were specifically observed in columnar epithelial cells within the lesion. Although it is still not known if differentially expressed C3 contributes to the more progressive PanIN phenotype, high C3 level is often correlated to inflammation in the body (Liu et a., 2016). Overall, these data confirmed the finding that the absence of epigenetic repressor EZH2 results in activation of expression of many genes including *C3*, and that inflammatory pathways could be closely related to the development of early PDAC. As the RNA-seq analysis was performed on tissue with a normal phenotype before progression to PanINs and without an injury stimulant, I next investigated the possibility that *KRAS^{G12D}Ezh2$^{\Delta SET}$* mice show a differential immune response to injury. Because the molecular response to *KRAS* activation could be dramatically changed in response to injury, work on gene expression profiles at later stages of PanIN progression is warranted in the future.

4.5 EZH2 plays a role in tumor microenvironment modulation

Recent studies revealed an immune modulatory function of EZH2 in the TME (Wang et al., 2019). To examine the immune response in the pancreas in the absence of EZH2 as well as $KRAS^{G12D}$ activation, I analyzed the effects of EZH2 knockout on accumulation of immune cell populations and CAFs following acute pancreatic injury. $KRAS^{G12D}Ezh2^{\Delta SET}$ mice exhibited a trend towards decreased accumulation of T cells and cytotoxic T cells in the TME compared to $KRAS^{G12D}$ mice, and this could correspond to a more aggressive phenotype of $KRAS^{G12D}Ezh2^{\Delta SET}$ tissues. T cells are a type of leucocyte that plays an important role in the body's immune system. It is previously demonstrated that aberrant EZH2 function plays a critical role in the recruitment of Tregs at the sites of inflammation, which perform immunosuppressive functions by restricting the T effector cells (DuPage et al., 2015; Yang et al., 2015). Overexpression of EZH2 in late-stage PDAC leads to excessive recruitment of Tregs, which largely inhibits infiltration of cytotoxic cells and therefore maintains a pro-tumor microenvironment. In this case, however, the deletion of EZH2 results in a slightly restricted recruitment of cytotoxic T cells compared to tissues with normal EZH2 function, suggesting distinct roles for EZH2 in the initiation and late stage of PDAC. EZH2 is deleted specifically in acinar cells as the driver gene *Mist1* is acinar-specific, which may also explain the inconsistency between previous study and this finding.

Surprisingly, I observed significantly more macrophages within the TME of $KRAS^{G12D}$ tissues. The amount of macrophage recruitment in the stroma largely varies in $KRAS^{G12D}$ samples from 0.20% to 2.25% positive stain verses the total lesion area, which may reflect the variability seen previously for the percentages of lesions area in $KRAS^{G12D}$. Macrophages are the most abundant immune cells in the TME and promote a favorable microenvironment for cancer cells by directly interacting and inhibiting cytotoxic T cells (Borrego et al., 1998). Therefore, the presence of macrophages is normally associated with immunosuppression and poor clinical outcome which is inconsistent with $KRAS^{G12D}$ $Ezh2^{\Delta SET}$ tissue having fewer macrophages in the TME but exhibiting a more advanced phenotype. Although it is hard to conclude the reason why this correlation appeared, it is

possible that expression of EZH2 in *KRAS*^{G12D} tissues increases the inflammatory response mediated by macrophages, which restrained the recruitment of CD3+ and CD8+ T cells to the sites of inflammation in the TME. However, this thesis only focussed on early pre-neoplastic events when the PanIN lesions just started to appear with *KRAS*^{G12D} as the only oncogenic mutation. This may explain the inconsistency since most previous studies looked at late-stage PDAC with additional oncogenic mutations such as *Tp53*. In addition, F4/80 is a global marker for macrophages, which includes anti-tumor inflammatory M1 subtype and tumorigenic immune-suppressive M2 subtype, making it hard to conclude whether the massive infiltration of macrophages in *KRAS*^{G12D} tissues plays a role in preventing or promoting PDAC.

The stromal response to pancreatic injury involves CAFs, which include myCAFs and iCAFs. MyCAFs are believed to promote tumorigenesis by secreting soluble factors and ECM proteins. In this study, however, no obvious differences were observed in the amount of myCAFs and total CAFs in the TME in both genotypes, suggesting EZH2 deletion does not enhance PDAC progression by altering CAFs in the TME. Combined, this data shows *Ezh2*$^{\Delta SET}$ deletion in KRAS^{G12D}-mediated PanIN progression decreases immune infiltration in pancreas but does not promote differences in CAFs remodeling.

In summary, EZH2's role in preventing the progression of *KRAS*-driven PanIN lesions is correlated with its function of epigenetically silencing immune-related genes and altering associated inflammatory response pathways, which leads to higher level of immune cell recruitment in the TME.

4.6 The role of EZH2 is context dependent

Next, I investigated whether the loss of *Ezh2* in acinar cells caused more progressive *KRAS*-mediated ADM formation without the presence of surrounding TME. To do this, the effects of EZH2 on the ADM process was assessed through primary acinar cultures. Oncogenic *KRAS*^{G12D} activation and *Ezh2* deletion were specifically induced in acinar cells 21 days before acinar cell isolation and culturing in 3D collagen culture. Type I collagen was specifically used for embedding acinar cells because collagen I is the most common type

of ECM protein found in skin, bones, and connective tissues, and is suitable for maintaining cells (Mochizuki et al., 2020). *KRAS*^{G12D}-expressing acinar cells, whether coupled with the loss of EZH2 or not, showed increased acinar cell dedifferentiation and formed duct-like cystic structures, suggesting a central role for *KRAS*^{G12D} in driving ADM, which is consistent with previous study. Interestingly, the loss of EZH2 function did not result in a greater percentage of *KRAS*-mediated ADM formation or significant increase in ADM size in *KRAS*^{G12D} *Ezh2*$^{\Delta SET}$ cells as predicted. This suggests that the effects of EZH2 alone are not able to cause visible phenotypic changes in acinar cells. Conversely, WT and *Ezh2*$^{\Delta SET}$ cells exhibited a limited ability to form ADM in the culture, and acinar cell clusters are short-lived. The size of cysts developed in WT and *Ezh2*$^{\Delta SET}$ were also considerably smaller than that in *KRAS*^{G12D} and *KRAS*^{G12D}*Ezh2*$^{\Delta SET}$ cultures. Similarly, the loss of EZH2 did not seem to promote or prevent the formation of cysts without *KRAS*^{G12D}. It is noted that following the first day in the culture, when KRAS^{G12D}-expressing cells rapidly underwent ADM, the survival rate of cysts dropped quickly after day 2 in all genotypes, suggesting a lack of the ability to proliferate. It is, however, expected because when these cells were isolated and plated in the culture, they are normal acinar cells with WT-like phenotype, not proliferating PDAC tumor cells that normally last longer in collagen culture. Overall, in the absence of the TME, the loss of EZH2 did not results in more progressed ADM formation even in the context of *KRAS*^{G12D}. This again suggests the role of EZH2 in preventing PanIN progress *in vivo* might be context dependent. It is likely that the effects of EZH2 in restricting PanIN progression is dependent on the TME.

However, it is possible that the deletion of EZH2 altered gene expression pattern in *KRAS*^{G12D}*Ezh2*$^{\Delta SET}$ cells but is not significant enough to lead to visible phenotypic changes to the cysts. Further research is required to investigate whether the absence of EZH2 changes the molecular response of acinar cells to *KRAS* oncogene.

4.7 Limitations and future directions

In this study, limitations of both *in vivo* and *in vitro* experiments exist. In acute models of PanIN, differences in collagen, myCAFs, and panCAFs in pancreatic tissues between genotypes could not be assessed due to insufficient n value. To complete these analysis,

repeated experiments with increased n values are needed. In terms of the *in vitro* work, maintaining acinar cells in good condition over five experimental days provided limitations to this study. In addition, technical difficulties in cysts isolation, fixation, and paraffin-embedding following five days in culture limit the possibilities in histological analysis of ADM.

In future studies, further efforts are required to establish the mechanisms by which EZH2 is restricting the progression of early PanIN lesions in the context of $KRAS^{G12D}$ hyperactivation. Performing ChIP-seq for H3K27me3 on acinar cells isolated at different time points, for examples 21 days after tamoxifen injection or five weeks after cerulein treatment, or five days after culturing, could be beneficial. This will allow us to determine potential targets of EZH2 by looking at H3K27me3 pattern in the genome. It would also help determine whether EZH2 has distinct roles in terms of the activation or silencing of genes at different time points during early PanIN progression. To investigate the involvement of EZH2 in intracellular mechanisms that restrict *KRAS*-mediated PanIN progression, several significant genes could be chosen for expression analysis by immunofluorescence (IF) or Western blotting to examine co-localization and amount of expression in pancreatic tissues, which may help with identifying the involvement of these genes in signaling pathways potentially affected by EZH2.

To further determine if the loss of EZH2 caused more progressive phenotype of ADM through modulating the TME, cysts growth could be examined in culture under additional conditions. Co-culture of mouse acinar cells and immune cells, including T cells and macrophages, could be used to investigate individual role of immune cell recruitment around ADM and whether *KRAS*-expressing cysts with EZH2 deletion will be more proliferative and grow bigger. Alternatively, we could treat cells with chemicals released by different immune cells, such as chemokines and cytokines, and monitor cyst growth to see if the presence of any factors contributes to a more advance phenotype of ADM.

4.8 Conclusion

In summary, the findings in this thesis support a preventive role for EZH2 in initiating *KRAS*-driven PDAC. In the context of acute pancreatic injury *in vivo,* the loss of EZH2 leads to greater extent of preneoplastic PanIN lesions without limiting PanIN lesion expansion. Although only a small number of genes are significantly dysregulated due to the lack of EZH2 function in response to $KRAS^{G12D}$, most of them are upregulated in the absence of EZH2 and are involved in multiple inflammatory response pathways, reflecting the role of EZH2 as an epigenetic suppressor. I also identified the role of EZH2 in modulating the tumor microenvironment by promoting recruitment of immune cells to the sites of inflammation, which might in turn contribute to the less progressive outcome in $KRAS^{G12D}$ tissues. However, EZH2 is not able prevent *KRAS*-driven acinar cell dedifferentiation in the cell culture, highlighting the context-dependent role of EZH2 in repressing *KRAS*-mediated ADM and PanIN through modulating the TME.

REFERENCE

Abukiwan, A., & R. Berger, M. (2019). Epigenetics: Dissecting Gene Expression Alteration in PDAC. In *DNA Repair- An Update*.

Adeegbe, D. O., & Nishikawa, H. (2013). Natural and induced T regulatory cells in cancer. In *Frontiers in Immunology* (Vol. 4, Issue JUL).

Adell, T., Gómez-Cuadrado, A., Skoudy, A., Pettengill, O. S., Longnecker, D. S., & Real, F. X. (2000). Role of the basic helix-loop-helix transcription factor p48 in the differentiation phenotype of exocrine pancreas cancer cells. *Cell Growth and Differentiation*, *11*(3).

Ambros, V. (2004). The functions of animal microRNAs. In *Nature* (Vol. 431, Issue 7006).

Antequera, F., & Bird, A. (1999). CpG islands as genomic footprints of promoters that are associated with replication origins. *Current Biology*, *9*(17).

Ardito, C. M., Grüner, B. M., Takeuchi, K. K., Lubeseder-Martellato, C., Teichmann, N., Mazur, P. K., DelGiorno, K. E., Carpenter, E. S., Halbrook, C. J., Hall, J. C., Pal, D., Briel, T., Herner, A., Trajkovic-Arsic, M., Sipos, B., Liou, G. Y., Storz, P., Murray, N. R., Threadgill, D. W., … Siveke, J. T. (2012). EGF Receptor Is Required for KRAS-Induced Pancreatic Tumorigenesis. *Cancer Cell*, *22*(3).

Audia, J. E., & Campbell, R. M. (2016). Histone modifications and cancer. *Cold Spring Harbor Perspectives in Biology*, *8*(4).

Azizi, N., Toma, J., Martin, M., Khalid, M. F., Mousavi, F., Win, P. W., Borrello, M. T., Steele, N., Shi, J., di Magliano, M. P., & Pin, C. L. (2021). Loss of activating transcription factor 3 prevents KRAS-mediated pancreatic cancer. *Oncogene*, *40*(17).

Bachem, M. G., Zhou, Z., Zhou, S., & Siech, M. (2006). Role of stellate cells in pancreatic fibrogenesis associated with acute and chronic pancreatitis. *Journal of Gastroenterology and Hepatology (Australia)*, *21*(SUPPL. 3).

Becker, A. E., Hernandez, Y. G., Frucht, H., & Lucas, A. L. (2014). Pancreatic ductal adenocarcinoma: Risk factors, screening, and early detection. In *World Journal of Gastroenterology* (Vol. 20, Issue 32).

Biffi, G. (2020). Tracing the Origin of Fibroblasts in Pancreatic Cancer. In *CMGH* (Vol. 10, Issue 3).

Binkley, C. E., Zhang, L., Greenson, J. K., Giordano, T. J., Kuick, R., Misek, D., Hanash, S., Logsdon, C. D., & Simeone, D. M. (2004). The molecular basis of pancreatic fibrosis: Common stromal gene expression in chronic pancreatitis and pancreatic adenocarcinoma. *Pancreas*, *29*(4).

Black, J. C., van Rechem, C., & Whetstine, J. R. (2012). Histone Lysine Methylation Dynamics: Establishment, Regulation, and Biological Impact. In *Molecular Cell* (Vol. 48, Issue 4).

Borrego, F., Ulbrecht, M., Weiss, E. H., Coligan, J. E., & Brooks, A. G. (1998). Recognition of human histocompatibility leukocyte antigen (HLA)-E complexed with HLA class I signal sequence-derived peptides by CD94/NKG2 confers protection from natural killer cell-mediated lysis. *Journal of Experimental Medicine*, *187*(5).

Bosetti, C., Bertuccio, P., Negri, E., la Vecchia, C., Zeegers, M. P., & Boffetta, P. (2012). Pancreatic cancer: Overview of descriptive epidemiology. *Molecular Carcinogenesis*, *51*(1).

Bournet, B., Muscari, F., Buscail, C., Assenat, E., Barthet, M., Hammel, P., Selves, J., Guimbaud, R., Cordelier, P., & Buscail, L. (2016). KRAS G12D mutation subtype is a prognostic factor for advanced pancreatic adenocarcinoma. *Clinical and Translational Gastroenterology*, *7*(3).

Boursi, B., Finkelman, B., Giantonio, B. J., Haynes, K., Rustgi, A. K., Rhim, A. D., Mamtani, R., & Yang, Y. X. (2017). A Clinical Prediction Model to Assess Risk for Pancreatic Cancer Among Patients With New-Onset Diabetes. *Gastroenterology*, *152*(4).

Brancaccio, M., Natale, F., Falco, G., & Angrisano, T. (2020). Cell-free dna methylation: The new frontiers of pancreatic cancer biomarkers' discovery. In *Genes* (Vol. 11, Issue 1).

Brembeck, F. H., Schreiber, F. S., Deramaudt, T. B., Craig, L., Rhoades, B., Swain, G., Grippo, P., Stoffers, D. A., Silberg, D. G., & Rustgi, A. K. (2003). The mutant K-ras oncogene causes pancreatic periductal lymphocytic infiltration and gastric mucous neck cell hyperplasia in transgenic mice. *Cancer Research*, *63*(9).

Buscail, L., Bournet, B., & Cordelier, P. (2020). Role of oncogenic KRAS in the diagnosis, prognosis and treatment of pancreatic cancer. In *Nature Reviews Gastroenterology and Hepatology* (Vol. 17, Issue 3).

Cao, R., Wang, L., Wang, H., Xia, L., Erdjument-Bromage, H., Tempst, P., Jones, R. S., & Zhang, Y. (2002). Role of histone H3 lysine 27 methylation in polycomb-group silencing. *Science*, *298*(5595).

Cao, R., & Zhang, Y. (2004). SUZ12 is required for both the histone methyltransferase activity and the silencing function of the EED-EZH2 complex. *Molecular Cell*, *15*(1).

Cardoso, C., Mignon, C., Hetet, G., Grandchamps, B., Fontes, M., & Colleaux, L. (2000). The human EZH2 gene: Genomic organisation and revised mapping in 7q35 within the critical region for malignant myeloid disorders. *European Journal of Human Genetics*, *8*(3).

Cargnello, M., & Roux, P. P. (2011). Activation and Function of the MAPKs and Their Substrates, the MAPK-Activated Protein Kinases. *Microbiology and Molecular Biology Reviews*, *75*(1).

Carrière, C., Young, A. L., Gunn, J. R., Longnecker, D. S., & Korc, M. (2009). Acute pancreatitis markedly accelerates pancreatic cancer progression in mice expressing oncogenic Kras. *Biochemical and Biophysical Research Communications*, *382*(3).

Chan-Seng-Yue, M., Kim, J. C., Wilson, G. W., Ng, K., Figueroa, E. F., O'Kane, G. M., Connor, A. A., Denroche, R. E., Grant, R. C., McLeod, J., Wilson, J. M., Jang, G. H., Zhang, A., Dodd, A., Liang, S. ben, Borgida, A., Chadwick, D., Kalimuthu, S., Lungu, I., … Notta, F. (2020). Transcription phenotypes of pancreatic cancer are driven by genomic events during tumor evolution. *Nature Genetics*, *52*(2).

Chen, N. M., Neesse, A., Dyck, M. L., Steuber, B., Koenig, A. O., Lubeseder-Martellato, C., Winter, T., Forster, T., Bohnenberger, H., Kitz, J., Reuter-Jessen, K., Griesmann, H., Gaedcke, J., Grade, M., Zhang, J. S., Tsai, W. C., Siveke, J., Schildhaus, H. U., Ströbel, P., … Hessmann, E. (2017). Context-Dependent Epigenetic Regulation of Nuclear Factor of Activated T Cells 1 in Pancreatic Plasticity. *Gastroenterology*, *152*(6).

Cheng, X., & Blumenthal, R. M. (2008). Mammalian DNA Methyltransferases: A Structural Perspective. In *Structure* (Vol. 16, Issue 3).

Chiappinelli, K. B., Zahnow, C. A., Ahuja, N., & Bylin, S. B. (2016). Combining epigenetic and immunotherapy to combat cancer. In *Cancer Research* (Vol. 76, Issue 7).

Chica, C., Louis, A., Roest Crollius, H., Colot, V., & Roudier, F. (2017). Comparative epigenomics in the Brassicaceae reveals two evolutionarily conserved modes of PRC2-mediated gene regulation. *Genome Biology*, *18*(1).

Clemens, D. L., Wells, M. A., Schneider, K. J., & Singh, S. (2014). Molecular mechanisms of alcohol associated pancreatitis. *World Journal of Gastrointestinal Pathophysiology*, *5*(3).

Collins, M. A., Bednar, F., Zhang, Y., Brisset, J. C., Galbán, S., Galbán, C. J., Rakshit, S., Flannagan, K. S., Adsay, N. V., & Pasca Di Magliano, M. (2012). Oncogenic Kras is required for both the initiation and maintenance of pancreatic cancer in mice. *Journal of Clinical Investigation*, *122*(2).

Collins, M. A., Yan, W., Sebolt-Leopold, J. S., & Pasca Di Magliano, M. (2014). MAPK signaling is required for dedifferentiation of acinar cells and development of pancreatic intraepithelial neoplasia in mice. *Gastroenterology*, *146*(3).

Collinson, A., Collier, A. J., Morgan, N. P., Sienerth, A. R., Chandra, T., Andrews, S., & Rugg-Gunn, P. J. (2016). Deletion of the Polycomb-Group Protein EZH2 Leads to Compromised Self-Renewal and Differentiation Defects in Human Embryonic Stem Cells. *Cell Reports*, *17*(10).

Collisson, E. A., Trejo, C. L., Silva, J. M., Gu, S., Korkola, J. E., Heiser, L. M., Charles, R. P., Rabinovich, B. A., Hann, B., Dankort, D., Spellman, P. T., Phillips, W. A., Gray, J. W., &

McMahon, M. (2012). A Central role for RAF→MEK→ERK signaling in the genesis of pancreatic ductal adenocarcinoma. *Cancer Discovery*, *2*(8).

Corbo, V., Tortora, G., & Scarpa, A. (2012). Molecular Pathology of Pancreatic Cancer: From Bench-to-Bedside Translation. *Current Drug Targets*, *13*(6).

Curiel, T. J., Coukos, G., Zou, L., Alvarez, X., Cheng, P., Mottram, P., Evdemon-Hogan, M., Conejo-Garcia, J. R., Zhang, L., Burow, M., Zhu, Y., Wei, S., Kryczek, I., Daniel, B., Gordon, A., Myers, L., Lackner, A., Disis, M. L., Knutson, K. L., … Zou, W. (2004). Specific recruitment of regulatory T cells in ovarian carcinoma fosters immune privilege and predicts reduced survival. *Nature Medicine*, *10*(9).

Dardare, J., Witz, A., Merlin, J. L., Gilson, P., & Harlé, A. (2020). SMAD4 and the TGFB pathway in patients with pancreatic ductal adenocarcinoma. In *International Journal of Molecular Sciences* (Vol. 21, Issue 10).

de La O, J. P., Emerson, L. L., Goodman, J. L., Froebe, S. C., Illum, B. E., Curtis, A. B., & Murtaugh, L. C. (2008). Notch and Kras reprogram pancreatic acinar cells to ductal intraepithelial neoplasia. *Proceedings of the National Academy of Sciences of the United States of America*, *105*(48).

di Magliano, M. P., & Logsdon, C. D. (2013). Roles for KRAS in pancreatic tumor development and progression. *Gastroenterology*, *144*(6).

Direnzo, D., Hess, D. A., Damsz, B., Hallett, J. E., Marshall, B., Goswami, C., Liu, Y., Deering, T., MacDonald, R. J., & Konieczny, S. F. (2012). Induced Mist1 expression promotes remodeling of mouse pancreatic acinar cells. *Gastroenterology*, *143*(2).

Distler, M., Aust, D., Weitz, J., Pilarsky, C., & Grützmann, R. (2014). Precursor lesions for sporadic pancreatic cancer: PanIN, IPMN, and MCN. In *BioMed Research International* (Vol. 2014).

Dobin, A., Davis, C. A., Schlesinger, F., Drenkow, J., Zaleski, C., Jha, S., Batut, P., Chaisson, M., & Gingeras, T. R. (2013). STAR: Ultrafast universal RNA-seq aligner. *Bioinformatics*, *29*(1).

Duan, R., Du, W., & Guo, W. (2020). EZH2: A novel target for cancer treatment. In *Journal of Hematology and Oncology* (Vol. 13, Issue 1).

Dunne, R. F., & Hezel, A. F. (2015). Genetics and Biology of Pancreatic Ductal Adenocarcinoma. In *Hematology/Oncology Clinics of North America* (Vol. 29, Issue 4).

DuPage, M., Chopra, G., Quiros, J., Rosenthal, W. L., Morar, M. M., Holohan, D., Zhang, R., Turka, L., Marson, A., & Bluestone, J. A. (2015). The chromatin-modifying enzyme Ezh2 is critical for the maintenance of regulatory T cell identity after activation. *Immunity, 42*(2).

Dvorak, H. F. (2015). Tumors: Wounds that do not heal-redux. *Cancer Immunology Research, 3*(1).

Elyada, E., Bolisetty, M., Laise, P., Flynn, W. F., Courtois, E. T., Burkhart, R. A., Teinor, J. A., Belleau, P., Biffi, G., Lucito, M. S., Sivajothi, S., Armstrong, T. D., Engle, D. D., Yu, K. H., Hao, Y., Wolfgang, C. L., Park, Y., Preall, J., Jaffee, E. M., … Tuveson, D. A. (2019). Cross-species single-cell analysis of pancreatic ductal adenocarcinoma reveals antigen-presenting cancer-associated fibroblasts. In *Cancer Discovery* (Vol. 9, Issue 8).

Ennis, C. (2014). Epigenetics 101: a beginner's guide to explaining everything. *The Guardian*.

Esposito, I., Haeberle, L., & Wirth, M. (2018). Pancreatic cancer: Pathology and genetics. In *Encyclopedia of Cancer*.

Etzerodt, A., Tsalkitzi, K., Maniecki, M., Damsky, W., Delfini, M., Baudoin, E., Moulin, M., Bosenberg, M., Graversen, J. H., Auphan-Anezin, N., Moestrup, S. K., & Lawrence, T. (2019). Specific targeting of CD163+ TAMs mobilizes inflammatory monocytes and promotes T cell-mediated tumor regression. *Journal of Experimental Medicine, 216*(10).

Feig, C., Gopinathan, A., Neesse, A., Chan, D. S., Cook, N., & Tuveson, D. A. (2012). The pancreas cancer microenvironment. In *Clinical Cancer Research* (Vol. 18, Issue 16).

Ferreira, R. M. M., Sancho, R., Messal, H. A., Nye, E., Spencer-Dene, B., Stone, R. K., Stamp, G., Rosewell, I., Quaglia, A., & Behrens, A. (2017). Duct- and Acinar-Derived Pancreatic

Ductal Adenocarcinomas Show Distinct Tumor Progression and Marker Expression. *Cell Reports*, *21*(4).

Foster, D. S., Jones, R. E., Ransom, R. C., Longaker, M. T., & Norton, J. A. (2018). The evolving relationship of wound healing and tumor stroma. In *JCI insight* (Vol. 3, Issue 18).

Gabrielson, A., Wu, Y., Wang, H., Jiang, J., Kallakury, B., Gatalica, Z., Reddy, S., Kleiner, D., Fishbein, T., Johnson, L., Island, E., Satoskar, R., Banovac, F., Jha, R., Kachhela, J., Feng, P., Zhang, T., Tesfaye, A., Prins, P., … He, A. R. (2016). Intratumoral CD3 and CD8 T-cell densities associated with relapse-free survival in HCC. *Cancer Immunology Research*, *4*(5).

Gentles, A. J., Newman, A. M., Liu, C. L., Bratman, S. v., Feng, W., Kim, D., Nair, V. S., Xu, Y., Khuong, A., Hoang, C. D., Diehn, M., West, R. B., Plevritis, S. K., & Alizadeh, A. A. (2015). The prognostic landscape of genes and infiltrating immune cells across human cancers. *Nature Medicine*, *21*(8).

Greer, E. L., & Shi, Y. (2012). Histone methylation: A dynamic mark in health, disease and inheritance. In *Nature Reviews Genetics* (Vol. 13, Issue 5).

Greer, R. L., Staley, B. K., Liou, A., & Hebrok, M. (2013). Numb regulates acinar cell dedifferentiation and survival during pancreatic damage and acinar-to-ductal metaplasia. *Gastroenterology*, *145*(5).

Grunstein, M. (1997). Histone acetylation in chromatin structure and transcription. In *Nature* (Vol. 389, Issue 6649).

Gu, M., Gao, Y., & Chang, P. (2021). KRAS mutation dictates the cancer immune environment in pancreatic ductal adenocarcinoma and other adenocarcinomas. In *Cancers* (Vol. 13, Issue 10).

Guerra, C., & Barbacid, M. (2013). Genetically engineered mouse models of pancreatic adenocarcinoma. In *Molecular Oncology* (Vol. 7, Issue 2).

Guerra, C., Collado, M., Navas, C., Schuhmacher, A. J., Hernández-Porras, I., Cañamero, M., Rodriguez-Justo, M., Serrano, M., & Barbacid, M. (2011). Pancreatitis-induced inflammation contributes to pancreatic cancer by inhibiting oncogene-induced senescence. *Cancer Cell*, *19*(6).

Guerra, C., Schuhmacher, A. J., Cañamero, M., Grippo, P. J., Verdaguer, L., Pérez-Gallego, L., Dubus, P., Sandgren, E. P., & Barbacid, M. (2007). Chronic Pancreatitis Is Essential for Induction of Pancreatic Ductal Adenocarcinoma by K-Ras Oncogenes in Adult Mice. *Cancer Cell*, *11*(3).

Guo, J., Xie, K., & Zheng, S. (2016). Molecular biomarkers of pancreatic intraepithelial neoplasia and their implications in early diagnosis and therapeutic intervention of pancreatic cancer. In *International Journal of Biological Sciences* (Vol. 12, Issue 3).

Habbe, N., Shi, G., Meguid, R. A., Fendrich, V., Esni, F., Chen, H., Feldmann, G., Stoffers, D. A., Konieczny, S. F., Leach, S. D., & Maitra, A. (2008). Spontaneous induction of murine pancreatic intraepithelial neoplasia (mPanIN) by acinar cell targeting of oncogenic Kras in adult mice. *Proceedings of the National Academy of Sciences of the United States of America*, *105*(48).

Haber, P. S., Keogh, G. W., Apte, M. v., Moran, C. S., Stewart, N. L., Crawford, D. H. G., Pirola, R. C., McCaughan, G. W., Ramm, G. A., & Wilson, J. S. (1999). Activation of pancreatic stellate cells in human and experimental pancreatic fibrosis. *American Journal of Pathology*, *155*(4).

Haeberle, L., & Esposito, I. (2019). Pathology of pancreatic cancer. In *Translational Gastroenterology and Hepatology* (Vol. 4, Issue June).

Haefner, M., Bluethner, T., Niederhagen, M., Moebius, C., Wittekind, C., Mossner, J., Caca, K., & Wiedmann, M. (2008). Experimental treatment of pancreatic cancer with two novel histone deacetylase inhibitors. *World Journal of Gastroenterology*, *14*(23).

Hahn, S. A., & Schmiegel, W. H. (1998). Recent discoveries in cancer genetics of exocrine pancreatic neoplasia. In *Digestion* (Vol. 59, Issue 5).

Hassan, Z., Schneeweis, C., Wirth, M., Veltkamp, C., Dantes, Z., Feuerecker, B., Ceyhan, G. O., Knauer, S. K., Weichert, W., Schmid, R. M., Stauber, R., Arlt, A., Krämer, O. H., Rad, R., Reichert, M., Saur, D., & Schneider, G. (2018). MTOR inhibitor-based combination therapies for pancreatic cancer. *British Journal of Cancer*, *118*(3).

He, A., Shen, X., Ma, Q., Cao, J., von Gise, A., Zhou, P., Wang, G., Marquez, V. E., Orkin, S. H., & Pu, W. T. (2012). PRC2 directly methylates GATA4 and represses its transcriptional activity. *Genes and Development*, *26*(1).

He, S., Liu, Y., Meng, L., Sun, H., Wang, Y., Ji, Y., Purushe, J., Chen, P., Li, C., Madzo, J., Issa, J. P., Soboloff, J., Reshef, R., Moore, B., Gattinoni, L., & Zhang, Y. (2017). Ezh2 phosphorylation state determines its capacity to maintain CD8+ T memory precursors for antitumor immunity. *Nature Communications*, *8*(1).

Hingorani, S. R., Petricoin, E. F., Maitra, A., Rajapakse, V., King, C., Jacobetz, M. A., Ross, S., Conrads, T. P., Veenstra, T. D., Hitt, B. A., Kawaguchi, Y., Johann, D., Liotta, L. A., Crawford, H. C., Putt, M. E., Jacks, T., Wright, C. V. E., Hruban, R. H., Lowy, A. M., & Tuveson, D. A. (2003). Preinvasive and invasive ductal pancreatic cancer and its early detection in the mouse. *Cancer Cell*, *4*(6).

Hingorani, S. R., Wang, L., Multani, A. S., Combs, C., Deramaudt, T. B., Hruban, R. H., Rustgi, A. K., Chang, S., & Tuveson, D. A. (2005). Trp53R172H and KrasG12D cooperate to promote chromosomal instability and widely metastatic pancreatic ductal adenocarcinoma in mice. *Cancer Cell*, *7*(5). https://doi.org/10.1016/j.ccr.2005.04.023

Hruban, R. H., Maitra, A., & Goggins, M. (2008). Update on pancreatic intraepithelial neoplasia. *International Journal of Clinical and Experimental Pathology*, *1*(4).

Hu, B., Wu, C., Mao, H., Gu, H., Dong, H., Yan, J., Qi, Z., Yuan, L., Dong, Q., & Long, J. (2022). Subpopulations of cancer-associated fibroblasts link the prognosis and metabolic features of pancreatic ductal adenocarcinoma. *Annals of Translational Medicine*, *10*(5).

Huang, H., Liu, Y., Daniluk, J., Gaiser, S., Chu, J., Wang, H., Li, Z. S., Logsdon, C. D., & Ji, B. (2013). Activation of nuclear factor-κB in acinar cells increases the severity of pancreatitis in mice. *Gastroenterology*, *144*(1).

Huang, H., Wang, Z., Zhang, Y., & Brekken, R. A. (2021). Mesothelial Cell-Derived Antigen-Presenting Cancer-Associated Fibroblasts Induce Expansion of Regulatory T Cells in Pancreatic Cancer. *SSRN Electronic Journal*.

Huang, J., Gou, H., Yao, J., Yi, K., Jin, Z., Matsuoka, M., & Zhao, T. (2021). The noncanonical role of EZH2 in cancer. In *Cancer Science* (Vol. 112, Issue 4).

Huang, L., Desai, R., Conrad, D. N., Leite, N. C., Akshinthala, D., Lim, C. M., Gonzalez, R., Muthuswamy, L. B., Gartner, Z., & Muthuswamy, S. K. (2021). Commitment and oncogene-induced plasticity of human stem cell-derived pancreatic acinar and ductal organoids. *Cell Stem Cell*, *28*(6).

Hyun, J. J., & Lee, H. S. (2014). Experimental models of pancreatitis. In *Clinical Endoscopy* (Vol. 47, Issue 3).

Hyun, K., Jeon, J., Park, K., & Kim, J. (2017). Writing, erasing and reading histone lysine methylations. In *Experimental and Molecular Medicine* (Vol. 49, Issue 4).

Iacobuzio-Donahue, C. A., Velculescu, V. E., Wolfgang, C. L., & Hruban, R. H. (2012). Genetic basis of pancreas cancer development and progression: Insights from whole-exome and whole-genome sequencing. *Clinical Cancer Research*, *18*(16).

Ida, S., Ohmuraya, M., Hirota, M., Ozaki, N., Hiramatsu, S., Uehara, H., Takamori, H., Araki, K., Baba, H., & Yamamura, K. ichi. (2010). Chronic pancreatitis in mice by treatment with choline-deficient ethionine-supplemented diet. *Experimental Animals*, *59*(4).

Jakubison, B. L., Schweickert, P. G., Moser, S. E., Yang, Y., Gao, H., Scully, K., Itkin-Ansari, P., Liu, Y., & Konieczny, S. F. (2018). Induced PTF1a expression in pancreatic ductal adenocarcinoma cells activates acinar gene networks, reduces tumorigenic properties, and sensitizes cells to gemcitabine treatment. *Molecular Oncology*, *12*(7).

Jazirehi, A. R., Wenn, P. B., & Damavand, M. (2012). Therapeutic implications of targeting the PI3Kinase/AKT/mTOR signaling module in melanoma therapy. *American Journal of Cancer Research, 2*(2).

Jiang, M., Azevedo-Pouly, A. C., Deering, T. G., Hoang, C. Q., DiRenzo, D., Hess, D. A., Konieczny, S. F., Swift, G. H., & MacDonald, R. J. (2016). MIST1 and PTF1 Collaborate in Feed-Forward Regulatory Loops That Maintain the Pancreatic Acinar Phenotype in Adult Mice. *Molecular and Cellular Biology*, *36*(23).

Johnson, C. L., Kowalik, A. S., Rajakumar, N., & Pin, C. L. (2004). Mist1 is necessary for the establishment of granule organization in serous exocrine cells of the gastrointestinal tract. *Mechanisms of Development*, *121*(3).

Jonckheere, N., Vasseur, R., & van Seuningen, I. (2017). The cornerstone K-RAS mutation in pancreatic adenocarcinoma: From cell signaling network, target genes, biological processes to therapeutic targeting. In *Critical Reviews in Oncology/Hematology* (Vol. 111).

Jones, P. A., Ohtani, H., Chakravarthy, A., & de Carvalho, D. D. (2019). Epigenetic therapy in immune-oncology. In *Nature Reviews Cancer* (Vol. 19, Issue 3).

Juiz, N., Elkaoutari, A., Bigonnet, M., Gayet, O., Roques, J., Nicolle, R., Iovanna, J., & Dusetti, N. (2020). Basal-like and classical cells coexist in pancreatic cancer revealed by single-cell analysis on biopsy-derived pancreatic cancer organoids from the classical subtype. *FASEB Journal*, *34*(9).

Kabacaoglu, D., Ruess, D. A., Ai, J., & Algül, H. (2019). NF-kB/rel transcription factors in pancreatic cancer: Focusing on relA, c-rel, and relB. In *Cancers* (Vol. 11, Issue 7).

Kanji, Z. S., & Gallinger, S. (2013). Diagnosis and management of pancreatic cancer. In *CMAJ* (Vol. 185, Issue 14).

Karagiannis, G. S., Poutahidis, T., Erdman, S. E., Kirsch, R., Riddell, R. H., & Diamandis, E. P. (2012). Cancer-associated fibroblasts drive the progression of metastasis through both paracrine and mechanical pressure on cancer tissue. In *Molecular Cancer Research* (Vol. 10, Issue 11).

Karantanos, T., Chistofides, A., Barhdan, K., Li, L., & Boussiotis, V. A. (2016). Regulation of T cell differentiation and function by EZH2. In *Frontiers in Immunology* (Vol. 7, Issue MAY).

Karki, A., Humphrey, S. E., Steele, R. E., Hess, D. A., Taparowsky, E. J., & Konieczny, S. F. (2015). Silencing Mist1 gene expression is essential for recovery from acute pancreatitis. *PLoS ONE*, *10*(12).

Kawaguchi, Y., Cooper, B., Gannon, M., Ray, M., MacDonald, R. J., & Wright, C. V. E. (2002). The role of the transcriptional regulator Ptf1a in converting intestinal to pancreatic progenitors. *Nature Genetics*, *32*(1).

Kim, E., Kim, M., Woo, D. H., Shin, Y., Shin, J., Chang, N., Oh, Y. T., Kim, H., Rheey, J., Nakano, I., Lee, C., Joo, K. M., Rich, J. N., Nam, D. H., & Lee, J. (2013). Phosphorylation of EZH2 Activates STAT3 Signaling via STAT3 Methylation and Promotes Tumorigenicity of Glioblastoma Stem-like Cells. *Cancer Cell*, *23*(6).

Kim, H. (2008). Cerulein Pancreatitis: Oxidative Stress, Inflammation, and Apoptosis. *Gut and Liver*, *2*(2).

Kim, K. H., Kim, W., Howard, T. P., Vazquez, F., Tsherniak, A., Wu, J. N., Wang, W., Haswell, J. R., Walensky, L. D., Hahn, W. C., Orkin, S. H., & Roberts, C. W. M. (2015). SWI/SNF-mutant cancers depend on catalytic and non-catalytic activity of EZH2. In *Nature Medicine* (Vol. 21, Issue 12).

Kirkegård, J., Mortensen, F. v., Heide-Jørgensen, U., & Cronin-Fenton, D. (2020). Predictors of underlying pancreatic cancer in patients with acute pancreatitis: a Danish nationwide cohort study. *HPB*, *22*(4).

Kopp, J. L., von Figura, G., Mayes, E., Liu, F. F., Dubois, C. L., Morris, J. P., Pan, F. C., Akiyama, H., Wright, C. V. E., Jensen, K., Hebrok, M., & Sander, M. (2012). Identification of Sox9-Dependent Acinar-to-Ductal Reprogramming as the Principal Mechanism for Initiation of Pancreatic Ductal Adenocarcinoma. *Cancer Cell*, *22*(6).

Korc, M. (2007). Pancreatic cancer-associated stroma production. *American Journal of Surgery*, *194*(4 SUPPL.).

Kubiczkova, L., Sedlarikova, L., Hajek, R., & Sevcikova, S. (2012). TGF-β - an excellent servant but a bad master. In *Journal of Translational Medicine* (Vol. 10, Issue 1).

Kunej, T., Godnic, I., Horvat, S., Zorc, M., & Calin, G. A. (2012). Cross talk between MicroRNA and coding cancer genes. In *Cancer Journal (United States)* (Vol. 18, Issue 3).

Laible, G., Wolf, A., Dorn, R., Reuter, G., Nislow, C., Lebersorger, A., Popkin, D., Pillus, L., & Jenuwein, T. (1997). Mammalian homologues of the Polycomb-group gene Enhancer of zeste mediate gene silencing in Drosophila heterochromatin and at S. cerevisiae telomeres. *EMBO Journal*, *16*(11).

Lawrence, C. L., & Baldwin, A. S. (2016). Non-canonical EZH2 transcriptionally activates RelB in triple negative breast cancer. *PLoS ONE*, *11*(10).

Lee, J. M., Lee, J. S., Kim, H., Kim, K. K., Park, H., Kim, J. Y., Lee, S. H., Kim, I. S., Kim, J., Lee, M., Chung, C. H., Seo, S. B., Yoon, J. B., Ko, E., Noh, D. Y., Kim, K. il, & Baek, S. H. (2012). EZH2 Generates a Methyl Degron that Is Recognized by the DCAF1/DDB1/CUL4 E3 Ubiquitin Ligase Complex. *Molecular Cell*, *48*(4).

Liao, Y., Smyth, G. K., & Shi, W. (2014). FeatureCounts: An efficient general purpose program for assigning sequence reads to genomic features. *Bioinformatics*, *30*(7).

Ling, J., Kang, Y., Zhao, R., Xia, Q., Lee, D. F., Chang, Z., Li, J., Peng, B., Fleming, J. B., Wang, H., Liu, J., Lemischka, I. R., Hung, M. C., & Chiao, P. J. (2012). KrasG12D-Induced IKK2/β/NF-κB Activation by IL-1α and p62 Feedforward Loops Is Required for Development of Pancreatic Ductal Adenocarcinoma. *Cancer Cell*, *21*(1).

Liou, G. Y., Döppler, H., Necela, B., Krishna, M., Crawford, H. C., Raimondo, M., & Storz, P. (2013). Macrophage-secreted cytokines drive pancreatic acinar-to-ductal metaplasia through NF-KB and MMPs. *Journal of Cell Biology*, *202*(3).

Liu, J., Akanuma, N., Liu, C., Naji, A., Halff, G. A., Washburn, W. K., Sun, L., & Wang, P. (2016). TGF-β1 promotes acinar to ductal metaplasia of human pancreatic acinar cells. *Scientific Reports*, *6*.

Liu, Z., Tang, Q., Wen, J., Tang, Y., Huang, D., Huang, Y., Xie, J., Luo, Y., Liang, M., Wu, C., Lu, Z., Tan, A., Gao, Y., Wang, Q., Jiang, Y., Yao, Z., Lin, X., Zhang, H., Mo, Z., & Yang, X. (2016). Elevated serum complement factors 3 and 4 are strong inflammatory markers of the metabolic syndrome development: A longitudinal cohort study. *Scientific Reports*, *6*.

Livshits, G., Alonso-Curbelo, D., Morris, J. P., Koche, R., Saborowski, M., Wilkinson, J. E., & Lowe, S. W. (2018). Arid1a restrains Kras-dependent changes in acinar cell identity. *ELife*, *7*.

Löhr, M., Klöppel, G., Maisonneuve, P., Lowenfels, A. B., & Lüttges, J. (2005). Frequency of K-ras mutations in pancreatic intraductal neoplasias associated with pancreatic ductal adenocarcinoma and chronic pancreatitis: A meta-analysis. *Neoplasia*, *7*(1).

Lomberk, G. A., & Urrutia, R. (2015). The Triple-Code Model for Pancreatic Cancer: Cross Talk Among Genetics, Epigenetics, and Nuclear Structure. In *Surgical Clinics of North America* (Vol. 95, Issue 5).

Longo, V., Brunetti, O., Gnoni, A., Cascinu, S., Gasparini, G., Lorusso, V., Ribatti, D., & Silvestris, N. (2016). Angiogenesis in pancreatic ductal adenocarcinoma: A controversial issue. In *Oncotarget* (Vol. 7, Issue 36).

Maddalena, M., Mallel, G., Nataraj, N. B., Shreberk-Shaked, M., Hassin, O., Mukherjee, S., Arandkar, S., Rotkopf, R., Kapsack, A., Lambiase, G., Pellegrino, B., Ben-Isaac, E., Golani, O., Addadi, Y., Hajaj, E., Eilam, R., Straussman, R., Yarden, Y., Lotem, M., & Oren, M. (2021). TP53 missense mutations in PDAC are associated with enhanced fibrosis and an immunosuppressive microenvironment. *Proceedings of the National Academy of Sciences of the United States of America*, *118*(23).

Magaña-Gómez, J., López-Cervantes, G., & Calderón de la Barca, A. M. (2006). Caerulin-induced pancreatitis in rats: Histological and genetic expression changes from acute phase to recuperation. *World Journal of Gastroenterology*, *12*(25).

Mahajan, U. M., Langhoff, E., Goni, E., Costello, E., Greenhalf, W., Halloran, C., Ormanns, S., Kruger, S., Boeck, S., Ribback, S., Beyer, G., Dombroswki, F., Weiss, F. U., Neoptolemos, J. P., Werner, J., D'Haese, J. G., Bazhin, A., Peterhansl, J., Pichlmeier, S., … Mayerle, J. (2018). Immune Cell and Stromal Signature Associated With Progression-Free Survival of Patients With Resected Pancreatic Ductal Adenocarcinoma. *Gastroenterology*, *155*(5).

Mallen-St. Clair, J., Soydaner-Azeloglu, R., Lee, K. E., Taylor, L., Livanos, A., Pylayeva-Gupta, Y., Miller, G., Margueron, R., Reinberg, D., & Bar-Sagi, D. (2012). EZH2 couples pancreatic regeneration to neoplastic progression. *Genes and Development*, *26*(5).

Margueron, R., Li, G., Sarma, K., Blais, A., Zavadil, J., Woodcock, C. L., Dynlacht, B. D., & Reinberg, D. (2008). Ezh1 and Ezh2 Maintain Repressive Chromatin through Different Mechanisms. *Molecular Cell*, *32*(4).

Mayerle, J., Sendler, M., Hegyi, E., Beyer, G., Lerch, M. M., & Sahin-Tóth, M. (2019). Genetics, Cell Biology, and Pathophysiology of Pancreatitis. *Gastroenterology*, *156*(7).

McCarthy, D. J., Chen, Y., & Smyth, G. K. (2012). Differential expression analysis of multifactor RNA-Seq experiments with respect to biological variation. *Nucleic Acids Research*, *40*(10).

McDonald, O. G. (2022). The biology of pancreatic cancer morphology. In *Pathology* (Vol. 54, Issue 2).

Mehmood, R., Varga, G., Mohanty, S. Q., Laing, S. W., Lu, Y., Johnson, C. L., Kharitonenkov, A., & Pin, C. L. (2014). Epigenetic reprogramming in Mist1-/- mice predicts the molecular response to cerulein-induced pancreatitis. *PLoS ONE*, *9*(1).

Mochizuki, M., Sagara, H., & Nakahara, T. (2020). Type i collagen facilitates safe and reliable expansion of human dental pulp stem cells in xenogeneic serum-free culture. *Stem Cell Research and Therapy*, *11*(1).

Moffitt, R. A., Marayati, R., Flate, E. L., Volmar, K. E., Loeza, S. G. H., Hoadley, K. A., Rashid, N. U., Williams, L. A., Eaton, S. C., Chung, A. H., Smyla, J. K., Anderson, J. M., Kim, H. J., Bentrem, D. J., Talamonti, M. S., Iacobuzio-Donahue, C. A., Hollingsworth, M. A., & Yeh, J. J. (2015). Virtual microdissection identifies distinct tumor- and stroma-specific subtypes of pancreatic ductal adenocarcinoma. *Nature Genetics*, *47*(10).

Morton, J. P., Timpson, P., Karim, S. A., Ridgway, R. A., Athineos, D., Doyle, B., Jamieson, N. B., Oien, K. A., Lowy, A. M., Brunton, V. G., Frame, M. C., Evans, T. R. J., & Sansom, O. J. (2010). Mutant p53 drives metastasis and overcomes growth arrest/senescence in pancreatic cancer. *Proceedings of the National Academy of Sciences of the United States of America*, *107*(1).

Mostafa, M. E., Erbarut-Seven, I., Pehlivanoglu, B., & Adsay, V. (2017). Pathologic classification of "pancreatic cancers": Current concepts and challenges. In *Chinese Clinical Oncology* (Vol. 6, Issue 6).

Murray, E. R., Menezes, S., Henry, J. C., Williams, J. L., Alba-Castellón, L., Baskaran, P., Quétier, I., Desai, A., Marshall, J. J. T., Rosewell, I., Tatari, M., Rajeeve, V., Khan, F., Wang, J., Kotantaki, P., Tyler, E. J., Singh, N., Reader, C. S., Carter, E. P., … Cameron, A. J. M. (2022). Disruption of pancreatic stellate cell myofibroblast phenotype promotes pancreatic tumor invasion. *Cell Reports*, *38*(4).

Nutt, S. L., Keenan, C., Chopin, M., & Allan, R. S. (2020). EZH2 function in immune cell development. In *Biological Chemistry* (Vol. 401, Issue 8).

Öhlund, D., Elyada, E., & Tuveson, D. (2014). Fibroblast heterogeneity in the cancer wound. In *Journal of Experimental Medicine* (Vol. 211, Issue 8).

Öhlund, D., Handly-Santana, A., Biffi, G., Elyada, E., Almeida, A. S., Ponz-Sarvise, M., Corbo, V., Oni, T. E., Hearn, S. A., Lee, E. J., Chio, I. I. C., Hwang, C. il, Tiriac, H., Baker, L. A., Engle, D. D., Feig, C., Kultti, A., Egeblad, M., Fearon, D. T., … Tuveson, D. A. (2017). Distinct populations of inflammatory fibroblasts and myofibroblasts in pancreatic cancer. *The Journal of Experimental Medicine*, *214*(3).

O'Meara, M. M., & Simon, J. A. (2012). Inner workings and regulatory inputs that control Polycomb repressive complex 2. In *Chromosoma* (Vol. 121, Issue 3).

Ougolkov, A. v., Bilim, V. N., & Billadeau, D. D. (2008). Regulation of pancreatic tumor cell proliferation and chemoresistance by the histone methyltransferase enhancer of zeste homologue 2. *Clinical Cancer Research*, *14*(21).

Özdemir, B. C., Pentcheva-Hoang, T., Carstens, J. L., Zheng, X., Wu, C. C., Simpson, T. R., Laklai, H., Sugimoto, H., Kahlert, C., Novitskiy, S. v., DeJesus-Acosta, A., Sharma, P., Heidari, P., Mahmood, U., Chin, L., Moses, H. L., Weaver, V. M., Maitra, A., Allison, J. P., … Kalluri, R. (2014). Depletion of carcinoma-associated fibroblasts and fibrosis induces immunosuppression and accelerates pancreas cancer with reduced survival. *Cancer Cell*, *25*(6).

Paradise, B. D., Barham, W., & Fernandez-Zapico, M. E. (2018). Targeting epigenetic aberrations in pancreatic cancer, a new path to improve patient outcomes? In *Cancers* (Vol. 10, Issue 5).

Parkin, D. M., Boyd, L., & Walker, L. C. (2011). The fraction of cancer attributable to lifestyle and environmental factors in the UK in 2010. *British Journal of Cancer*, *105*.

Patil, S., Steuber, B., Kopp, W., Kari, V., Urbach, L., Wang, X., Kuffer, S., Bohnenberger, H., Spyropoulou, D., Zhang, Z., Versemann, L., Bosherz, M. S., Brunner, M., Gaedcke, J., Strobel, P., Zhang, J. S., Neesse, A., Ellenrieder, V., Singh, S. K., … Hessmann, E. (2021). EZH2 regulates pancreatic cancer subtype identity and tumor progression via transcriptional repression of gata6. *Cancer Research*, *80*(21).

Pengelly, A. R., Copur, Ö., Jäckle, H., Herzig, A., & Müller, J. (2013). A histone mutant reproduces the phenotype caused by loss of histone-modifying factor polycomb. *Science*, *339*(6120).

Peters, A. H. F. M., Kubicek, S., Mechtler, K., O'Sullivan, R. J., Derijck, A. A. H. A., Perez-Burgos, L., Kohlmaier, A., Opravil, S., Tachibana, M., Shinkai, Y., Martens, J. H. A., &

Jenuwein, T. (2003). Partitioning and Plasticity of Repressive Histone Methylation States in Mammalian Chromatin. *Molecular Cell*, *12*(6).

Peterson, S. L., Nguyen, H. X., Mendez, O. A., & Anderson, A. J. (2017). Complement Protein C3 Suppresses Axon Growth and Promotes Neuron Loss. *Scientific Reports*, *7*(1).

Pin, C. L., Michael Rukstalis, J., Johnson, C., & Konieczny, S. F. (2001). The bHLH transcription factor Mist1 is required to maintain exocrine pancreas cell organization and acinar cell identity. *Journal of Cell Biology*, *155*(3).

Prabhu, L., Mundade, R., Korc, M., Loehrer, P. J., & Lu, T. (2014). Critical role of NF-κB in pancreatic cancer. In *Oncotarget* (Vol. 5, Issue 22).

Provenzano, P. P., Cuevas, C., Chang, A. E., Goel, V. K., von Hoff, D. D., & Hingorani, S. R. (2012). Enzymatic Targeting of the Stroma Ablates Physical Barriers to Treatment of Pancreatic Ductal Adenocarcinoma. *Cancer Cell*, *21*(3).

Ray, K. C., Bell, K. M., Yan, J., Gu, G., Chung, C. H., Washington, M. K., & Means, A. L. (2011). Epithelial tissues have varying degrees of susceptibility to KrasG12D-initiated tumorigenesis in a mouse model. *PLoS ONE*, *6*(2).

Robinson, M. D., McCarthy, D. J., & Smyth, G. K. (2009). edgeR: A Bioconductor package for differential expression analysis of digital gene expression data. *Bioinformatics*, *26*(1).

Rodolosse, A., Chalaux, E., Adell, T., Hagège, H., Skoudy, A., & Real, F. X. (2004). PTF1alpha/p48 transcription factor couples proliferation and differentiation in the exocrine pancreas [corrected]. *Gastroenterology*, *127*(3).

Rozenblum, E., Schutte, M., Goggins, M., Hahn, S. A., Panzer, S., Zahurak, M., Goodman, S. N., Sohn, T. A., Hruban, R. H., Yeo, C. J., & Kern, S. E. (1997). Tumor-suppressive pathways in pancreatic carcinoma. *Cancer Research*, *57*(9).

Saitou, M., Goto, M., Horinouchi, M., Tamada, S., Nagata, K., Hamada, T., Osako, M., Takao, S., Batra, S. K., Aikou, T., Imai, K., & Yonezawa, S. (2005). MUC4 expression is a novel

prognostic factor in patients with invasive ductal carcinoma of the pancreas. *Journal of Clinical Pathology*, *58*(8).

Sarantis, P., Koustas, E., Papadimitropoulou, A., Papavassiliou, A. G., & Karamouzis, M. v. (2020). Pancreatic ductal adenocarcinoma: Treatment hurdles, tumor microenvironment and immunotherapy. In *World Journal of Gastrointestinal Oncology* (Vol. 12, Issue 2).

Sato, N., Ohta, T., Kitagawa, H., Kayahara, M., Ninomiya, I., Fushida, S., Fujimura, T., Nishimura, G. I., Shimizu, K., & Miwa, K. (2004). FR901228, a novel histone deacetylase inhibitor, induces cell cycle arrest and subsequent apoptosis in refractory human pancreatic cancer cells. *International Journal of Oncology*, *24*(3).

Sauvageau, M., & Sauvageau, G. (2010). Polycomb group proteins: Multi-faceted regulators of somatic stem cells and cancer. In *Cell Stem Cell* (Vol. 7, Issue 3).

Sawey, E. T., Johnson, J. A., & Crawford, H. C. (2007). Matrix metalloproteinase 7 controls pancreatic acinar cell transdifferentiation by activating the Notch signaling pathway. *Proceedings of the National Academy of Sciences of the United States of America*, *104*(49).

Schlitter, A. M., Segler, A., Steiger, K., Michalski, C. W., Jäger, C., Konukiewitz, B., Pfarr, N., Endris, V., Bettstetter, M., Kong, B., Regel, I., Kleeff, J., Klöppel, G., & Esposito, I. (2017). Molecular, morphological and survival analysis of 177 resected pancreatic ductal adenocarcinomas (PDACs): Identification of prognostic subtypes. *Scientific Reports*, *7*.

Schneider, G., Krämer, O. H., Schmid, R. M., & Saur, D. (2011). Acetylation as a transcriptional control mechanism-HDACs and HATs in pancreatic ductal adenocarcinoma. *Journal of Gastrointestinal Cancer*, *42*(2).

Seeley, E. S., Carrière, C., Goetze, T., Longnecker, D. S., & Korc, M. (2009). Pancreatic cancer and precursor pancreatic intraepithelial neoplasia lesions are devoid of primary cilia. *Cancer Research*, *69*(2).

Shen, H., & Laird, P. W. (2013). Interplay between the cancer genome and epigenome. In *Cell* (Vol. 153, Issue 1).

Shi, G., Direnzo, D., Qu, C., Barney, D., Miley, D., & Konieczny, S. F. (2013). Maintenance of acinar cell organization is critical to preventing Kras-induced acinar-ductal metaplasia. *Oncogene*, *32*(15).

Shinkawa, T., Ohuchida, K., Mochida, Y., Sakihama, K., Iwamoto, C., Abe, T., Ideno, N., Mizuuchi, Y., Shindo, K., Ikenaga, N., Moriyama, T., Nakata, K., Oda, Y., & Nakamura, M. (2022). Subtypes in pancreatic ductal adenocarcinoma based on niche factor dependency show distinct drug treatment responses. *Journal of Experimental and Clinical Cancer Research*, *41*(1).

Simon, J. A., & Lange, C. A. (2008). Roles of the EZH2 histone methyltransferase in cancer epigenetics. In *Mutation Research - Fundamental and Molecular Mechanisms of Mutagenesis* (Vol. 647, Issues 1–2).

Siveke, J. T., Einwächter, H., Sipos, B., Lubeseder-Martellato, C., Klöppel, G., & Schmid, R. M. (2007). Concomitant Pancreatic Activation of KrasG12D and Tgfa Results in Cystic Papillary Neoplasms Reminiscent of Human IPMN. *Cancer Cell*, *12*(3).

Slack, J. M. W. (2020). Molecular biology of the cell. In *Principles of Tissue Engineering*.

Sousa, C. M., & Kimmelman, A. C. (2014). The complex landscape of pancreatic cancer metabolism. In *Carcinogenesis* (Vol. 35, Issue 7).

Stock, J. K., Giadrossi, S., Casanova, M., Brookes, E., Vidal, M., Koseki, H., Brockdorff, N., Fisher, A. G., & Pombo, A. (2007). Ring1-mediated ubiquitination of H2A restrains poised RNA polymerase II at bivalent genes in mouse ES cells. *Nature Cell Biology*, *9*(12).

Storz, P. (2017). Acinar cell plasticity and development of pancreatic ductal adenocarcinoma. In *Nature Reviews Gastroenterology and Hepatology* (Vol. 14, Issue 5).

Sung, B. H., & Weaver, A. M. (2017). Exosome secretion promotes chemotaxis of cancer cells. *Cell Adhesion and Migration*, *11*(2).

Tan, A. C., Jimeno, A., Lin, S. H., Wheelhouse, J., Chan, F., Solomon, A., Rajeshkumar, N. v., Rubio-Viqueira, B., & Hidalgo, M. (2009). Characterizing DNA methylation patterns in pancreatic cancer genome. *Molecular Oncology*, *3*(5–6).

Thompson, M. J., Rubbi, L., Dawson, D. W., Donahue, T. R., & Pellegrini, M. (2015). Pancreatic cancer patient survival correlates with DNA methylation of pancreas development genes. *PLoS ONE*, *10*(6).

Tie, F., Banerjee, R., Stratton, C. A., Prasad-Sinha, J., Stepanik, V., Zlobin, A., Diaz, M. O., Scacheri, P. C., & Harte, P. J. (2009). CBP-mediated acetylation of histone H3 lysine 27 antagonizes Drosophila Polycomb silencing. *Development*, *136*(18).

Tjomsland, V., Niklasson, L., Sandström, P., Borch, K., Druid, H., Bratthäll, C., Messmer, D., Larsson, M., & Spångeus, A. (2011). The desmoplastic stroma plays an essential role in the accumulation and modulation of infiltrated immune cells in pancreatic adenocarcinoma. *Clinical and Developmental Immunology*, *2011*.

Tomasek, J. J., Gabbiani, G., Hinz, B., Chaponnier, C., & Brown, R. A. (2002). Myofibroblasts and mechano: Regulation of connective tissue remodelling. In *Nature Reviews Molecular Cell Biology* (Vol. 3, Issue 5).

Tracy, S., Höfling, K., Pirruccello, S., Lane, P. H., Reyna, S. M., & Gauntt, C. J. (2000). Group B coxsackievirus myocarditis and pancreatitis: Connection between viral virulence phenotypes in mice. *Journal of Medical Virology*, *62*(1).

Truong, L. H., & Pauklin, S. (2021). Pancreatic cancer microenvironment and cellular composition: Current understandings and therapeutic approaches. In *Cancers* (Vol. 13, Issue 19).

Tsai, H. J., & Chang, J. S. (2019). Environmental risk factors of pancreatic cancer. In *Journal of Clinical Medicine* (Vol. 8, Issue 9).

Vaish, U., Jain, T., Are, A. C., & Dudeja, V. (2021). Cancer-associated fibroblasts in pancreatic ductal adenocarcinoma: An update on heterogeneity and therapeutic targeting. In *International Journal of Molecular Sciences* (Vol. 22, Issue 24).

Vaziri, N. D. (2004). Roles of oxidative stress and antioxidant therapy in chronic kidney disease and hypertension. In *Current Opinion in Nephrology and Hypertension* (Vol. 13, Issue 1).

Versemann L, Patil S, Steuber B, Zhang Z, Kopp W, Krawczyk HE, Kaulfuß S, Wollnik B, Ströbel P, Neesse A, Singh SK, Ellenrieder V, Hessmann E. TP53-Status-Dependent Oncogenic EZH2 Activity in Pancreatic Cancer. Cancers (Basel). 2022 Jul 15;14(14):3451.

Vigil, D., Cherfils, J., Rossman, K. L., & Der, C. J. (2010). Ras superfamily GEFs and GAPs: Validated and tractable targets for cancer therapy? In *Nature Reviews Cancer* (Vol. 10, Issue 12).

Vincent, A., Omura, N., Hong, S. M., Jaffe, A., Eshleman, J., & Goggins, M. (2011). Genome-wide analysis of promoter methylation associated with gene expression profile in pancreatic adenocarcinoma. *Clinical Cancer Research*, *17*(13).

Völkel, P., Dupret, B., le Bourhis, X., & Angrand, P. O. (2015). Diverse involvement of EZH2 in cancer epigenetics. In *American Journal of Translational Research* (Vol. 7, Issue 2).

Vonlaufen, A., Phillips, P. A., Xu, Z., Zhang, X., Yang, L., Pirola, R. C., Wilson, J. S., & Apte, M. v. (2011). Withdrawal of alcohol promotes regression while continued alcohol intake promotes persistence of LPS-induced pancreatic injury in alcohol-fed rats. *Gut*, *60*(2).

Vujasinovic, M., Dugic, A., Maisonneuve, P., Aljic, A., Berggren, R., Panic, N., Valente, R., Mucelli, R. P., Waldthaler, A., Ghorbani, P., Kordes, M., Hagström, H., & Löhr, J. M. (2020). Risk of developing pancreatic cancer in patients with chronic pancreatitis. *Journal of Clinical Medicine*, *9*(11).

Waddell, N., Pajic, M., Patch, A. M., Chang, D. K., Kassahn, K. S., Bailey, P., Johns, A. L., Miller, D., Nones, K., Quek, K., Quinn, M. C. J., Robertson, A. J., Fadlullah, M. Z. H., Bruxner, T. J. C., Christ, A. N., Harliwong, I., Idrisoglu, S., Manning, S., Nourse, C., … Grimmond, S. M. (2015). Whole genomes redefine the mutational landscape of pancreatic cancer. *Nature*, *518*(7540).

Wang, D., Quiros, J., Mahuron, K., Pai, C. C., Ranzani, V., Young, A., Silveria, S., Harwin, T., Abnousian, A., Pagani, M., Rosenblum, M. D., van Gool, F., Fong, L., Bluestone, J. A., &

DuPage, M. (2018). Targeting EZH2 Reprograms Intratumoral Regulatory T Cells to Enhance Cancer Immunity. *Cell Reports*, *23*(11).

Wang, L., Xie, D., & Wei, D. (2019). Pancreatic acinar-to-ductal metaplasia and pancreatic cancer. In *Methods in Molecular Biology* (Vol. 1882).

Wang, R., Xin, M., Li, Y., Zhang, P., & Zhang, M. (2016). The Functions of Histone Modification Enzymes in Cancer. *Current Protein & Peptide Science*, *17*(5).

Wang, W., Qin, J. J., Voruganti, S., Nag, S., Zhou, J., & Zhang, R. (2015). Polycomb Group (PcG) Proteins and Human Cancers: Multifaceted Functions and Therapeutic Implications. *Medicinal Research Reviews*, *35*(6). https://doi.org/10.1002/med.21358

Wang, X., Brea, L. T., & Yu, J. (2019). Immune modulatory functions of EZH2 in the tumor microenvironment: implications in cancer immunotherapy. *American Journal of Clinical and Experimental Urology*, *7*(2).

Waters, A. M., & Der, C. J. (2018). KRAS: The critical driver and therapeutic target for pancreatic cancer. *Cold Spring Harbor Perspectives in Medicine*, *8*(9).

Whatcott, C. J., Diep, C. H., Jiang, P., Watanabe, A., Lobello, J., Sima, C., Hostetter, G., Shepard, H. M., von Hoff, D. D., & Han, H. (2015). Desmoplasia in primary tumors and metastatic lesions of pancreatic cancer. *Clinical Cancer Research*, *21*(15).

Winter, J., Jung, S., Keller, S., Gregory, R. I., & Diederichs, S. (2009). Many roads to maturity: MicroRNA biogenesis pathways and their regulation. In *Nature Cell Biology* (Vol. 11, Issue 3).

Wu, Y., Zhang, C., Jiang, K., Werner, J., Bazhin, A. v., & D'Haese, J. G. (2021). The Role of Stellate Cells in Pancreatic Ductal Adenocarcinoma: Targeting Perspectives. In *Frontiers in Oncology* (Vol. 10).

Xu, B., Konze, K. D., Jin, J., & Wang, G. G. (2015). Targeting EZH2 and PRC2 dependence as novel anticancer therapy. In *Experimental Hematology* (Vol. 43, Issue 8).

Xu, K., Wu, Z. J., Groner, A. C., He, H. H., Cai, C., Lis, R. T., Wu, X., Stack, E. C., Loda, M., Liu, T., Xu, H., Cato, L., Thornton, J. E., Gregory, R. I., Morrissey, C., Vessella, R. L., Montironi, R., Magi-Galluzzi, C., Kantoff, P. W., … Brown, M. (2012). EZH2 Oncogenic Activity in Castration-Resistant Prostate Cancer Cells Is Polycomb-Independent. *Science*, *338*(6113).

Xu, Y., Liu, J., Nipper, M., & Wang, P. (2019). Ductal vs. acinar? Recent insights into identifying cell lineage of pancreatic ductal adenocarcinoma. In *Annals of Pancreatic Cancer* (Vol. 2).

Yang, X. P., Jiang, K., Hirahara, K., Vahedi, G., Afzali, B., Sciume, G., Bonelli, M., Sun, H. W., Jankovic, D., Kanno, Y., Sartorelli, V., O'Shea, J. J., & Laurence, A. (2015). EZH2 is crucial for both differentiation of regulatory T cells and T effector cell expansion. *Scientific Reports*, *5*.

Yao, Y., Hu, H., Yang, Y., Zhou, G., Shang, Z., Yang, X., Sun, K., Zhan, S., Yu, Z., Li, P., Pan, G., Sun, L., Zhu, X., & He, S. (2016). Downregulation of enhancer of zeste homolog 2 (EZH2) is essential for the induction of autophagy and apoptosis in colorectal cancer cells. *Genes*, *7*(10).

Yin, X., Yang, S., Zhang, M., & Yue, Y. (2019). The role and prospect of JMJD3 in stem cells and cancer. In *Biomedicine and Pharmacotherapy* (Vol. 118).

Yonemori, K., Kurahara, H., Maemura, K., & Natsugoe, S. (2017). MicroRNA in pancreatic cancer. In *Journal of Human Genetics* (Vol. 62, Issue 1).

Yu, G. (2018). clusterProfiler: An universal enrichment tool for functional and comparative study. *BioRxiv*.

Yu, G., Wang, L. G., Han, Y., & He, Q. Y. (2012). ClusterProfiler: An R package for comparing biological themes among gene clusters. *OMICS A Journal of Integrative Biology*, *16*(5).

Yu, Y., Xiao, C. H., Tan, L. D., Wang, Q. S., Li, X. Q., & Feng, Y. M. (2014). Cancer-associated fibroblasts induce epithelial-mesenchymal transition of breast cancer cells through paracrine TGF-β signalling. *British Journal of Cancer*, *110*(3).

Yuan, T. L., & Cantley, L. C. (2008). PI3K pathway alterations in cancer: Variations on a theme. In *Oncogene* (Vol. 27, Issue 41).

Zamora, A. E., Crawford, J. C., & Thomas, P. G. (2018). Hitting the Target: How T Cells Detect and Eliminate Tumors. *The Journal of Immunology*, *200*(2).

Zee, B. M., Levin, R. S., Xu, B., LeRoy, G., Wingreen, N. S., & Garcia, B. A. (2010). In vivo residue-specific histone methylation dynamics. *Journal of Biological Chemistry*, *285*(5).

Zhang, L., Qiao, Z., Feng, H., & Shen, J. (2020). The early predictive role of complement C3 and C4 in patients with acute pancreatitis. *Journal of Clinical Laboratory Analysis*, *34*(5).

Zhang, R., Liu, Q., Li, T., Liao, Q., & Zhao, Y. (2019). Role of the complement system in the tumor microenvironment. In *Cancer Cell International* (Vol. 19, Issue 1).

Zhang, X. J., Ye, H., Zeng, C. W., He, B., Zhang, H., & Chen, Y. Q. (2010). Dysregulation of miR-15a and miR-214 in human pancreatic cancer. *Journal of Hematology and Oncology*, *3*. https://doi.org/10.1186/1756-8722-3-46

Zhao, E., Maj, T., Kryczek, I., Li, W., Wu, K., Zhao, L., Wei, S., Crespo, J., Wan, S., Vatan, L., Szeliga, W., Shao, I., Wang, Y., Liu, Y., Varambally, S., Chinnaiyan, A. M., Welling, T. H., Marquez, V., Kotarski, J., … Zou, W. (2016). Cancer mediates effector T cell dysfunction by targeting microRNAs and EZH2 via glycolysis restriction. *Nature Immunology*, *17*(1). https://doi.org/10.1038/ni.3313

Zhao, R., Choi, B. Y., Lee, M. H., Bode, A. M., & Dong, Z. (2016). Implications of Genetic and Epigenetic Alterations of CDKN2A (p16INK4a) in Cancer. In *EBioMedicine* (Vol. 8). https://doi.org/10.1016/j.ebiom.2016.04.017

Zhao, X. D., Han, X., Chew, J. L., Liu, J., Chiu, K. P., Choo, A., Orlov, Y. L., Sung, W. K., Shahab, A., Kuznetsov, V. A., Bourque, G., Oh, S., Ruan, Y., Ng, H. H., & Wei, C. L. (2007). Whole-Genome Mapping of Histone H3 Lys4 and 27 Trimethylations Reveals Distinct Genomic Compartments in Human Embryonic Stem Cells. *Cell Stem Cell*, *1*(3). https://doi.org/10.1016/j.stem.2007.08.004

Zhou, H., Qin, Y., Ji, S., Ling, J., Fu, J., Zhuang, Z., Fan, X., Song, L., Yu, X., & Chiao, P. J. (2018). SOX9 activity is induced by oncogenic Kras to affect MDC1 and MCMs expression in pancreatic cancer. *Oncogene*, *37*(7). https://doi.org/10.1038/onc.2017.393

Zhou, Q., & Melton, D. A. (2018). Pancreas regeneration. In *Nature* (Vol. 557, Issue 7705). https://doi.org/10.1038/s41586-018-0088-0

Zhu, L., Shi, G., Schmidt, C. M., Hruban, R. H., & Konieczny, S. F. (2007). Acinar cells contribute to the molecular heterogeneity of pancreatic intraepithelial neoplasia. *American Journal of Pathology*, *171*(1). https://doi.org/10.2353/ajpath.2007.061176

Curriculum Vitae

Name: Xiaoyi (Jessie) Wang

Post-secondary Education and Degrees:

The University of Western Ontario 2020-2022 M.A.
London, Ontario, Canada

- Master of Science
- Physiology and Pharmacology

University of Western Ontario 2015-2020 B.A.
London, Ontario, Canada

- Master of Science
- Bachelor of Science Honours
- Minor in Pharmacology

Honours and Awards:

- Physiology and Pharmacology Annual Research Day Poster Presentation Award 2020
- Dean's Honour List 2017-2020
- The University of Western Ontario Entrance Scholarship 2015-2016

Related Work Experience

Victoria Research Lab, Children's Health Research Institute 2020-2022

- Supervisor: Dr. Christopher Pin
- Lab research assistant

Teaching Assistant

- The University of Western Ontario, Department of Physiology and Pharmacology 2020-2022
- PhysPharm 3000E and Pharm 3620